MichiganTech
Create the Future

Michigan Technological University
Digital Commons @ Michigan Tech

Dissertations, Master's Theses and Master's Reports - Open

Dissertations, Master's Theses and Master's Reports

2014

DYNAMICS AND CONTROL OF REACTIVE DISTILLATION PROCESS FOR MONOMER SYNTHESIS OF POLYCARBONATE PLANTS

Mathkar Alawi A Alharthi
Michigan Technological University

Follow this and additional works at: https://digitalcommons.mtu.edu/etds

Part of the Chemical Engineering Commons

Recommended Citation

Alharthi, Mathkar Alawi A, "DYNAMICS AND CONTROL OF REACTIVE DISTILLATION PROCESS FOR MONOMER SYNTHESIS OF POLYCARBONATE PLANTS", Dissertation, Michigan Technological University, 2014.
https://digitalcommons.mtu.edu/etds/929

Follow this and additional works at: https://digitalcommons.mtu.edu/etds

Part of the Chemical Engineering Commons

DYNAMICS AND CONTROL OF REACTIVE DISTILLATION PROCESS FOR MONOMER SYNTHESIS OF POLYCARBONATE PLANTS

By

Mathkar Alawi A Alharthi

A DISSERTATION

Submitted in partial fulfillment of the requirements for the degree of

DOCTOR OF PHILOSOPHY

In Chemical Engineering

MICHIGAN TECHNOLOGICAL UNIVERSITY

2014

This dissertation has been approved in partial fulfillment of the requirements for the degree of DOCTOR OF PHILOSOPHY in Chemical Engineering.

Department of Chemical Engineering

Dissertation Co-Advisor: *Prof. Tomas B. Co*

Dissertation Co-Advisor: *Prof. Gerard T. Caneba*

Committee Member: *Prof. Tony N. Rogers*

Committee Member: *Prof. Jeffery B. Burl*

Department Chair: *Prof. S. Komar Kawatra*

Table of Contents

3

List of Figures

7

List of Tables

Acknowledgement

Abstract

Polycarbonate (PC) is an important engineering thermoplastic that is currently produced in large industrial scale using bisphenol A and monomers such as phosgene. Since phosgene is highly toxic, a non-phosgene approach using diphenyl carbonate (DPC) as an alternative monomer, as developed by Asahi Corporation of Japan, is a significantly more environmentally friendly alternative. Other advantages include the use of CO_2 instead of CO as raw material and the elimination of major waste water production. However, for the production of DPC to be economically viable, reactive-distillation units are needed to obtain the necessary yields by shifting the reaction-equilibrium to the desired products and separating the products at the point where the equilibrium reaction occurs. In the field of chemical reaction engineering, there are many reactions that are suffering from the low equilibrium constant. The main goal of this research is to determine the optimal process needed to shift the reactions by using appropriate control strategies of the reactive distillation system. An extensive dynamic mathematical model has been developed to help us investigate different control and processing strategies of the reactive distillation units to increase the production of DPC. The high-fidelity dynamic models include extensive thermodynamic and reaction-kinetics models while incorporating the necessary mass and energy balance of the various stages of the reactive distillation units. The study presented in this document shows the possibility of producing DPC via one reactive distillation instead of the conventional two-column, with a production rate of 16.75 tons/h corresponding to start reactants materials of 74.69 tons/h of Phenol and 35.75 tons/h of Dimethyl Carbonate. This represents a threefold increase over the projected production rate given in the literature based on a two-column configuration. In addition, the purity of the DPC produced could reach levels as high as 99.5% with the effective use of controls. These studies are based on simulation done using high-fidelity dynamic models.

1. Introduction

1.1 Polycarbonate

Polycarbonate (PC) is an important engineering thermoplastic that is produced in large industrial scale from bisphenol A and a monomer such as phosgene or diphenyl carbonate (DPC). Applications of the PC can be found in electronic components, data storage (CDs, DVDs, and Blue-ray discs), automobiles, mobile phones, personal computers, construction materials, etc. The main properties of PC are the high heat resistance, excellent impact resistance, structure stability, and optical transparency (Brunelle and Korn, 2005).

Polycarbonate was first discovered by Dr. Hermann Schnell of Bayer in Germany (Schnell, 1959), and was also discovered independently by Dr. Daniel Fox of GE in the United States (Fox, 1964). The original discovery was based on the phosgene process, and both Bayer and GE (Now SABIC Innovative Plastics) commercialized PC production in 1958 and 1960, respectively. Other companies followed in Japan from 1960-1975. They are Petrochemicals, Teijin Chemicals, Mitsubishi Gas Chemical; and Mitsubishi Chemical. The Dow Chemical followed in 1985 (Fukuoka et al., 2010b). The majority of polycarbonate industry has used the phosgene as the monomer.

The overall steps of this process are shown in Figure 1.1. In this conventional process, also called interfacial process, the reaction is carried out in the presence of catalyst at low temperatures using phosgene gas, solid bisphenol A, and aq. NaOH. Also, dichloromethane (CH_2Cl_2) and water are used as solvents. Drawbacks and disadvantageous of this process can be harmful environmentally and economically because phosgene is very dangerous and CH_2Cl_2 is very corrosive (Fukuoka et al., 2007).

A non-phosgene method using carbon monoxide (CO), oxygen (O_2), and MeOH as starting materials have been commercialized for PC production by GE in 1978. However, the major problems of this alternative are low selectivity of dimethyl carbonate (DMC), low purity of DMC, corrosive reaction, and the removal of water.
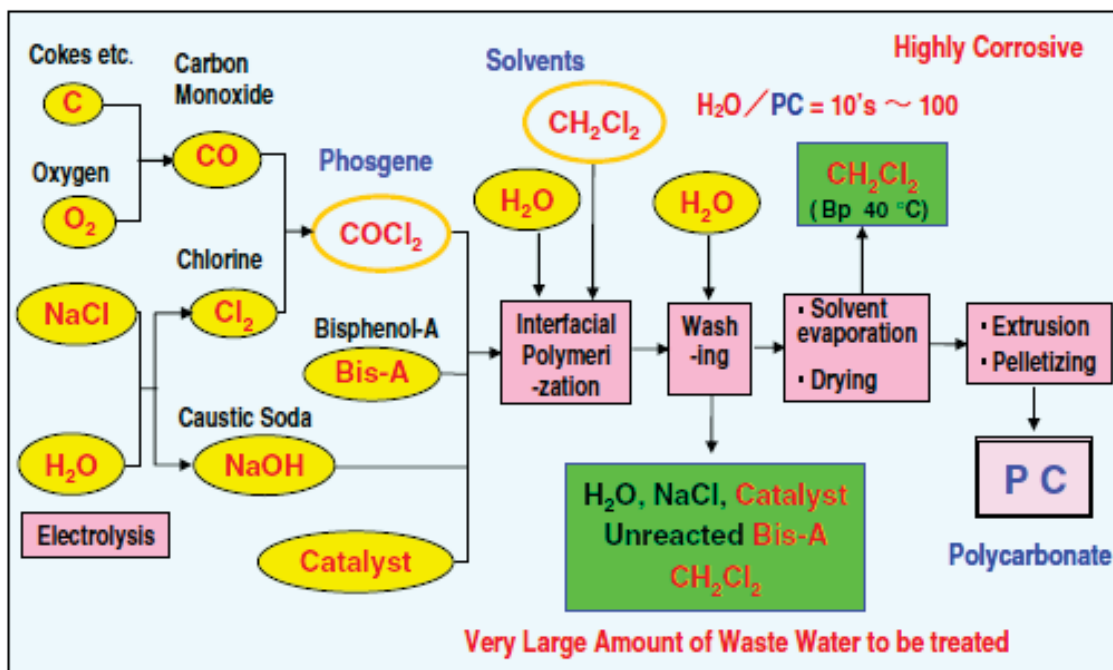
Figure 1.1 : Phosgene Process for PC Production. *Reprinted by permission from Macmillan Publishers Ltd: Polymer Journal, Vol. 39, No. 2, pp. 91– 114, copyright (2007)*

All these problems appear to be overcome by a new process developed by Asahi Corporation in Japan using CO_2 instead of CO (Fukuoka et al., 2003). It is also a non-phosgene synthesis in which diphenyl carbonate (DPC) is used as monomer instead of the highly toxic phosgene. In the Asahi process (see Figure 1.2), the raw materials used are carbon dioxide (CO_2), ethylene oxide (EO), and 2,2-bis-(4-hydroxyphenyl)-propane (bisphenol-A). Three steps are produced and the final polycarbonate products have been formed to have high purity and excellent properties. The first step (EC-DMC step) is the production of dimethyl carbonate (DMC) and monoethylene glycol (MEG) from methanol (MeOH) and ethylene carbonate (EC). EC is synthesized from raw feed of CO_2 and EO. The second step (DPC step) is the production of DPC and MeOH, where MeOH will be recycled to the EC-DMC step, from DMC and phenol (PhOH). The final step (PC production step) is the production of PC and PhOH, where PhOH will be recycled to the DPC step, from bisphenol-A and DPC.

13
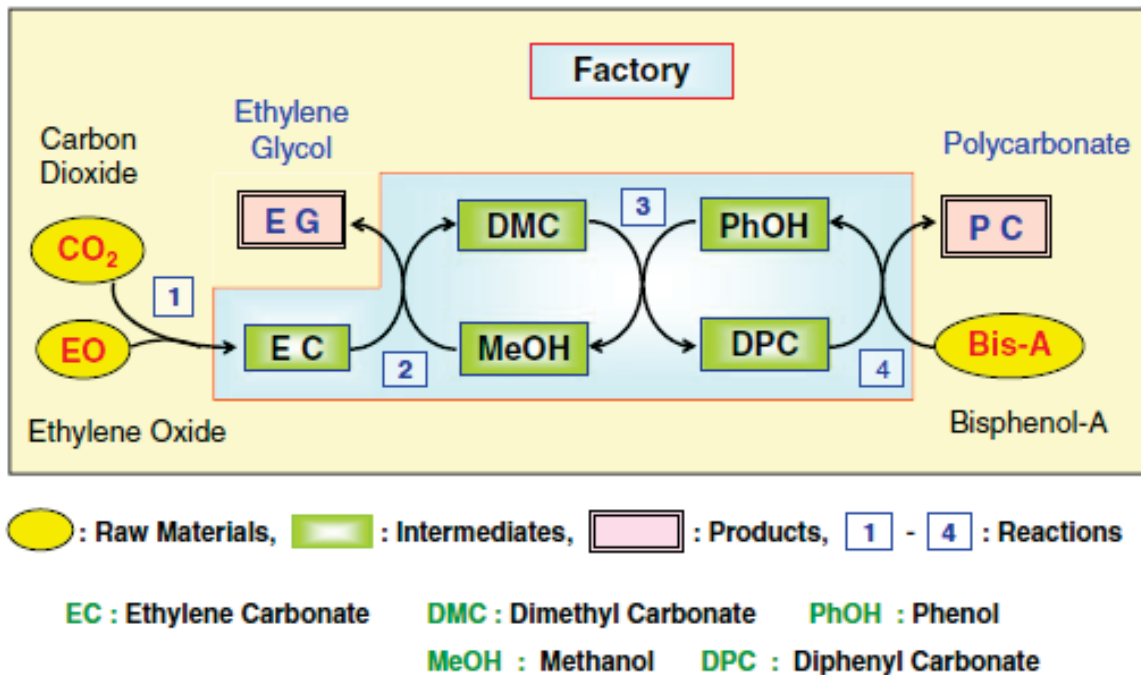
Figure 1.2 : Asahi Kasei's Non-Phosgene PC Process. *Reprinted by permission from Macmillan Publishers Ltd: Polymer Journal, Vol. 39, No. 2, pp. 91–114, copyright (2007)*

The ideal case of producing PC would be to synthesize it from CO_2 and bisphenol-A, but this remains difficult if not impossible (see Figure 1.3 and Figure 1.4). Nonetheless, the Asahi way comes close to the ideal case, and it is also environmentally benign (Fukuoka et al., 2010b; Fukuoka et al., 2003).

So far, five commercial plants have been operated successfully using Asahi process. Saudi Kayan, which is affiliated with Saudi Basic Industry Corporation (SABIC), has started producing polycarbonate in 2011 using the Asahi method with a production rate of 260,000 t/year. Before that, a plant of 150,000 t/y in Taiwan, two plants of 65,000 t/y in Korea, and another plant of 65,000 t/y in Russia have been built and operated successfully using this process (Fukuoka et al., 2010b). Also, as reported by SABIC, another plant with a production rate of 260,000 t/y will be started by 2015 in China.

Figure 1.3 : Ideal Process for PC Production. *Reprinted by permission from Macmillan Publishers Ltd: Polymer Journal, Vol. 39, No. 2, pp. 91–114, copyright (2007)*

Figure 1.4 : Asahi Kasei's New Process: Closest to the Ideal Process. *Reprinted by permission from   Macmillan Publishers Ltd: Polymer Journal, Vol. 39, No. 2, pp. 91–114, copyright (2007)*
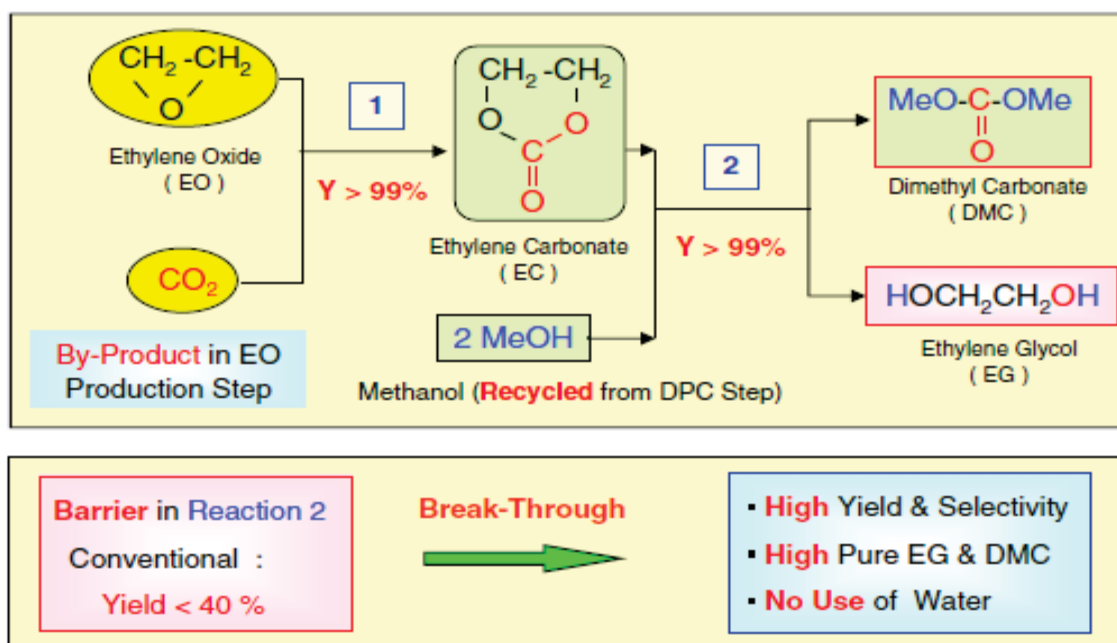
Figure 1.5 : Break-through (1) in the Monomer Production Step (EC and DMC Steps).
Reprinted by permission from Macmillan Publishers Ltd: Polymer Journal, Vol. 39, No. 2, pp. 91–114, copyright (2007)

The overall plant shown in Figure 1.2 can be divided to three parts. Each part contains important break-through for the whole integrated plant. The three breaks-through are shown in Figure 1.5, Figure 1.6, and Figure 1.7. The first part is constructed as a first step for DMC production (see Figure 1.5).

In order to obtain PC with high purity, the monomer used needs to also have high purity (Fukuoka et al., 2007). The non phosgene polycarbonate processes use DPC monomer instead of phosgene as shown in Figure 1.6. The last part of this plant is for the polymerization plant. The final polycarbonate product undergoes three processes, namely pre-polymerization, crystallization, and solid state polymerization as shown in Figure 1.7. The importance of DPC is clearly evident in the production of PC. Therefore, the study of DPC synthesis has grown through the past three decades. In the following section, the focus will be directed toward the DPC production process describing two different chemical reaction mechanisms for DPC synthesis.
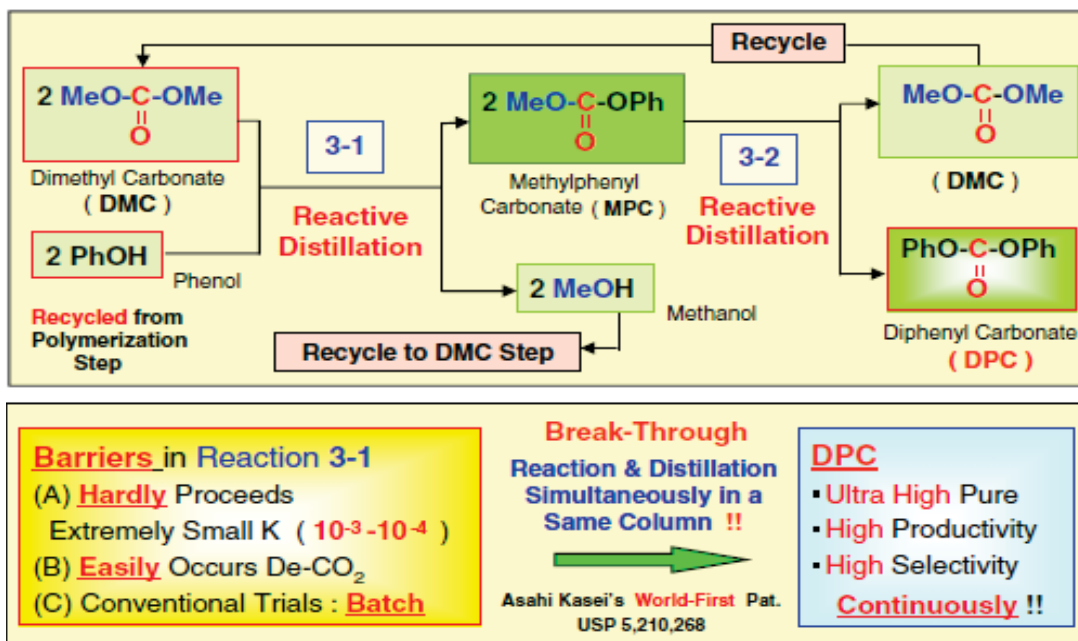
Figure 1.6 : Break-through (2) in the Monomer Production Step (DPC Step). *Reprinted by permission from Macmillan Publishers Ltd: Polymer Journal, Vol. 39, No. 2, pp. 91–114, copyright (2007)*
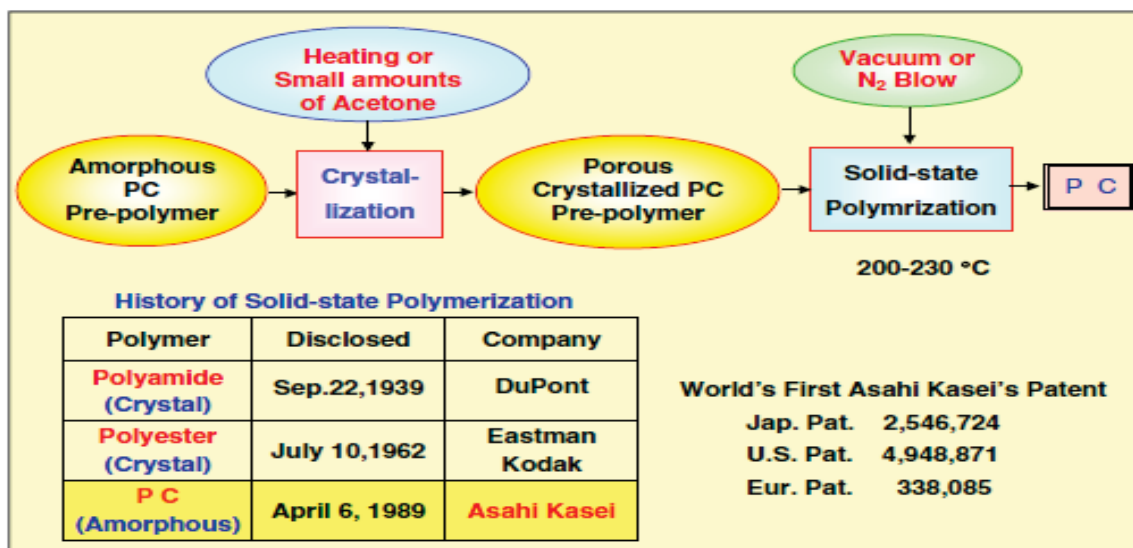
Figure 1.7 : Break-through (3) in the Polymer Production Step: Solid-State Polymerization of PC. *Reprinted by permission from Macmillan Publishers Ltd: Polymer Journal, Vol. 39, No. 2, pp. 91–114, copyright (2007)*

1.2 Diphenyl Carbonate (DPC) Production

Within the whole PC plant, DPC synthesis can be achieved by either transesterification of DMC with phenol or phosgenation of phenol. This study will be on the DMC transesterification using reactive distillation technology. The following sections include a brief description of both GE/SABIC-IP process and Asahi process. Although our focus will be on Asahi process, the GE/SABIC-IP process is still commercially competitive. However, the overall advantages of using CO_2 as raw material, as well as the benefit of reactive distillation, makes the Asahi process more sustainable in the future.

The use of CO_2 as raw material for DMC chemical process is considered by Ashai Kasei Corporation. It has become a commercial process since 2002, and has been run successfully (Fukuoka et al., 2010b; Fukuoka et al., 2003). The chemical reactions to produce DPC are shown in Figure 1.9. The first reaction has been studied and developed sufficiently since the middle of the last century (Peppel, 1958). The ethylene carbonate is commonly produced with high yield. For instance, The Dow Chemical Company has improved this process successfully (Raines and Ainsworth, 1980). Also, Asahi has worked to improve EC process for long time, and plan to commercialize their own invention (Okamoto and Someya, 2007).

1.2.1 GE (SABIC IP) Process

For this process, DMC and water are produced using the monoxide carbon (CO), oxygen (O_2), and MeOH as starting materials through the first reaction shown in Figure 1.8. This reaction is catalyzed by copper compounds (Romano et al., 1980). The second reaction is a transestrification of DMC with phenol in two steps to yield DPC. In the first step, phenyl methyl carbonate (PMC) is produced using a molecular sieve and some catalyst. In the second step, PMC is heated to remove PhOH, MeOH and DMC leaving DPC as the main product (Hallgren, 1983; Illuminati et al., 1980).

$$2CH_3OH + CO + \tfrac{1}{2}\,O_2 \longrightarrow C_3H_6O_3 + H_2O \qquad\qquad \text{Reaction 1}$$

(MeOH)   **(DMC)**

$$2C_6H_5OH + C_3H_6O_3 \longleftrightarrow C_{13}H_{10}O_3 + 2CH_3OH \qquad\qquad \text{Reaction 2}$$

(PhOH)   **(DMC)**   **(DPC)**   **(MeOH)**
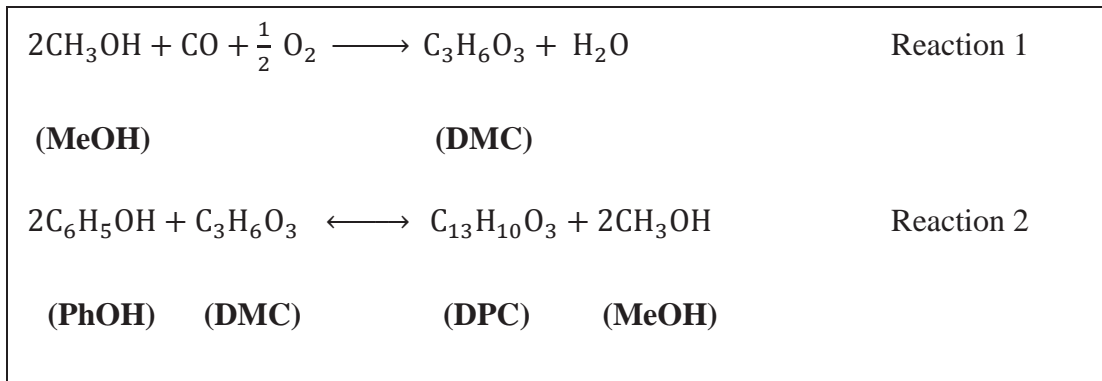
Figure 1.8 : GE (SABIC IP) Process

1.2.2 Asahi Kasei Process

The second reaction is a transesterification of EC with low equilibrium constant.
Different types of reactor technologies have been used to carry out this reaction. Since
this reaction is equilibrium-limited, the best technology to achieve the reaction
completion is reactive distillation as used by Asahi, resulting in high yield of DMC and
MEG (Fukuoka et al., 2006). An integrated process have been depicted well for both
reactions 1 and 2 (Buchanan et al., 2006).

$$C_2H_3OH + CO_2 \longrightarrow C_3H_4O_3 \qquad\qquad \text{Reaction 1}$$

(EO)   **(EC)**

$$C_3H_4O_3 + 2CH_3OH \longleftrightarrow C_3H_6O_3 + C_2H_6O \qquad\qquad \text{Reaction 2}$$

(EC)   **(MeOH)**   **(DMC)**   **(MEG)**

$$2C_6H_5OH + C_3H_6O_3 \longleftrightarrow C_{13}H_{10}O_3 + 2CH_3OH \qquad\qquad \text{Reaction 3}$$

(PhOH)   **(DMC)**   **(DPC)**   **(MeOH)**
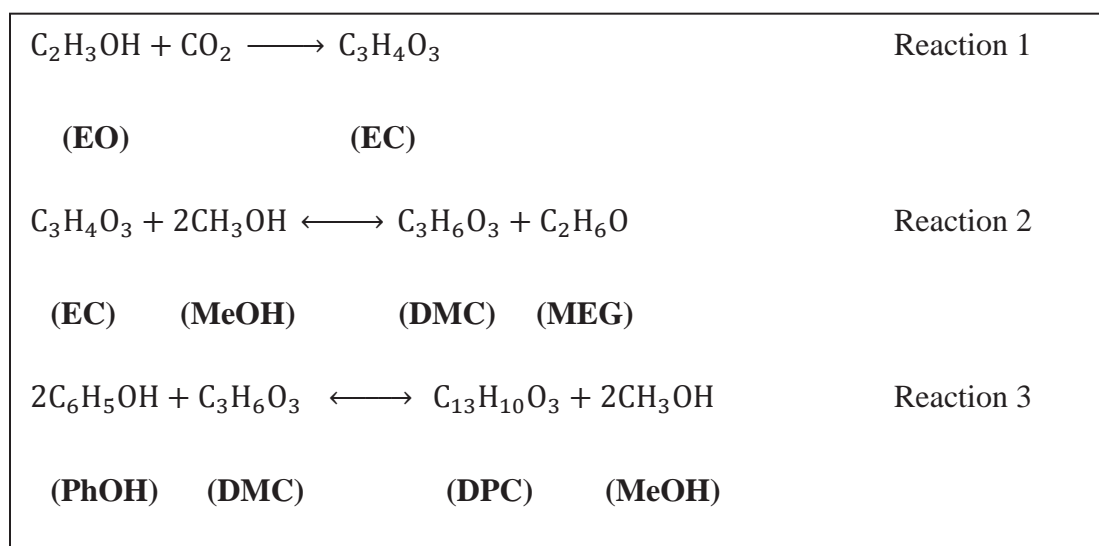
Figure 1.9 : Asahi Kasei Process

19

The third reaction is also equilibrium-limited, but with a very low equilibrium constant. To enhance the reaction toward completion, reactive distillation has been also used by Asahi. A series of two reactive distillations will be efficient to carry this reaction in two steps, to attain DPC with high purity (Fukuoka et al., 1993; Fukuoka et al., 2009; Fukuoka et al., 2010a). Our study will be focused on the optimization and control of the reactive distillation units as applied to the Asahi process. Therefore, a lot of discussion about reactive distillation will be covered in the next chapters. To summarize, the DPC synthesis using CO_2 has the following main advantages (Fukuoka et al., 2010b):

a. CO_2 will be used as raw material.
b. DPC is much safer than phosgene.
c. No water and chlorine are present.
d. MEG is one of the byproducts and it is another valuable chemical.
e. Reactive distillation technologies will produce high yields and selectivity.
f. No solvents or chemical modifications are needed.
g. All the intermediates are recycled.

1.3 Reactive Distillation Technology

The reactive distillation unit is a relatively new and important unit that combines reaction and separation in one unit operation. This technology is most useful in systems where reactions have low chemical equilibrium constants. By separating volatile products from the reaction regime, it will increase the reaction conversion significantly by shifting the chemical equilibrium to the forward reaction. In some cases, removing the most volatile materials can also reduce the side reactions; thereby increase the desired product selectivity. Also, the azeotropes of the non-reactive mixtures may also change or disappear by during reactive distillation.

Reactive distillation has been successfully applied industrially over the world for many chemicals synthesis, especially esterification and etherification processes. One of the main benefits of reactive distillation is to minimize several complex units into one reactive distillation column, thus lowering plant capital and energy costs. Often low chemical equilibrium constants can be overcome by continuously removing one of the products while the reaction is taking place, and thus increase the productivity towards the desired product (Luyben and Yu, 2009; Sundmacher and Kienle, 2006). One of the most successful cases of reactive distillation was reported by Eastman Chemical for producing high purity methyl acetate (Agreda et al., 1990). By using this technology, the capital and energy costs have been reported to be five times lower than those using conventional technologies (Siirola, 1996). Active research in reactive distillation include phase equilibrium models, reactions and catalysis, and equipment design and control alternatives (Malone and Doherty, 2000).

The conflict between yield and purity is still an issue in many of the reactive distillation systems. One important limitation of reactive distillation is coming from the reaction and separation temperatures disagreement. More research is needed to focus on finding new relationships between separation and reaction involved in the reactive distillation systems that can be used to improve both yield and purity simultaneously. The system investigated in this work is an example where yield and purity will need to be balanced.

21

1.4 Dynamics and Control of Reactive Distillations

The dynamics and control study of reactive distillation has not received much attention in the literature. The nonlinearity and the complexity of this system present significant challenges. A book has been published recently about the design and control of reactive distillation to provide a general overview of reactive distillation technology by presenting different ideal and non-ideal systems (Luyben and Yu, 2009).

The objective of process control in the industry is mainly focused on the following important issues: environmental and safety considerations, economic measures in terms of cost and profit, and the quality of the required product. In order to choose the suitable control methodology, the chemical process has to be sufficiently understood. For reactive distillation, the design and control may not be generalized for all chemical processes in consideration of the non-ideal cases. The study involves conversion of the limiting reactant as well as the separation efficiency in term of purity. Therefore, each chemical system has its own characteristics and limitations from reaction and separation points of view. Our work is focused on the production of Diphenyl carbonate (DPC), which is currently one of the most important industrial. The successful production method using reactive distillation to produce DPC has been applied recently (Fukuoka, 2012). In the next outlines, we will introduce a brief background of reactive distillation control. A comparison was made between two control structures for controlling two temperatures points in a reactive distillation (Kaymak and Luyben, 2005). The first type was published late 1980s for the control of reactive distillation where a quaternary reaction is involved (A+B <==> C+D) while the catalyst is used as a saturated liquid (Roat et al., 1986).

The methyl acetate reactive distillation system is used as an example for this reaction. The two control structures of this study were to control two temperatures at both the reactive and stripping sections by manipulating the two feeds of A and B while fixing the reboiler heat input to handle the production rate. The second type of this comparison has been discussed recently, through a private communication between Dr. Luyben and Dr. Yu, by considering one of the feeds and the reboiler heat input as manipulated variables to control the two temperatures while the second feed is used to handle the production

rate (Kaymak and Luyben, 2005). It has been shown that the stability of the system can be affected by using the second control structure due to the manipulation of one of the column feeds.

In term of batch process, investigations were carried out on a batch reactive distillation showing the controllability dependency on the operating conditions and the run time (Sørensen and Skogestad, 1994). The system Sørensen and Skogestad studied consists of reactor/reboiler connected with the distillation column above it. Their target is to increase the reaction temperature while shifting the equilibrium toward the production side by using the distillation column to remove one or more of the light components. The strategy of controlling a tray temperature within the column (one-point column control) has been shown to improve the control of this system. Other strategies are presented in this study such as controlling the reactor temperature (one-point bottom control) and controlling both the reactor temperature as well as the distillate compositions (two-point control); however, they are shown to be difficult strategies for controlling the batch reactive distillation. Sharma and Singh have reviewed the control of reactive distillation to provide extensive literature references about this subject (Sharma and Singh, 2010). How to control the column to shift the reaction toward the product side is a critical subject. However, there are many control methodologies. The classical Proportional-Integral-Derivative (PID) control is still effective and widely used in the actual plants, but the advanced controls such as Model Predictive Controls (MPC) have received more and more attention from industry. The control techniques in this work will be limited to classical PID controls. The main objective of PID control remains to minimize the error between the required set point and the system output driving the dynamic behavior of the system toward its steady state point.

The control output of PID can be estimated as

$$u(t) = K_p e(t) + K_i \int_0^t e(\tau)d\tau + K_d \frac{de(t)}{dt} \qquad (1.1)$$

where the three parameters K_p, K_i, and K_d are the gains of proportional, integral, and derivative terms. The function $e(t)$ is the error that needs to be minimized. The proportional term is driving the system toward the set point based on the present error while the integral and derivative terms are treating the system based on the past accumulated errors and the predicted future errors, respectively.

1.5 Dissertation Methodology

The main objective of this research is the study of reactive distillation technology. Modeling, simulation, and control of different ideal and non-ideal systems are studied using Aspen Plus and MATLAB softwares. The strategy of this document is summarized as following:

1- The required model for reactive simulation will be discussed through the second chapter providing the high-fidelity model for reactive distillation simulation. The model can be simplified based on the simulated system assumptions.

2- Based on the model, the next chapter will be dealing with the design and control of two different systems. The first one will be the ideal binary reactive distillation which represents the isomerization process of n-butane to the isobutane. The design of this system is based on maximizing the conversion while holding the purities at the required levels. The control configuration is setup to hold the design specifications. The other system is a quaternary system with two feeds and two products. The dynamic model is used to reach the steady states by controlling the top product purity and the column base level.

3- The next chapter will be discussing the preliminary conceptual design of diphenyl carbonate (DPC) system. An azeotropic study will be discussed to identify the azeotropes of the DPC system in order to consider it through the design and control. This study is based on an experimental data collected from the literature, and the UNIFAC thermodynamic activity coefficient is used to measure the non-ideal behavior of the liquid phase. Since the operation pressure is low, the vapor phase is assumed to be ideal.

4- The last part of this document will be discussing the design and control of DPC system. Systematic design procedures will be presented based on maximizing the yield and purity while observing the total annual cost (TAC). The control configuration is used effectively to hold the purity of DPC while keeping the yield at the optimal value.

2. Reactive Distillation Modeling

To model the process in reactive distillation units, many fundamental concepts are needed such as vapor-liquid equilibrium, mass transfer, chemical reaction kinetics, and catalyst diffusion process (Taylor and Krishna, 2000). The additional complexity results from combining reaction and separation steps in one unit. Different strategies have to be applied to optimize the process.

2.1 Chemical System

Diphenyl carbonate is produced via transesterification reaction between phenol and dimethyl carbonate. In this chapter, we will present the fundamental concepts of reactive distillation modeling. The typical reactive distillation is shown in Figure 2.1 with total number of trays equal to N_T.
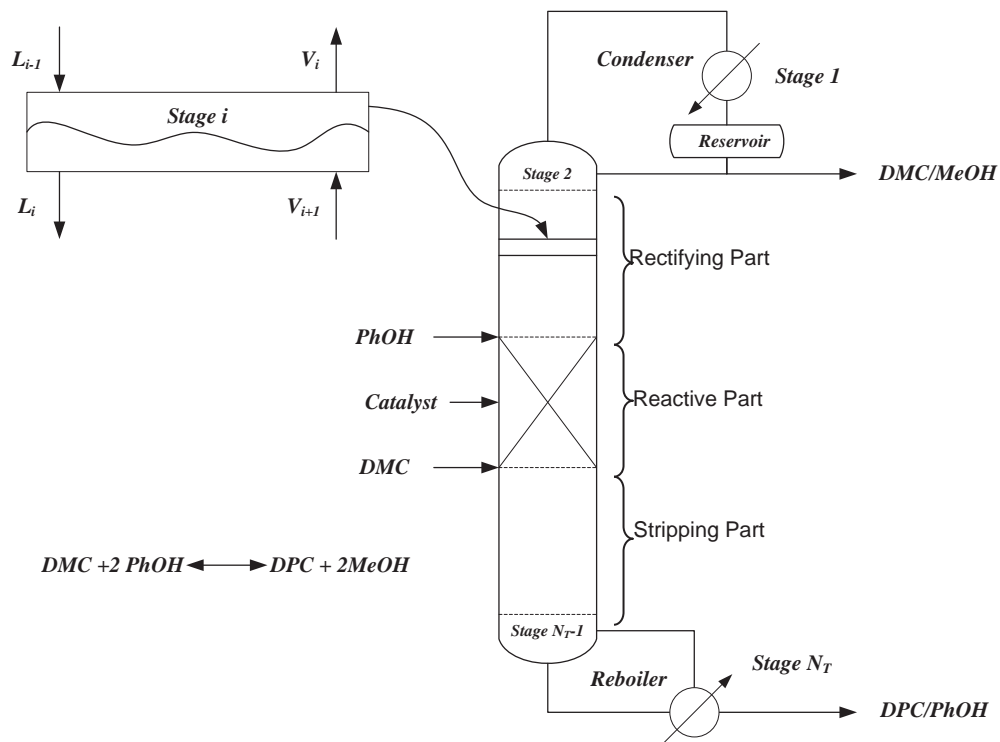
Figure 2.1 : Typical Reactive Distillation Diagram

2.2 Equilibrium Stage Model

The equations used to describe each stage within the reactive distillation column will involve material balance equations, phase equilibrium relations, summation relations, and energy balance equations. We refer to this collection of equations as Material balance, Equilibrium, Summation, and Heat balance (MESH) (Taylor and Krishna, 2000). From the typical schematic diagram of the reactive distillation is represented by Figure 2.1, the modeling of one stage is the base for constructing the column model. Figure 2.2 is used for a single stage modeling. For $i = 2, \ldots, N_T - 1$, the total dynamic mass balance around one stage can be expressed as following:

$$\frac{dM_i}{dt} = V_{i+1} + L_{i-1} + F_i - (1 + r_i^V)V_i - (1 + r_i^L)L_i + \sum_{m=1}^{n} \sum_{j=1}^{c} v_{j,m} \, R_{m,i} \, \varepsilon_i \quad (2.1)$$

where

M_i = stage i molar hold up (mole),

V_{i+1} = vapor flow rate coming from stage $i + 1$ (mole/s),

L_i = Liquid flow rate leaving stage $i - 1$ (mole/s),

F_i = feed flow rate in stage i (mole/s),

r_i^V = ratio of vapor side stream flow to vapor interstage flow on stage i [ ],

r_i^L = ratio of liquid side stream flow to liquid interstage flow on stage i [ ],

F_i = feed flow rate in stage i (mole/s),

m = reaction index

n = number of components

j = component index

c = number of components

$v_{j,m}$ = stoichiometric coefficient of component j in reaction m [ ],

$R_{m,i}$ = reaction m taken place in stage i

ε_i = reaction volume in stage i (m^3),
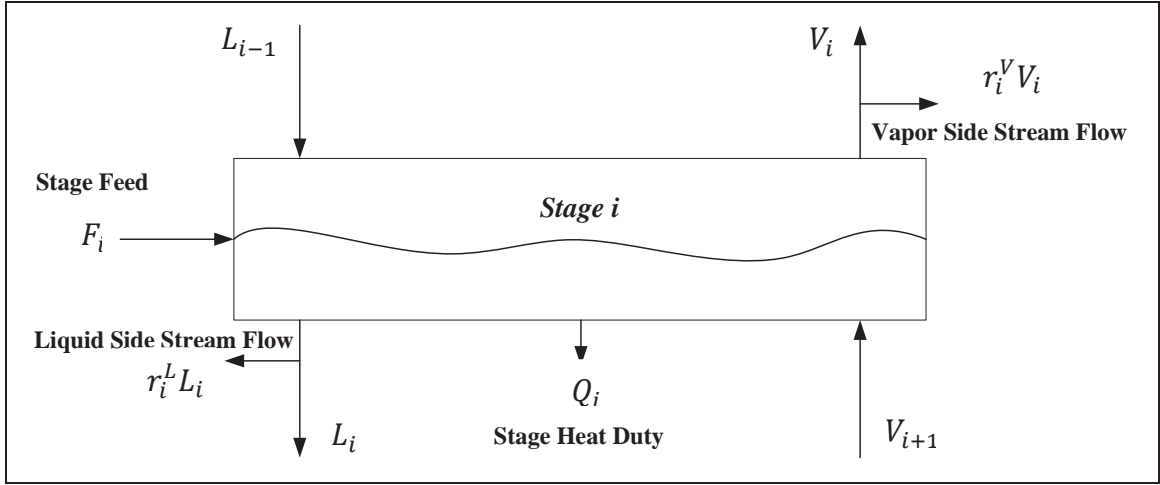
Figure 2.2 : Schematic Diagram of Single Equilibrium Stage

Note that stage 1 and stage NT are not considered in the equilibrium stage model because they are used for representing condenser and reboiler respectively. To evaluate the component composition at each stage, the composition material balance has to be used which is based on the overall material balance expressed by equation (2.1). The component material balance at stage i for $i = 2, \dots, N_T - 1$ is written to be

$$\frac{dM_i x_{j,i}}{dt} = V_{i+1}\, y_{j,i+1} + L_{i-1}\, x_{j,i-1} + F_i\, z_{j,i} - (1 + r_i^V)V_i\, y_{j,i}$$

$$- (1 + r_i^L)L_i\, x_{j,i} + \sum_{m=1}^{n} \nu_{j,m}\, R_{m,i}\, \varepsilon_i \qquad (2.2)$$

where

$x_{j,i}$ = the liquid composition of component j at stage i [ ],

$y_{j,i}$ = the vapor composition of component j at stage i [ ],

$z_{j,i}$ = the composition of feed coming in stage i [ ],

The energy equation of stage i for $i = 2, \ldots, N_T - 1$ yields

$$\frac{dM_i H_i^L}{dt} = V_{i+1} H_{i+1}^V + L_{i-1} H_{i-1}^L + F_i H_i^F - \left(1 + r_i^V\right) V_i H_i^V - \left(1 + r_i^L\right) L_i H_i^L + Q_i \quad (2.3)$$

where

H_i^L = the liquid enthalpy at stage i (J/mole),

H_i^V = the vapor enthalpy at stage i (J/mole),

H_i^F = the feed fluid enthalpy at stage i (J/mole),

Q_i = the heat duty of stage i (J/s),

For the condenser (stage 1), equations (2.1), (2.2), and (2.3) can be reproduced

$$\frac{dM_1}{dt} = V_2 + L_1 + D \quad (2.4)$$

$$\frac{dM_1 x_{j,1}}{dt} = V_2 \, y_{j,2} + L_1 \, x_{j,1} + D \, x_{j,1} \quad (2.5)$$

$$\frac{dM_1 H_1^L}{dt} = V_2 H_2^V + L_1 H_1^L + D H_1^L - Q_C \quad (2.6)$$

The reboiler balance equations yields

$$\frac{dM_{N_T}}{dt} = L_{N_T - 1} - B - V_b \quad (2.7)$$

$$\frac{dM_{N_T} x_{j,N_T}}{dt} = L_{N_T - 1} x_{j,N_T - 1} - B \, x_{j,N_T} - V_b \, y_{j,N_T} \quad (2.8)$$

$$\frac{dM_{N_T} H_{N_T}^L}{dt} = L_{N_T - 1} H_{N_T - 1}^L - B \, H_{N_T}^L - V_b H_{N_T}^V + Q_R \quad (2.9)$$

where D is the distillate flow rate (mole/s), Q_C is the condenser heat duty (J/s), B is the bottom flow rate (mole/s), V_b is the reboiler boil up flow rate (mole/s), and Q_R is the reboiler heat duty (J/s).

The Francis weir equation is commonly used to calculate the liquid flow rates through the column trays $(2, \dots, N_T - 1)$ which is (Ferrio, 1999)

$$L_i = \frac{f_c \, \rho_{L,i} \, L_{w,i} \, H_c^{3/2}}{MW_{L,i}}, \qquad with \ \ H_c = h_i - h_{w,i} \geq 0 \qquad (2.10)$$

where

f_c = corrected factor [ ],

$\rho_{L,i}$ = the liquid density at stage i (kg/m^3),

$L_{w,i}$ = the weir length at stage i (m),

H_c = the crest height of stage i (m),

h_i = the liquid height at stage i (m),

$h_{w,i}$ = the weir height of stage i (m),

$MW_{L,i}$ = the liquid mixture molecular weight at stage i [ ],

The vapor flow through the column trays $(2, \dots, N_T - 1)$ can be calculated using the pressure drop within the trays. Therefore, the vapor flow as a function of the pressure drop yields

$$V_{i+1} = \frac{f_c \, A_h \, \rho_{V,i} \, C_i}{MW_{V,i}} \sqrt{\frac{2\Delta P_{d,i}}{\rho_{V,i}}} \qquad with \quad \Delta P_{d,i} = \Delta P_i - \Delta P_h \geq 0 \qquad (2.11)$$

where

f_c = corrected factor [ ],

$\rho_{V,i}$ = the vapor density at stage i (kg/m^3),

C_i = the pressure drop coefficient at stage i [ ],

$\Delta P_{d,i}$ = the pressure drop through the dry stage i (atm),

ΔP_i = the total pressure drop of stage i (atm),

ΔP_h = the hydrostatic pressure drop of the liquid at stage i (atm),

$MW_{V,i}$ = the vapor mixture molecular weight at stage i [ ],

2.3 Phase Equilibria

The equilibrium between liquid and vapor phases is crucial when modeling any separation system. There are many thermodynamic models that can be used to calculate the vapor composition from its corresponding liquid composition when the vapor liquid equilibrium is reached. For the ideal system, Raoult's law equation is used to express this relationship between the two phases as follows:

$$P \, y_j = x_j \, P_j^s \tag{2.12}$$

where P is the total vapor pressure and P_j^s is the saturated vapor pressure of component j. The saturated vapor pressure P_j^s is calculated by Antoine equation as

$$\ln P_j^s = A_j - \frac{B_j}{T + C_j} \tag{2.13}$$

where A_j, B_j, and C_j are called Antoine parameters for component j.

To describe the phase equilibria for the non ideal chemical systems, major modification has to be applied on equation (2.12) to correct the equilibrium behavior between liquid and vapor. Two important parameters have been added: the fugacity coefficient, ϕ, which is used to reflect the vapor non ideality, and the activity coefficient, γ, which accounts for the non ideality of the liquid phase (Prausnitz et al., 1999). Including these two parameters, equation (2.12) becomes

$$\phi_i \, P \, y_j = \gamma_i \, x_j \, P_j^s \tag{2.14}$$

One of the equations of state can be used to predict the fugacity coefficient (ϕ) while the activity coefficient (γ) can be predicted by various liquid activity coefficient models. This work will be considering Soave-Redlich-Kwong equation of state for vapor fugacity prediction and UNIFAC model for estimating the liquid activity coefficient which is explained through the next chapters.

2.4 Reaction Kinetics

Reactive distillation is different from the conventional distillation because reaction taken place simultaneously while the chemicals are separated. The rate of the reaction is needed for modeling reactive distillation. The simple reversible reaction $(A \leftrightarrow B)$ is taken as example. The rate of this reaction as function of the liquid fractions at each reactive stage within the column yields

$$R_i = M_i(k_f \, x_{A,i} - k_b \, x_{B,i}) \tag{2.15}$$

The rate constants $(k_f \; and \; k_b)$ is calculated by Arrhenius equation to be:

$$k_f = k_{0,f} \exp\left(-\frac{E_{A,f}}{R_{gas}T}\right) \tag{2.16}$$

$$k_b = k_{0,b} \exp\left(-\frac{E_{A,b}}{R_{gas}T}\right) \tag{2.17}$$

where

$k_{0,f}$ = pre-exponential factor of the forward reaction [s^{-1}],

$k_{0,b}$ = pre-exponential factor of the backward reaction [s^{-1}],

$E_{A,f}$ = the activation energy of forward reaction (kJ/mole),

$E_{A,b}$ = the activation energy of backward reaction (kJ/mole),

R_{gas} = the ideal gas constant (kJ/mole.K),

T = reaction temperature (K),

At chemical equilibrium, the rate constants is related to each other by the equilibrium constant (K_{eq}) to yield

$$K_{eq} = \frac{k_f}{k_b} \tag{2.18}$$

3. Ideal Reactive Distillation

In this chapter, two ideal reactive distillations will be presented. The first is a binary chemical system while the second will be the quaternary DPC system. Parametric investigations have been studied to explore the different effective parameters of reactive distillation. Although the ideal system can be used to represent a lot of the scientific concepts, the deviation of the ideal results from reality still not small. This comparison between ideal and real systems will be explained using the main chemical system of this dissertation (i.e. the production of diphenyl carbonate). In the next section, we will discuss in detail the binary reactive distillation.

3.1 Binary System $(A \leftrightarrow B)$

3.1.1 Problem Definition

Isomerization is an appropriate chemical system to be carried by reactive distillation. The conceptual design of this system was investigated from equipment point of view (Sundmacher and Kienle, 2006). It has been shown the advantage of using reactive distillation as comparison with other two kinds of equipments. The first one is the reactor following by conventional distillation column while the second is a distillation on the top of reactive reboiler. The isomerization of n-butane to isobutene is picked to be our example for binary reactive distillation study. The symbol A will be used to refer n-butane, and the symbol B will be used for isobutene. The chemical reaction of this isomerization system can be written as

$$A \underset{k_b}{\overset{k_f}{\Longleftrightarrow}} B \tag{3.1}$$
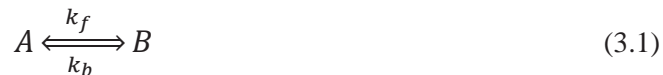
The column flow sheet is explained by Figure 3.1. The kinetics of reaction (3.1) is listed in Table 3.1. The design procedures of reactive distillation for this binary chemical system will be discussed in the next section.
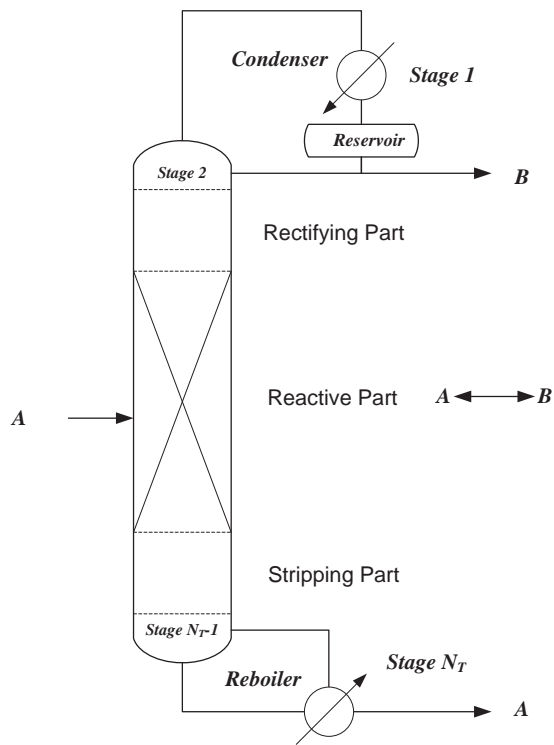
Figure 3.1: Binary Reactive Distilaltion

Table 3.1: Kinetics Parameters of Binary System

Forward pre-exponential factor (s^{-1})	0.06
Backward pre-exponential factor (s^{-1})	0.03
Forward activation energy (kJ/mole)	32.2
Forward activation energy (kJ/mole)	15.3

3.1.2 Design Procedure

Since we are dealing with reactive distillation, the number of stages wouldn't be as in the usual distillation. As shown in Figure 3.1, there are three sections and each of them has its own number of stages. Therefore, the design of reactive distillation stages consists of the design of each of these sections. There are three numbers that have to be optimized instead of focusing on one number as in the conventional distillation. The cross-reference N_r is used for defining the number of rectifying stages while N_{rx} and N_s are used for reactive stages number and stripping stages number respectively. The objective of this column is to maximize both of the yield and purity simultaneously. The required top mole purity of B is 99% while the bottom mole purity of A also 99%. The conversion of A is driven to complete conversion as much as possible. The reference steady state conditions that we got are listed in Table 3.2. The temperature and compositions profiles are illustrated by Figure 3.2 and Figure 3.3.

Table 3.2: Steady State Conditions

Feed flow of A (mole/s)	100	
Reflux ratio	3.35	
Rectifying stages including condenser	5	
Reactive stages	22	
Stripping stages including reboiler	12	
Holdup (m^3)	1.3	
Feed stage	19	
Pressure (atm)	1.0	
Product Purity (Mole Fraction)	Distillate	Bottoms
A	0.01	0.99
B	0.99	0.01
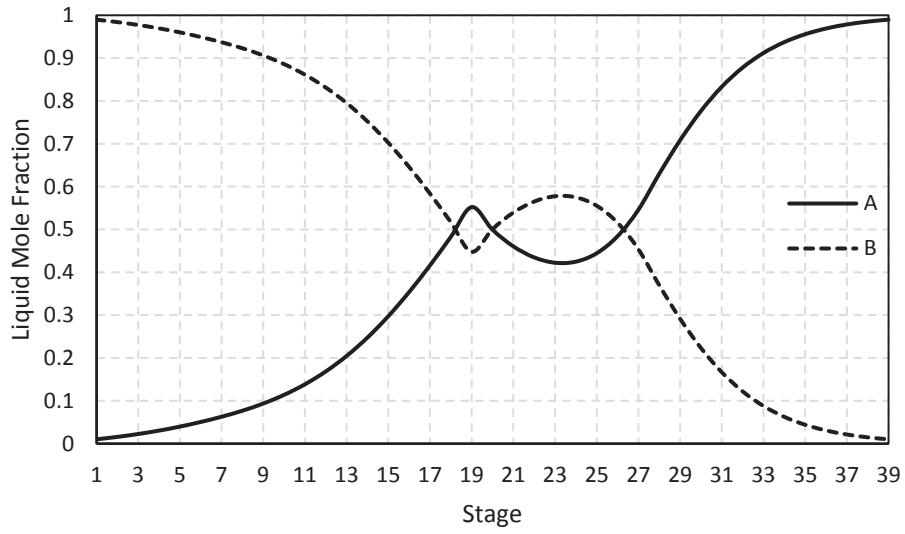
Figure 3.2: Composition Profiles of Binary System
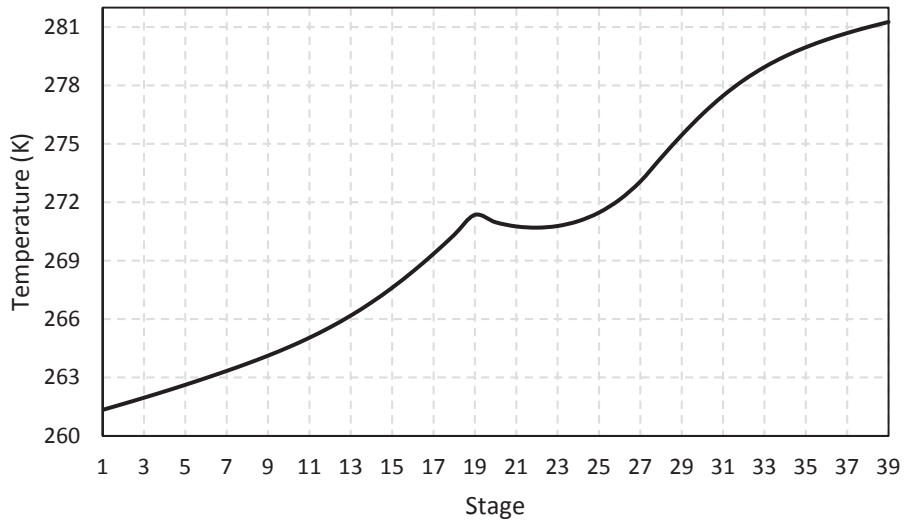
Figure 3.3: Temperature Profile of Binary System

The steps listed below are the systematic design procedures for the binary system under study to reach above reference steady state conditions.

1- The pressure is fixed at 1 atm.

2- The total number of stages is guessed to be 34 that give good purity and yield.

3- The numbers of reactive, rectifying, and stripping stages are guessed taking into consideration the required yield and purity. By taking $N_{rx} = 22$, $N_r = 4$, and $N_s = 8$, the conversion of A will be 89.76% while the mole purity of the A at the top will reach 97.53% and the bottom mole purity of B at the bottoms will be 99.13% . The feed stage is the last reactive stage ($N_f = 26$).

4- The reflux ratio and the reboiler heat duty are manipulated until the required purity specifications are met.

5- Back to step 3, N_{rx} is fixed as guessed while N_s and N_r are calculated using Fenske equation (Seader et al., 2011) which yields:

$$N_s = 2 \frac{\log\left(\frac{x_{B,27}}{x_{A,27}} \frac{x_{A,34}}{x_{B,34}}\right)}{\log(\alpha_{AB})} = 12.44 \tag{3.2}$$

$$N_r = 2 \frac{\log\left(\frac{x_{B,1}}{x_{A,1}} \frac{x_{A,4}}{x_{B,4}}\right)}{\log(\alpha_{AB})} = 5.39 \tag{3.3}$$

6- The new values of N_s and N_r are entered. The feed stage will be changed to be $N_f = 28$, and the simulation is executed again.

7- The step 4 is repeated until the required purity specifications are met. The conversion is calculated to be 65.8 % which confirms the conflict between purity and yield in reactive distillation design.

8- The feed stage (N_f) is changed until the required conversion is met. The change of conversion with respect to the feed location can be read from Figure 3.4 which shows that maximum conversion (86.54%) can be achieved when $N_f = 19$. This is corresponding to a reflux ratio of 3.35. The relationship between the feed

location and the reflux ratio are explained by Figure 3.5 that shows a minimum reflux ratio of 2.01 when $N_f = 28$. This is another conflict destination between separation and reaction because more reflux means more heat duty as shown in Figure 3.6.
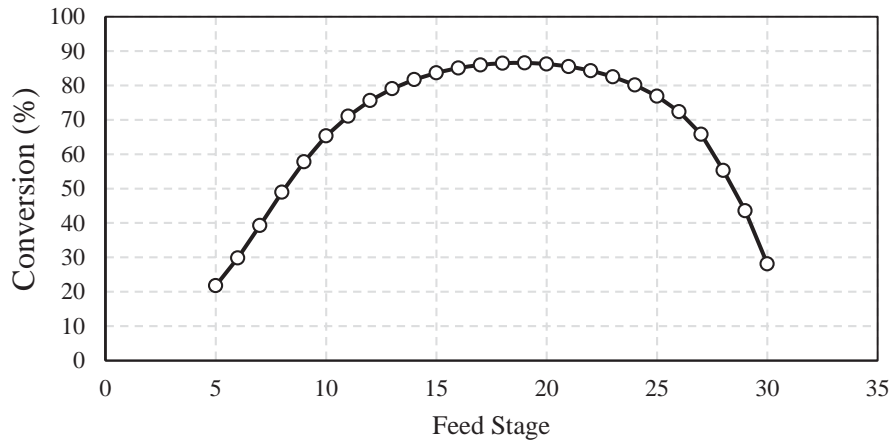
Figure 3.4: Effect of Feed Stage on Reaction Converison
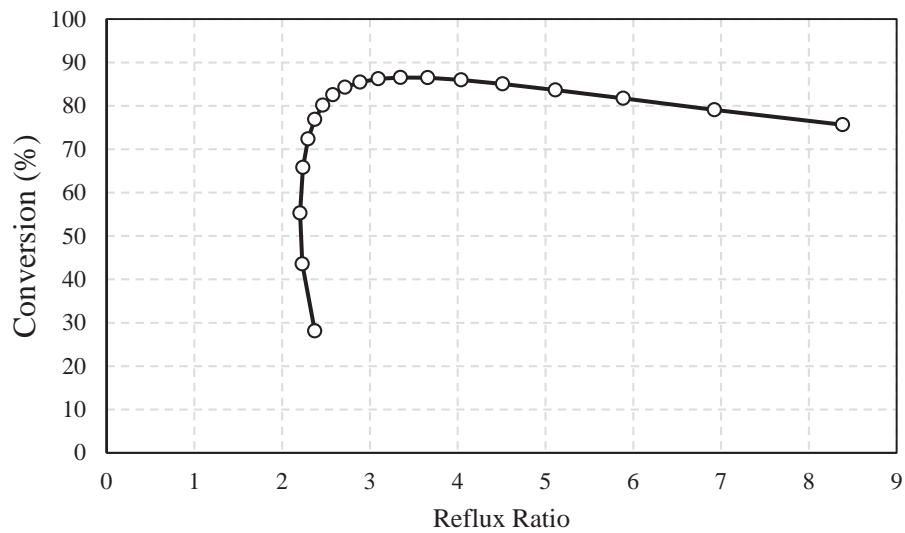
Figure 3.5: Conversion Response to Reflux Ratio
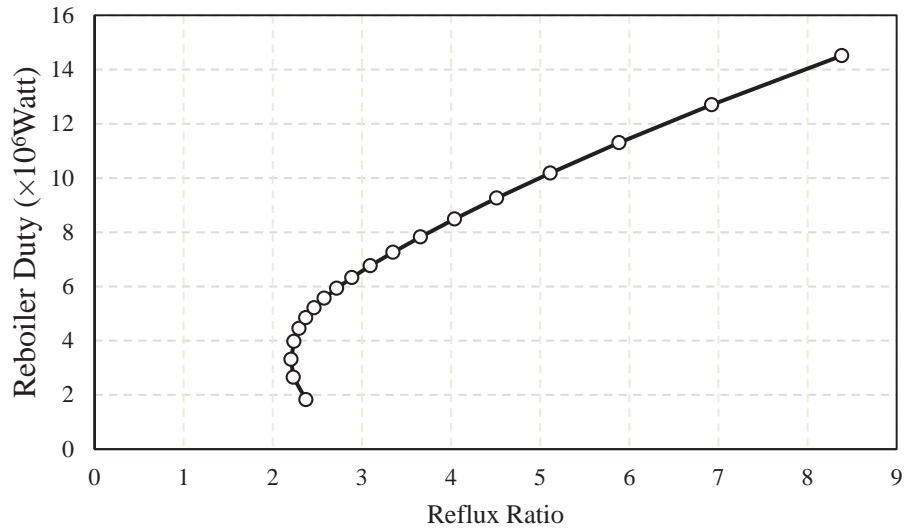
Figure 3.6: Reboiler Heat Response to Reflux Ratio Change

3.1.3 Residence Time and Reactive Stages

In the previous section, we could build design procedures for the binary reactive distillation. Due to the conflict between reaction and separation, the fact that the complete conversion could not be achieved is shown at step 8. However, the conversion can be increased by increasing the reactive stages or by increasing the reaction residence time (i.e. the holdup of each reactive stage) while keeping the numbers of rectifying and stripping stages constants. For example, by increasing the reactive stages, the conversion of 99% can be achieved with $N_T = 49$ when $N_r = 5$, $N_{rx} = 32$, and $N_s = 12$. This is also with holding the purity at their required points at both the distillate and bottoms. As a result, we end with higher reflux ratio and the required duty for the column will be increased as well (Reflux Ratio $= 3.33$, $Q_R = 8248.79$ KW, $Q_C = -9178.35$ KW). Increasing the holdup is critical because it is also related to the mechanical design of the equipment. The physical geometry of the stage volume has to be large enough to contain the specified liquid volume.

3.1.4 Pressure of Reactive Distillation

The pressure is very sensitive because it affects the reaction rate and the equilibrium. Sometimes, the pressure plays a positive effect while it may give negative response in other cases. In the previous section, the conversion is increased by changing the number of the reactive trays. Instead of changing this number, the pressure can be used to increase the conversion. For instance, when the pressure is set at 1.8 atm, the conversion can reach 93.94 % with reflux ratio of 4.69 and Q_R = 10278.1 KW, Q_C = -10916.7 KW. The pressure effect of different values is shown in Table 3.3. The positive effect of the column pressure can be seen on both the reflux ratio and the duty. However, if the column stages are higher (e.g. N_T = 60), the pressure effect will be negative. This design difference is coming from the fact that each chemical system has its own characteristics.

Table 3.3: Pressue Effect

Pressure (atm)	Conversion (%)	Reflux Ratio	Qr (KW)	Qc (KW)
1	86.5375	3.34892	7260.71	-8063.38
1.1	87.7188	3.46532	7556.88	-8336.46
1.2	88.7808	3.5978	7875.79	-8633.05
1.3	89.7458	3.74559	8217.81	-8953.44
1.4	90.6318	3.90806	8583.10	-9297.82
1.5	91.4535	4.08464	8971.75	-9666.24
1.6	92.2230	4.27487	9383.82	-10058.70
1.7	92.9499	4.47837	9819.33	-10475.30
1.8	93.6421	4.69484	10278.40	-10916.00
1.9	94.3041	4.92397	10760.70	-11380.50

3.2 Control of Binary Reactive Distillation

The control of the binary reactive distillation presented in the previous section will be discussed thoroughly. Our control study is practical based with effective industrial control methods. In general, the reactive distillation still has the main controls that are usually used for most of the distillation columns. The complexity is coming from considering the reaction conversion beside the purity of the desired products. Therefore, the selected control variables should affect both of conversion and separation. The control variables that are usually observed for any distillation column (reactive or non-reactive) are listed below:

1- The level of the column base.
2- The level of the top reservoir.
3- The column pressure.
4- The feed and products flows.
5- The composition of any component at specific point.
6- The temperatures of all sensitive stages.

The first four control variables are standard and must be under control. The composition control is not preferred because it is expensive and suffers from large time delay. The maintenance of this control is also a problem. The temperature control is widely used as alternative to the direct composition control since it is inexpensive and fast. In addition, the indirect measurement and control of the composition can be achieved via temperature control using cascade composition-temperature control. The system control will be first discussed without cascade control, then; the cascade will be added to explore its ability to hold the purity of the desired product B. There are many criteria that can be used to identify the appropriate control variable. The steady state gain matrix will be used in this study to identify which stage temperature should be controlled. The next section will discuss the steady state gain matrix that is used for temperature sensitivity analysis for identifying the stages to which we have to pay our attention.

3.2.1 Steady State Gain Matrix

Several choices for manipulation variables are available for controlling the temperatures of the sensitive stages. In our design, the reflux ratio and reboiler heat duty will be the chosen manipulated variables. They have been used effectively to hold the purity of products while driving the conversion toward the completion. The gain matrix of the temperatures can then be constructed as following:

$$
G = \begin{bmatrix}
\dfrac{\partial T_1}{\partial R_r} & \dfrac{\partial T_1}{\partial Q_r} \\
\vdots & \vdots \\
\dfrac{\partial T_i}{\partial R_r} & \dfrac{\partial T_i}{\partial R_r} \\
\vdots & \vdots \\
\dfrac{\partial T_{N_T}}{\partial R_r} & \dfrac{\partial T_{N_T}}{\partial Q_r}
\end{bmatrix}
$$

where G is the steady state gain matrix of reactive distillation temperatures, T_i is the temperature of stage i, R_r is the reflux ratio, and Q_r is the reboiler heat duty. The following steps explain how to determine the gain matrix (G) elements.

1- The simulation is run at the design values. Then, the temperatures are recorded.
2- While holding the reboiler heat duty (Q_r) at its design value, the reflux ratio (R_r) is perturbed with about 0.08% ($i.e.$ $\delta R_r = R_r - 0.0008 R_r$); then, the simulation is run again. The temperatures are subtracted from those we got from the first step to give us a column vector ($\boldsymbol{\delta T}$).
3- Dividing the column vector $\boldsymbol{\delta T}$ by δR_r will give us the first column of the gain matrix G.
4- Steps 1 to 3 are repeated by changing the reboiler heat duty to be ($\delta Q_r = Q_r - 0.0008 Q_r$) while holding the reflux ratio constant at its design value to give us the second column of the gain matrix G.

The plot of each column of the gain matrix G versus the stages number is shown in Figure 3.7 and Figure 3.8. The first graph shows the open loop gains between each stage temperature and the reflux ratio while the second graph gives us the open loop gains

between each stage temperature and with respect to the reboiler heat duty as a manipulated variable. It can be concluded that stage 29 is the most sensitive location. Negative gain between temperatures and reflux ratio are shown in the first plot. The second plot shows positive gains between temperatures and reboiler heat duty.
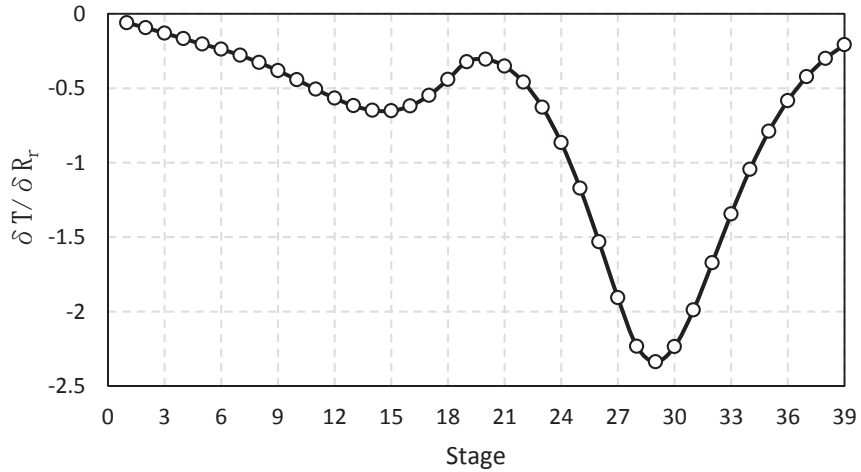
Figure 3.7: Openloop Gains between Temperatures and Reflux Ratio
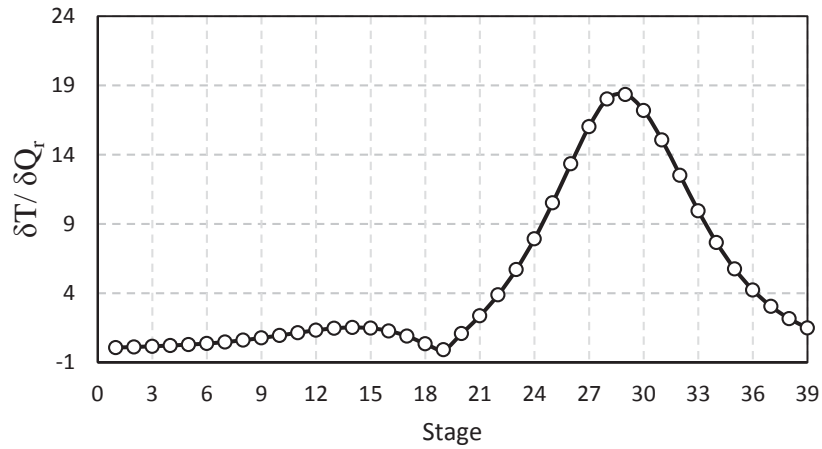
Figure 3.8: Openloop Gains between Temperatures and Reboiler Duty

43

3.2.2 Control Configuration

It is shown in the previous section that stage 29 is the most sensitive temperature stage. Therefore, the control configuration will be considering this stage. The control configuration structure is shown in Figure 3.9 which has five controls including the control of the temperature on stage 29. These controls are listed below:

1- P controller for the column base level (CBC).
2- PI controller for the feed flow (FC).
3- P controller for the accumulator level at the top (ALC).
4- PI controller for the column pressure (CPC).
5- PI controller for the stage 29 temperature (T29C).
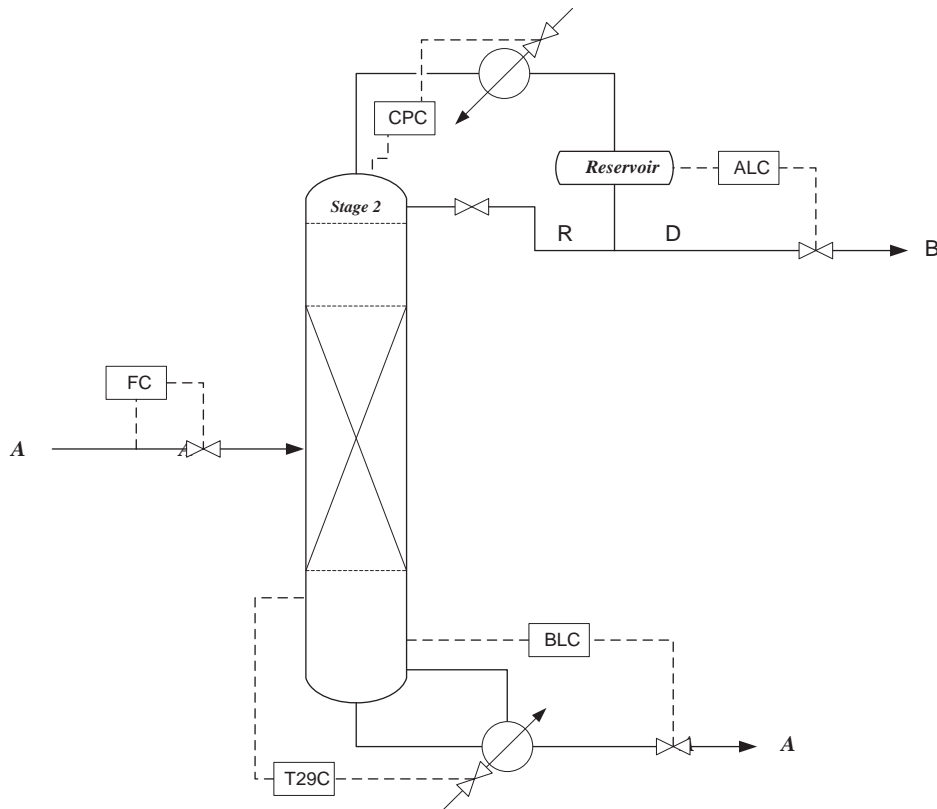
Figure 3.9: Control Configuration of Binary System without Cascade Control

The proportional controls (CBC and ALC) are used with 2.5 gains while the PI flow control is used with the conventional flow controller tuning (gain of 0.5 and integral time of 0.3). The temperature controller (T29C) was tuned using the relay-feedback method for calculating the ultimate gain and frequency. The gain and integral time is determined by Tyreus-Luyben equations as

$$K_c = \frac{K_u}{3.2} \tag{3.4}$$

$$\tau_I = 2.2\, P_u \tag{3.5}$$

After finishing the relay-feedback test, the parameters were calculated to be $K_c = 1.22$ and $\tau_I = 5.28$.

3.2.3 Control Response to Disturbances

To test the control performance, the feed flow rate was increased by 10%. The control could maintain the temperature at the steady state set point while the top product (component B) purity changed from 0.99 to 0.9872. When the feed flow rate was decreased by 10%, the controller was able to also maintain the temperature, and the top product purity changed from 0.99 to 0.9921. These responses are shown graphically via Figure 3.10. The responses of the bottoms product reflux ratio and reboiler duty are represented by Figure 3.11 and Figure 3.12, respectively. Although temperature has been kept at the set point, the purity has shifted. Other configurations have been applied such as controlling the compositions of the two products; however, they are not effective when having any disturbance being not able to keep the column at the required operation conditions.
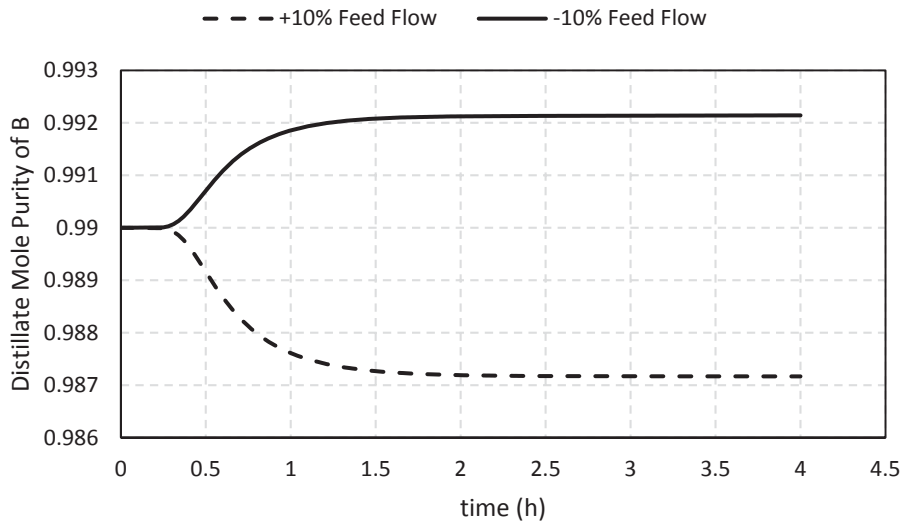
Figure 3.10: Component B Purity Response at the Top
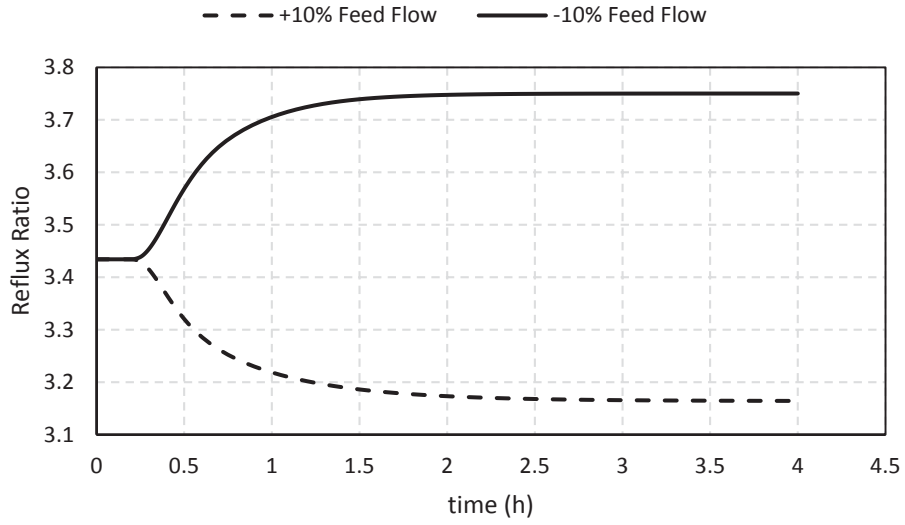
Figure 3.11: Reflux Ratio Response
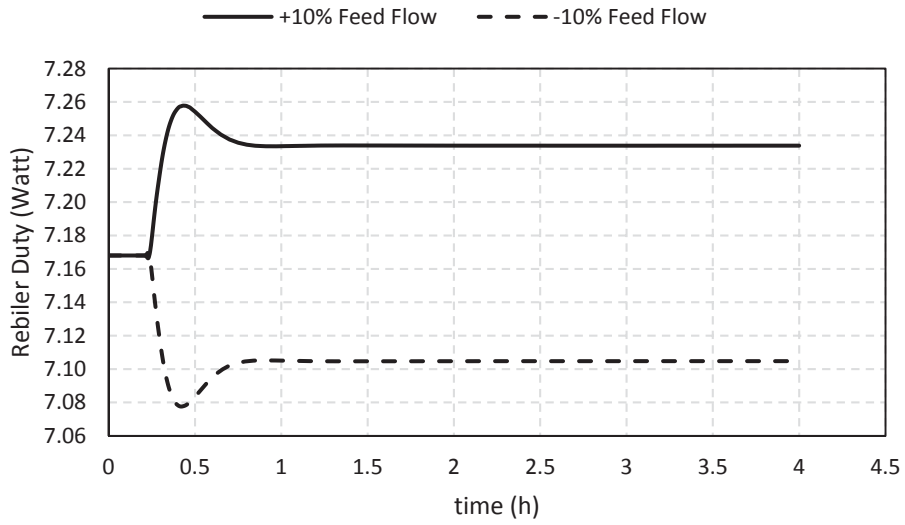
Figure 3.12: Reboiler Heat Duty Response

3.2.4 Cascade Control

Using the fast temperature control instead of the slow composition control will not hold the desired purity at the design levels as shown in Figure 3.10. The cascade control strategy will be able to meet the composition purity using the temperature control. The control configuration is represented by Figure 3.13. The main control becomes the composition control, and the output signal of this control would be the temperature reference point which is adjusted to always keep the set point of the composition control at the desired value. A relay-feedback test has to be applied on the composition control. The gain and integral time is determined by Tyreus-Luyben equations (3.4) and (3.5) to be $K_c = 5.29$ and $\tau_I = 50.16$. The disturbances +10% and -10% of the feed flow was applied. The cascade control could maintain the composition of B at the desired value. The response of the purity to the disturbances is shown by Figure 3.14, and Figure 3.15 shows the temperature behavior to both disturbances.
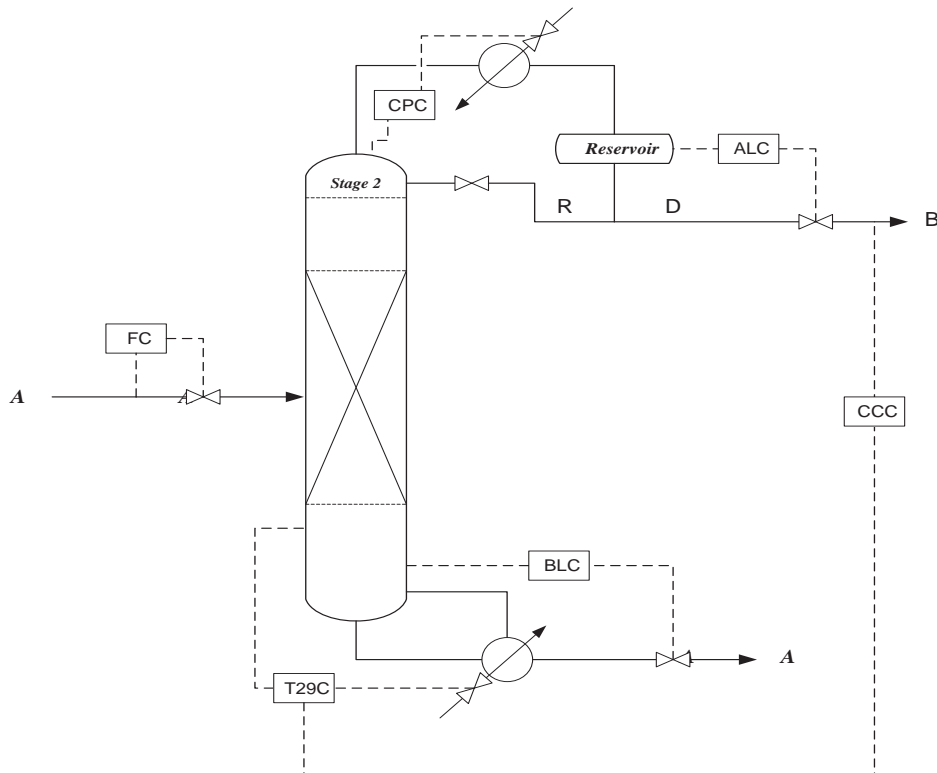
Figure 3.13: Control Configuration of Binay System with Cascade Control
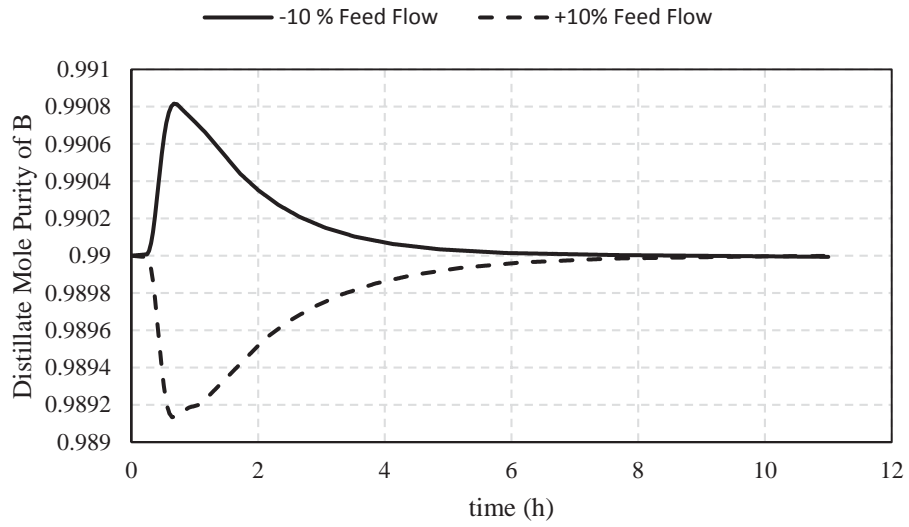
Figure 3.14: Component B Purity Response at the Top after Adding Cascade Control
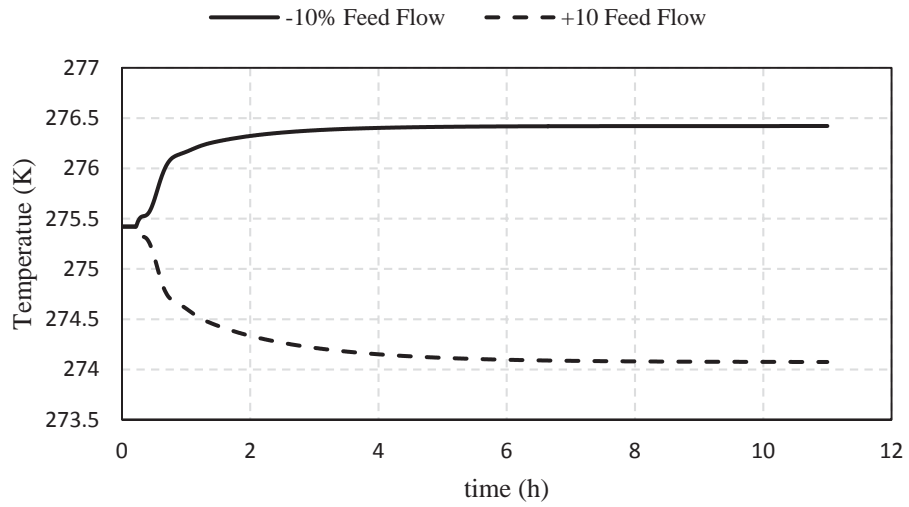
Figure 3.15: Temperature Response with Cascade Structure

3.3 Comparison between Reactive and Non-Reactive Systems

Before moving to the quaternary system, the advantage of using reactive distillation can be shown by comparing it with the conventional non-reactive distillation using the binary system under study. The design of non-reactive distillation is basically determined by the McCabe-Thiele method considering the design specifications of the reactive distillation in the previous sections. The VaxaSoftware can be used to calculate the McCabe-Thiele diagram for the non-reactive distillation as shown in Figure 3.16. This binary system is the same system presented in the previous sections of n-butane(A)/iso-butane(B) mixture at 1 atm, which follows constant molar overflow distillation condition because it is thermodynamically an ideal solution. In Figure 3.16, the McCabe-Thiele construction (based on B mole fractions) for the number of stages is obtained from a simple steady-state distillation system with saturated liquid feed, a total condenser, and a partial reboiler. For a saturated liquid feed of 20 mole % iso-butane, iso-butane distillate and bottoms compositions are 99 % and 1 %, respectively; the total number of stages for a reflux ratio of 11.7 is 39. Finally the feed is injected above stage 19 from the top of the column. For its reactive analog, as described in the above-mentioned section 3.2 that
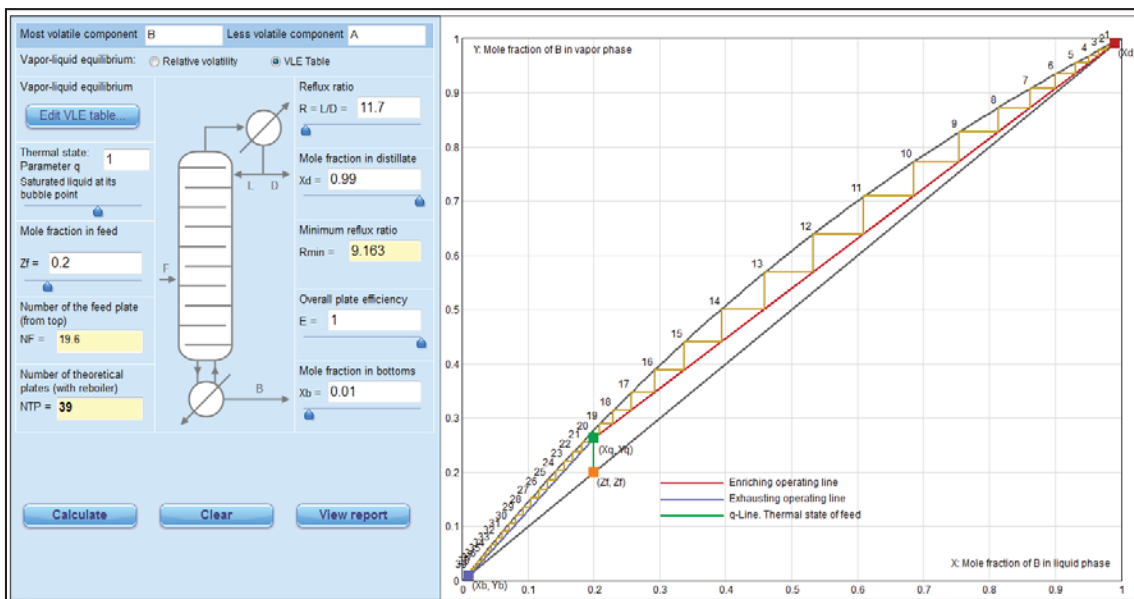
Figure 3.16: Non Reactive McCabe-Thiele diagram for a simple distillation system of iso-butane/n-butane, with compositions based on iso-butane at 1 atm

includes the isomerization of n-butane to iso-butane, the McCabe-Thiele diagram of this reactive system is shown by Figure 3.17. The reflux ratio has been lowered to 3.04 even though the feed seems to be in a suboptimal at the same stage number from the top location as that in the nonreactive analog (Figure 3.16). Note that the lowering of the reflux ratio (L/D) means that the distillate (D) yield has increased, while the internal column flows (L and V) have decreased in the reactive binary system, resulting in higher production rate with a smaller diameter column. In Figure 3.18, the optimal location of the feed at stage 27 from the top indicates an even lower reflux ratio of 2.22. This is manifested by the absence of a loop operating curve pattern around the feed stage in the diagram, in a similar way to what is shown in Figure 3.17. Another way of looking at the optimal feed location from Figure 3.17 is through its equivalent liquid composition profile diagram, as shown in Figure 3.19. The looping of the operating curve shown in Figure 3.17 is represented by local minima and maxima of component compositions around the feed stage.
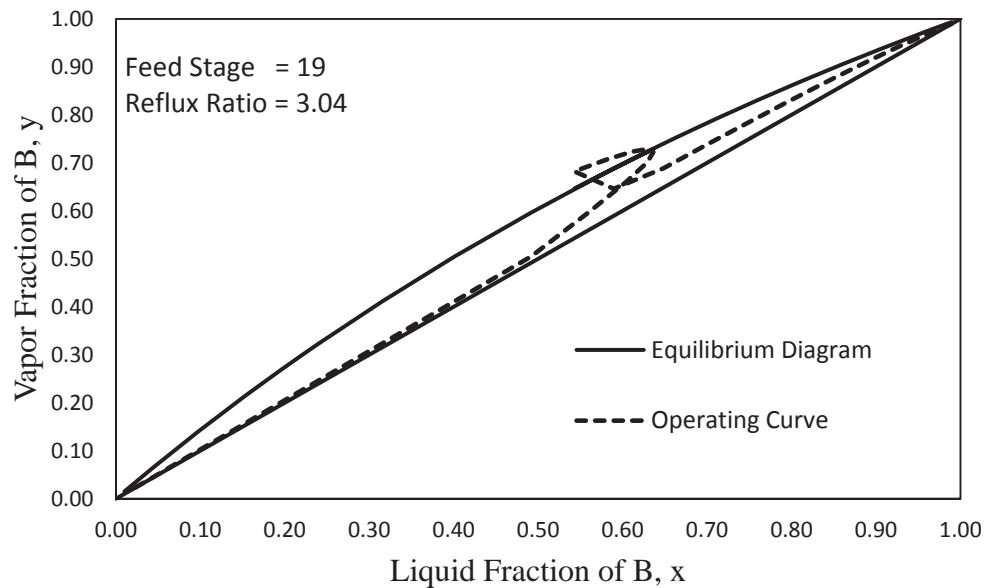
Figure 3.17: McCabe-Thiele diagram of the reactive analog of Figure 3.16 when the feed stage = 19

51

As for Figure 3.18 with optimal feed location, its column liquid composition profiles are shown in Figure 3.20, in which the profiles are monotonically behaved (i.e., no local minimum and maximum in the entire composition range). This is also represented by the behavior of four components systems as we can see in the next section of the quaternary reactive distillation. All these McCabe-Thiele and liquid composition profile plots indicate that the search for optimality in multicomponent reactive distillation systems has not be possible for all its components, based on the total cost-based optimization criterion used in this work. As shown in the literature (King, 1980), the combination of monotonic composition profiles with those containing local minima and maxima around the feed stages are found in nonreactive multicomponent systems used in industrial operations. Whether the system is a binary or a multicomponent distillation system, the reflux ratio and total number of stages can be reduced when the appropriate chemical reaction is carried out with the separation process. In future studies, other optimization criteria can be investigated which might result in monotonically behaved composition profiles for more if not all the components along the reactive column in the material system of interest in this work.
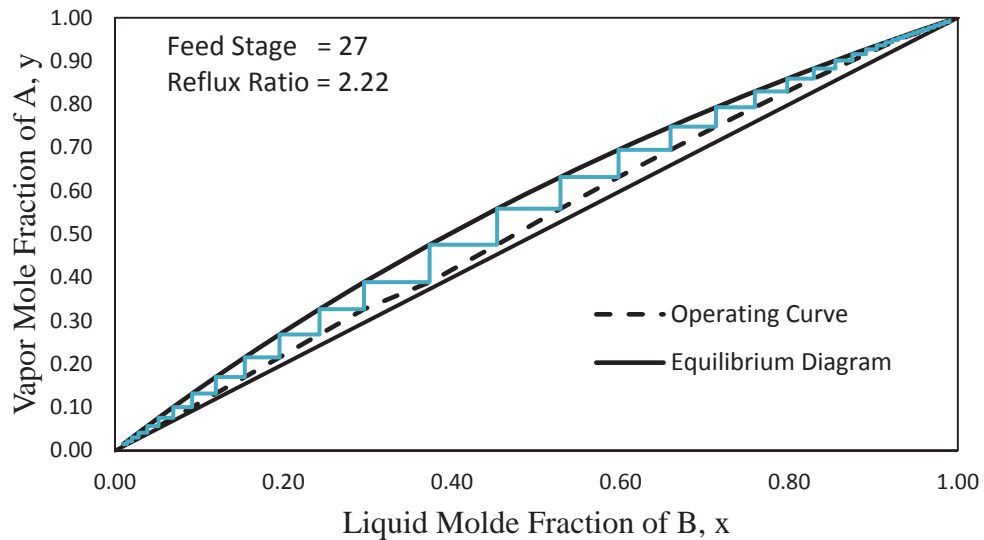
Figure 3.18: McCabe-Thiele diagram of the reactive analog of Figure 3.16 when the feed stage = 17
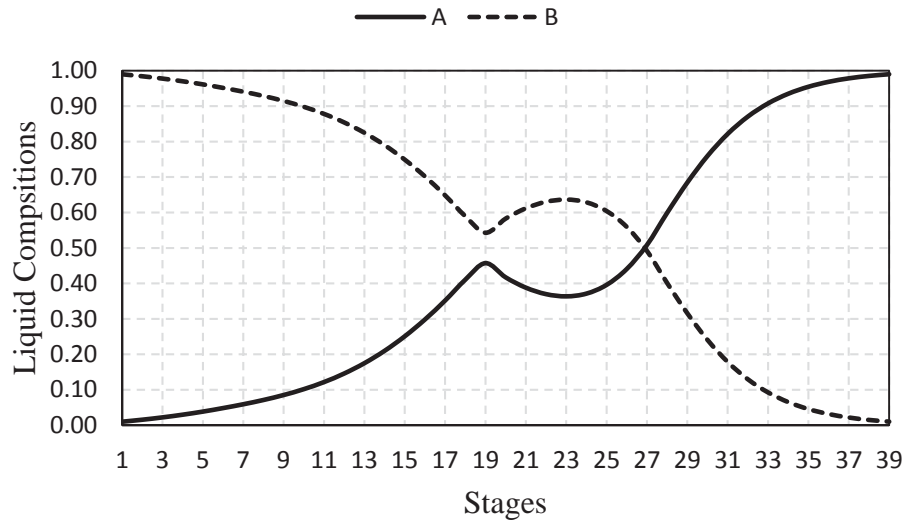
Figure 3.19: Liquid compositions profiles for the reactive binary system in Figure 3.17, where in the feed stage = 19
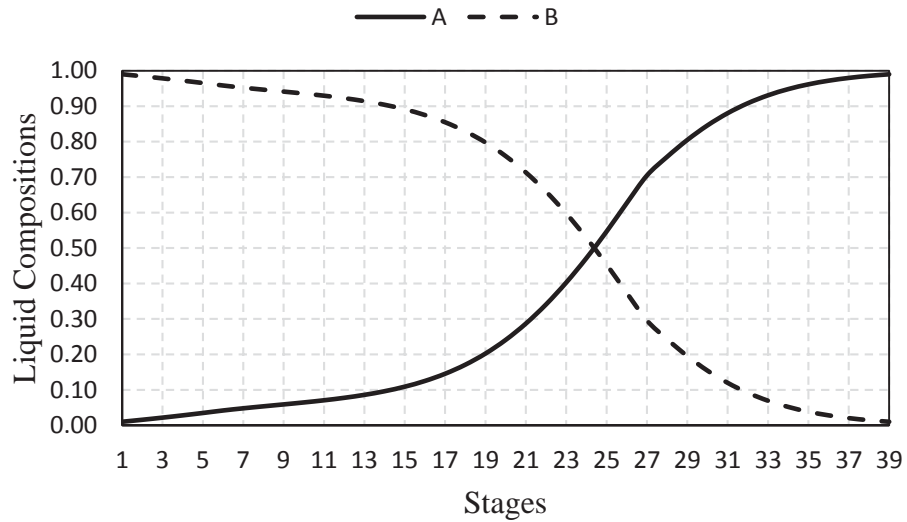
Figure 3.20: Liquid compositions profiles for the reactive binary system in Figure 4, where in the feed stage = 27

3.4 Quatenary Ideal Reactive Distillation

The quaternary ideal system have been studied thoroughly by Luyben and Yu (Luyben and Yu, 2009). The schematic diagram in Figure 3.21 defines the quaternary system. The reversible exothermic reaction of two reactants and two products is used through most of their studies. The reaction is expressed as

$$A + B \underset{k_b}{\overset{k_f}{\Longleftrightarrow}} C + D \tag{3.6}$$

The rate of reaction can be expressed using equation (2.15), so the reaction rate is expressed as

$$R_i = M_i \left(k_{f,i} \, x_{A,i} x_{B,i} - k_{b,i} \, x_{C,i} x_{D,i} \right) \tag{3.7}$$
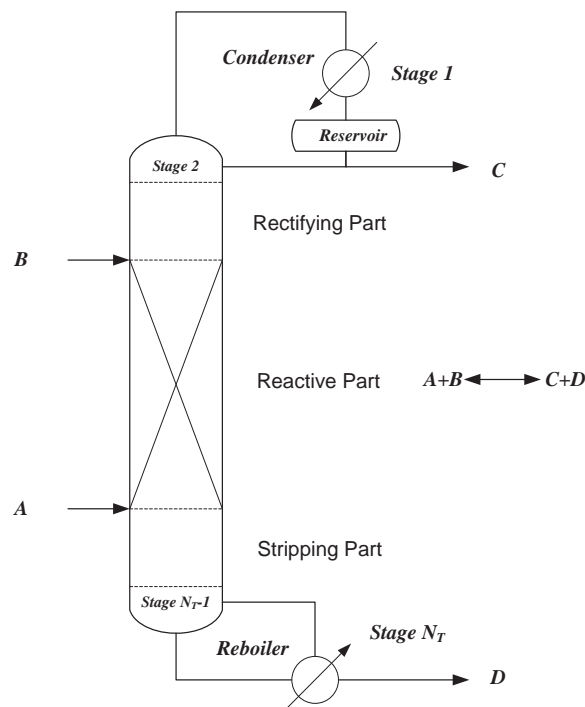
Figure 3.21: Quatenary Reactive Distilaltion

Component C has lowest boiling point while component D is the highest boiling point. Component A is lighter than B. The Antoine equation (2.13) is used for calculating the vapor compositions based on the Raoult's law (2.12). We could reproduce their results by developing MATLAB program for solving complex system of differential algebraic equations (DAEs) using built in functions that could simulate the DAEs simultaneously. Our results are based on Runge-Kutta numerical method which is more accurate than those results based on Euler numerical method. Through the next section, a brief background is presented about the DAEs.

3.4.1 Differential Algebraic Equations (DAEs)

Combining ordinary differential equations with a set of algebraic equations can be found in many engineering applications (Co, 2013). The reactive distillation is one of the physical systems that are described by a set of ordinary differential equations combined with a set of algebraic equations to yield different algebraic equations (DAEs).

The ordinary differential equations are those describing the liquid compositions at each stage of the reactive distillation. Algebraic equations are coming from vapor liquid equilibrium equations (Raoult's equation) to calculate the vapor compositions at each stage. The mathematical formulations of reactive distillation with n stages and m components can be expressed as

$$f\left(t, x, \frac{d}{dt}x, y\right) = 0 \tag{3.8}$$

where t is the time, x is $n \times m$ state variables matrix of the liquid compositions states through the column, y is $n \times m$ state variables matrix of the vapor compositions through the column. Considering the vapor liquid equilibrium at each stage, Raoult's law is applied for vapor compositions calculations to yield

$$f_{VLE}(t, x, y) \tag{3.9}$$

To formulate the DAEs system, equations (3.8) and (3.9) are combined to give

$$\begin{pmatrix} f\left(t, x, \frac{d}{dt}x, y\right) \\ f_{VLE}(t, x, y) \end{pmatrix} = F\left(t, z, \frac{d}{dt}z\right) \tag{3.10}$$

where $z = (x, y)^T$ is an extended state vector.

The above DAEs form is implemented by different solvers such as ode25s or ode23s in MATLAB. These solvers defines DAEs as mass matrix form that is

$$M(t, x)\frac{d}{dt}x = f(t, x) \tag{3.11}$$

where M is the mass matrix.

3.4.2 Steady States Simulation

The modeling of the quaternary system is based on the equilibrium stage model presented in the second chapter. The steady state can be reached using relaxation method by running the dynamic system until achieving the steady state solution (Rose et al., 1958). The assumptions made on this model are summarized below:

1- Ideal vapor liquid equilibrium.
2- Constant liquid holdups on the stages.
3- Constant liquid and vapor flow rates through the non-reactive stages. These rates are correlated in the reactive stages by adding the effect of the heat of reaction. Therefore, the following equations have been used to calculate the liquid and vapor flows through the reactive section:

$$L_i = L_{i+1} + \frac{\Delta H_R}{\Delta H_V} R_{i,comp} \tag{3.12}$$

$$V_i = V_{i+1} + \frac{\Delta H_R}{\Delta H_V} R_{i,comp} \tag{3.13}$$

To solve this complex nonlinear system, the relaxation method strategy is applied while controlling the top product purity and the column base level. Simple proportional control is used for the column base by manipulating the boilup ratio. PI control is used to hold 95% mole purity of component C at the top by manipulating the reflux ratio. It is found that the total annual cost (TAC) is minimum by holding the 95% mole purity of C at the distillate and 95% mole purity of D at the bottoms (Luyben and Yu, 2009). The composition and temperature profiles are represented by Figure 3.22 and Figure 3.23. In Figure 3.22, the reactants compositions show a maximum at the feed stages while the products show a minimum at these locations. This behavior is the same as those of components A and B in the binary system shown in Figure 3.19 in the previous section. This behavior confirms how the distribution of the components along the column would be in suboptimal way in reactive distillation systems. The required parameters for operating at steady state are listed in Table 3.4.

Table 3.4: Required Parameters for Operation at Steady State

Feed flow of A (mole/s)	12.6
Feed flow of B (mole/s)	12.6
Reflux flow (mole/s)	33.55
Rectifying stages including condenser	6
Reactive stages	9
Stripping stages including reboiler	6
Reactive Stages Holdup (mole)	1000
Stripping and Rectifying Holdup (mole)	400
Pressure (atm)	8
Conversion (%)	95

Product Purity (Mole Fraction)	Distillate	Bottoms
A	0.03	0.02
B	0.02	0.03
C	0.95	0.00
D	0.00	0.95

Kinetic Parameters	
Forward pre-exponential factor (s^{-1})	0.008
Backward pre-exponential factor (s^{-1})	0.004
Forward activation energy (cal/mole)	30000
Forward activation energy (cal/mole)	40000

Pure Component Vapor pressure $\quad \ln P_{s,i} = a_j - \dfrac{b_i}{T} \quad$ where T in K

Comp i	A	B	C	D
a	12.34	11.45	13.04	10.96
b	3862	3862	3862	3862
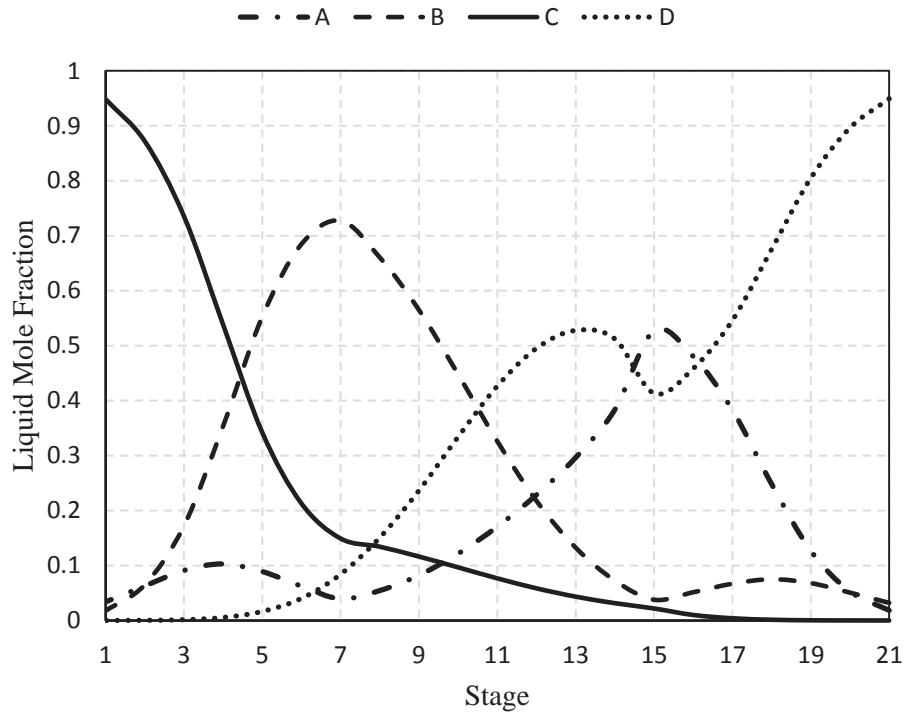
Figure 3.22: Composition Profiles of Ideal Quaternary Reactive Distillation
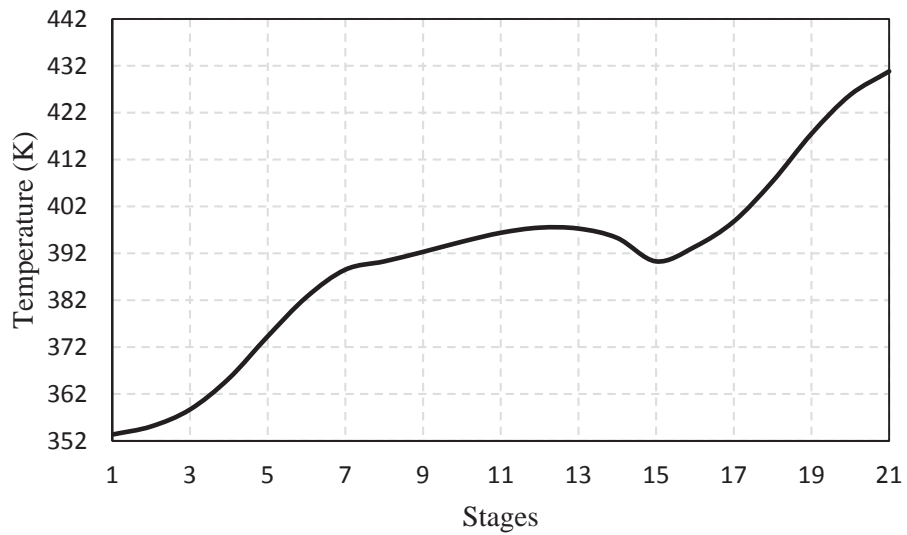
Figure 3.23: Temperature Profile of Ideal Quaternary Reactive Distillation

4. Preliminary Conceptual Design of DPC System

4.1 Process Description

As reported in the DPC production section of chapter 1, the transesterification reaction (reaction 3 in Figure 1.9) is equilibrium limited with very low equilibrium constant. The reaction can be carried out in two steps. The first step is a transesterification reaction between DMC and PhOH to the MPC and MeOH. The second step can be either reaction 2 or reaction 3 shown in Figure 4.1(Haubrock et al., 2008a). The side reactions 4 and 5 are easily carried out to produce anisole and CO_2 (Ono, 1997; Tundo et al., 1988). Since the equilibrium constant of transesterification reaction between DMC and PhOH is very low($10^{-3} - 10^{-4}$) (Fukuoka et al., 2007), this reaction is not favored from thermodynamic point of view. Therefore, it is impossible to carry out the DPC production in a closed system using this reaction. Most volatile components in reactor (which is MeOH in our case) should be continuously removed from the reactor to improve yield, and reactive distillation technology offers this capability. The continuous withdrawal of MeOH from the reactive distillation enhances the equilibrium shifting toward the desired production side increasing the yield of the wanted product. The homogeneous or heterogeneous catalysts can be used for producing diphenyl carbonate. Our references (Fukuoka et al., 2009; Fukuoka et al., 2010a) show that the real plants are using the homogeneous catalyst which restricts the reactive distillation study to consider only the rectifying and reactive sections because the reactive section will start from the catalyst feed stage down to column base removing the stripping part. The industrial production of DPC is achieved by using two consecutive reactive distillations as shown in Figure 4.2. The first column is for producing the intermediate methyl phenyl carbonate (MPC) which is fed to the second column to yield the final product (DPC). It is claimed that this configuration is mandatory because carrying the two reaction steps in one column will cause economic and operations problems. Our study will focus on one column to explore the reactions and separation limitations via feasibility analysis. We have proposed different control configuration to achieve as much productivity and purity as possible by just using one reactive distillation column.
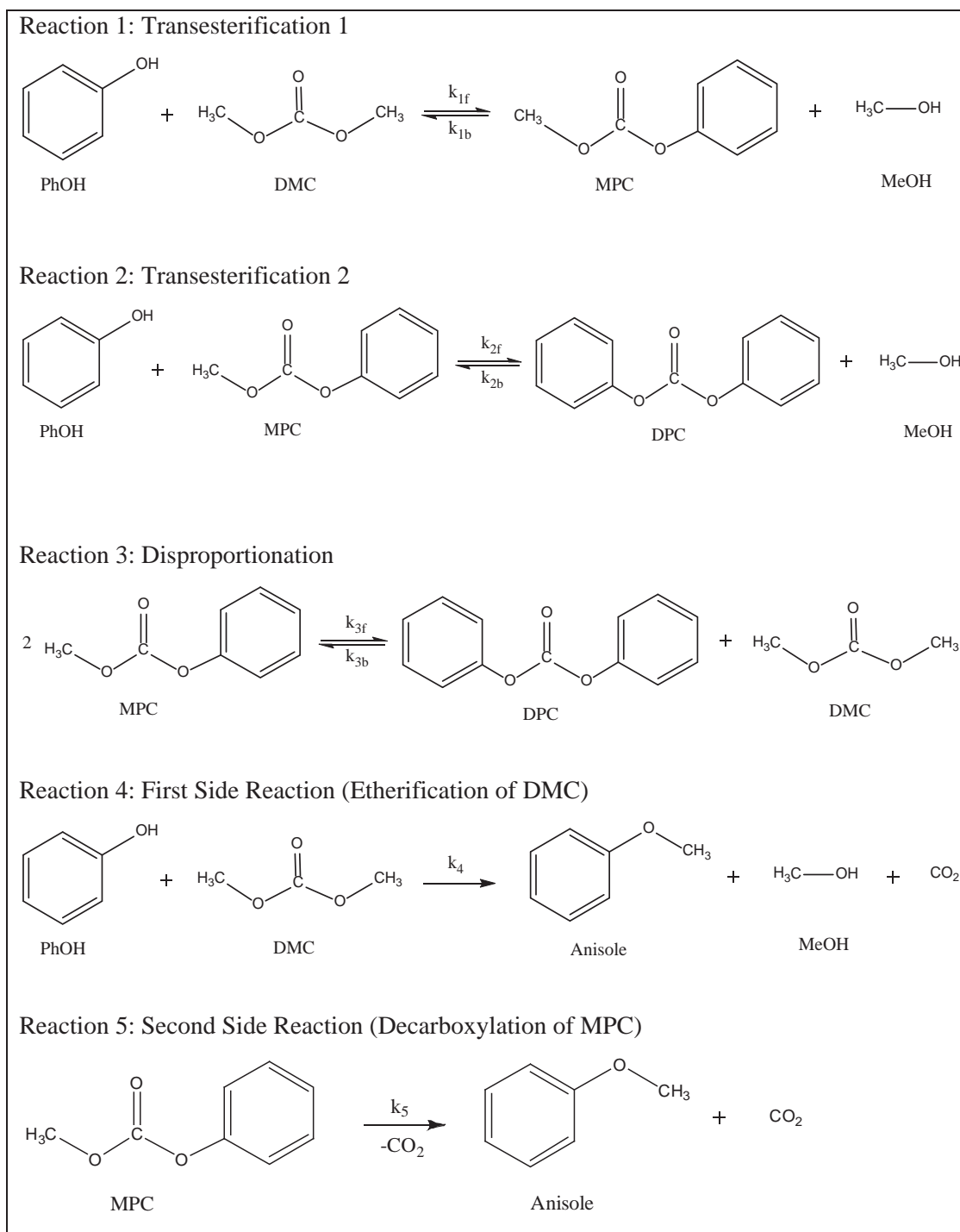
Figure 4.1: Reactions of Diphenyl Carbonate Production Process
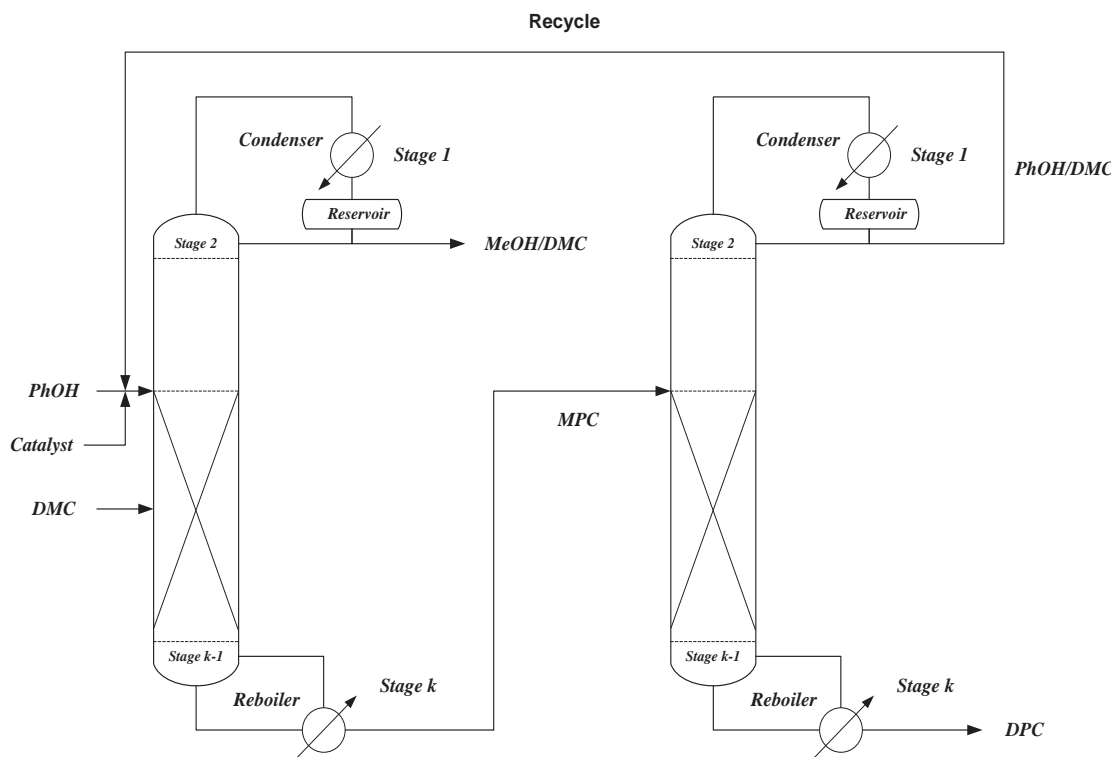
Figure 4.2: Consecutive Reactive Distillations for DPC Production

To investigate other constraints of the DPC process, an azeotropic study was performed using the residue curve maps (RCMs). In the next section, dynamic mathematical models for non-reactive and reactive systems are presented, which have been used to generate the RCMs in order to identify azeotropes involved in the DPC chemical system.

4.2 Residue curve maps

Residue curve maps (RCMs) are multiple trajectories which describe the dynamic behavior of the liquid compositions of a mixture while the vapor is formed and removed from a simple flash distillation shown in Figure 4.3.
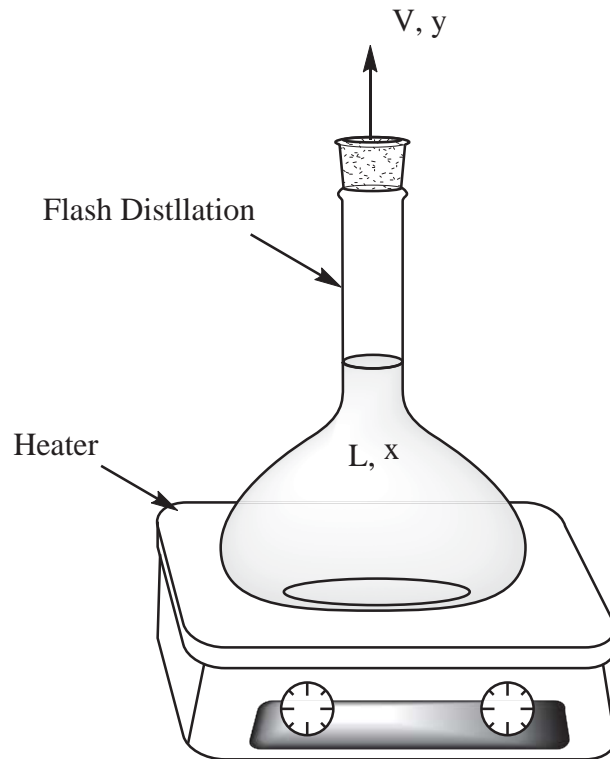
Figure 4.3: Simple Flash Distillation

The RCMs method has been used to determine the existence of azeotrope for the design of the conventional distillation process. The azeotrope is the point where the liquid compositions equal to the vapor compositions. At this point, no separation can be achieved, representing what is called "distillation boundary". RCMs have also been found to be useful for the design of reactive distillation systems by observing new reactive azeotropes that appear after the inclusion of reaction kinetics. A complete information about this topic have been documented by Doherty and Malone (Doherty and Malone, 2001).

4.3 RCMs Mathematical Models

By simulating the mass balance ordinary differential equation of the simple flash distillation, the RCMs can be generated using thermodynamic and physical parameters of a specific chemical system. Phase equilibria equations are required for equilibrium compositions calculations. The mass balance of the simple flash distillation shown in Figure 4.3 can be expressed for component i as follows

$$\frac{dL}{dt} = -V \tag{4.1}$$

$$L\frac{dx_i}{dt} + x_i\frac{dL}{dt} = -Vy_i \tag{4.2}$$

where L is the liquid residual in the flash, x_i is the liquid composition of component i, V is the vapor flow removed from the still, and y_i is the vapor composition of component i. From equations (4.1) and (4.2), the a *non reactive RCMs model* can be derived to become (Doherty and Perkins, 1978):

$$\frac{dx_i}{d\tau} = x_i - y_i \qquad i = 1, \dots, N_c - 1 \tag{4.3}$$

where τ is a dimensionless time. From equations (4.3) and (4.1), the expression for defining τ can be found as

$$d\tau = \frac{V}{L}\,dt \tag{4.4}$$

For more details about the mathematical derivation, the reader should go through the pioneering article by Doherty and Perkins (Doherty and Perkins, 1978). The non reactive model given in (4.3) has been extended to account the reactions taken place in the chemical mixtures system (Barbosa and Doherty, 1988).

A complex reactive flash distillation system would be the new case after adding the chemical reaction to the normal flash distillation resulting in different observations. Further more studies have been done taken into consideration the mixtures with multiple chemical reactions (Ung and Doherty, 1995a; Ung and Doherty, 1995b). Therefore, the reactive model of the system shown in Figure 4.3 can be derived starting from the mass balance considering the reactions taking place in the system. In the case of chemical equilibrium, the rate of these reactions is assumed to be infinitely fast. Thus, the mass balance for component i can be written as:

$$\frac{dL}{dt} = -V + \sum_{k=1}^{N_r} \sum_{i=1}^{N_c} v_{i,k} r_k L \tag{4.5}$$

$$\frac{dLx_i}{dt} = -Vy_i + \sum_{k=1}^{N_r} v_{i,k} r_k L \tag{4.6}$$

where N_r is the number of reactions, N_c is the number of components, $v_{i,k}$ is the moles of component i in reaction k, and r_k is the rate of reaction k. In case of equilibrium reactive distillation, the equilibrium is assumed to be continuous through time for both phase and reactions. To simplify equation (4.6) even more for N_r independent reactions, the transformed compositions have been introduced by Ung and Doherty as:

$$X_i = \frac{x_i - \boldsymbol{v}_i^T (\boldsymbol{v}_{ref})^{-1} \boldsymbol{x}_{ref}}{1 - \boldsymbol{v}_{tot}^T (\boldsymbol{v}_{ref})^{-1} \boldsymbol{x}_{ref}} \tag{4.7}$$

$$Y_i = \frac{y_i - \boldsymbol{v}_i^T (\boldsymbol{v}_{ref})^{-1} \boldsymbol{y}_{ref}}{1 - \boldsymbol{v}_{tot}^T (\boldsymbol{v}_{ref})^{-1} \boldsymbol{y}_{ref}} \tag{4.8}$$

where ν_i^T is a vector of the stoichiometric coefficients of component i in the considered reactions, ν_{ref} is square matrix of the N_r stoichiometric coefficients for N_r reference components in the considered independent N_r reactions, x_{ref} is a vector of the liquid compositions of N_r reference components, ν_{tot}^T is a vector of the sum of the stoichiometric coefficients for each reaction, and y_{ref} is a vector of the vapor compositions of N_r reference components. Equations (4.7) and (4.8) are subject to the following constrains:

$$\sum_{i=1}^{N_c-N_r} X_i = \sum_{i=1}^{N_c-N_r} Y_i = 1 \tag{4.9}$$

Taking the transformed compositions into account and substituted to (4.5) and (4.6), the equilibrium reactive RCMs model has been derived (Ung and Doherty, 1995a; Ung and Doherty, 1995c) to be:

$$\frac{dX_i}{d\tau} = X_i - Y_i \qquad i = 1, \dots, N_c - R - 1 \tag{4.10}$$

where τ is a dimensionless time having different definition from that presented in the non reactive RCMs (i.e. equation (4.3)). Because of the transformed compositions variables, the dimensionless time in equation (4.10) has been defined by:

$$d\tau = \frac{V}{L}\left(\frac{y_i - \boldsymbol{\nu}_{tot}^T(\boldsymbol{\nu}_{ref})^{-1}\boldsymbol{y}_{ref}}{1 - \boldsymbol{\nu}_{tot}^T(\boldsymbol{\nu}_{ref})^{-1}\boldsymbol{y}_{ref}}\right)dt \tag{4.11}$$

At this point, the difference between non reactive model represented by equation (4.3) and the reactive model represented by equation (4.10) should be understood. The liquid and vapor compositions are related to each other by only phase equilibria in the non reactive model while the transformed liquid and vapor compositions relationship is based on the phase and reaction equilibria. These relationships are formulated based on the

66

thermodynamic and kinetic concepts that will be discussed in the next section. Before going through these concepts, we should present another reactive RCMs model that is kinetically controlled in order to overcome the reaction equilibrium over wide range of the process time. From equations (4.5) and (4.6), the kinetic controlled model is

$$L\frac{dx_i}{dt} + x_i\left(-V + \sum_{k=1}^{N_r}\sum_{i=1}^{N_c} v_{i,k}r_kL\right) = -Vy_i + \sum_{k=1}^{N_r} v_{i,k}r_kL \qquad (4.12)$$

By arranging equation (4.12), the final form of the kinetic controlled reactive RCMs can be formulated as:

$$\frac{dx_i}{d\tau} = x_i - y_i + \frac{L}{V}\left(\sum_{k=1}^{N_r} v_{i,k}r_k - x_i\sum_{k=1}^{N_r}\sum_{i=1}^{N_c} v_{i,k}r_k\right) \qquad (4.13)$$

To solve equation (4.13), further modification is needed because L/V still unknown quantity. The Damkohler number is a dimensionless parameter expressed by dividing the timescale of the reaction by the transport phenomena time scale. This number has been used in the model shown by equation (4.13) to fix the L/V problem (Venimadhavan et al., 1994). The effect of this number in the reactive distillation systems also have investigated by Doherty and his coworkers (Doherty and Malone, 2001; Rev, 1994; Thiel et al., 1997) which is expressed by

$$Da = \frac{L_0\,k_{ref}}{V_0} \qquad (4.14)$$

By substituting equation (4.14) into (4.13), we can end with the following form:

$$\frac{dx_i}{d\tau} = x_i - y_i + \frac{Da}{k_{ref}} \frac{L}{L_0} \frac{V_0}{V} \left(\sum_{k=1}^{N_r} v_{i,k} r_k - x_i \sum_{k=1}^{N_r} \sum_{i=1}^{N_c} v_{i,k} r_k \right) \begin{cases} i = 1, ..., N_c - 1 \\ k = 1, ..., N_r \end{cases} \quad (4.15)$$

The model in (4.15) represents the kinetically controlled reactive RCMs model that is relates the liquid and vapor compositions via phase equilibria and reactions kinetics. In this model, the quantity of $\frac{L}{L_0}$ has been calculated by combining equations (4.1) and (4.4) to yield (Venimadhavan et al., 1994)

$$\frac{dL}{d\tau} = -L \quad (4.16)$$

Analytically, the below solution of equation (4.16) could be found with considering the initial condition H_0 at $\tau = 0$

$$\frac{L}{L_0} = e^{-\tau} \quad (4.17)$$

Also, they reported two approaches of representing the term $\frac{V}{V_0}$ which reflects the rate of heating control. The first one is when $\frac{V}{V_0} = \frac{L}{L_0}$ resulting in equation (4.15) to be time invariant while the second one is by setting $V = V_0$ meaning a constant supply of the heat resulting in equation (4.15) to be time variant model. In summary, the three different models have been presented for residue curve maps calculations. To solve these models, we need to add the phase equilibria model to relate the liquid composition with the vapor composition. Also, we need to add the kinetics expressions to represent the rate of reactions value as a function of the liquid compositions. Through the following section, the thermodynamic phase equilibrium will be presented, and the following section will represent the reactions kinetics of the chemical system under study.

4.4 Thermodynamic Activity Model

It is essential to use some of the activity coefficients models (UNIQUAC, UNIFAC, Wilson, or NRTL) to account for the non ideal behavior of the liquid phase within the system. As for the vapor phase, it is assumed to be ideal; otherwise, one of the equations of states should be considered to calculate the deviation parameter (vapor fugacity coefficient) from the ideal situation. The advantage of using UNIFAC comes when VLE experimental data are not available. UNIFAC is a group contribution method used predict the activity coefficients in liquid mixtures (Fredenslund et al., 1975). The UNIFAC model is based on the UNIQUAC one unless the later is based on the binary interaction parameter between each two different molecules within the mixture while UNIFAC is based on the interaction parameters between the different functional groups which are used to build the structure of the mixture components. For a chemical mixture system, the UNIFAC model to predict the activity coefficient has been reported to be (Fredenslund et al., 1975):

$$\ln \gamma_i = \underset{combinatorial}{\ln \gamma_i^C} + \underset{residual}{\ln \gamma_i^R} \tag{4.18}$$

where

$$\ln \gamma_i^C = \ln \frac{\phi_i}{x_i} + \frac{z}{2} q_i \ln \frac{\theta_i}{\phi_i} + l_i - \frac{\phi_i}{x_i} \sum_j x_j \, l_j$$

$$l_i = \frac{z}{2}(r_i - q_i) - (r_i - 1); \quad z = 10$$

$$r_i = \sum_k v_k^i R_k; \quad q_i = \sum_k v_k^i Q_k$$

$$\theta_i = \frac{q_i x_i}{\sum_j q_j \, x_j}; \quad \phi_i = \frac{r_i x_i}{\sum_j r_j \, x_j}$$

while

$$\ln \gamma_i^R = \sum_k v_k^i \left(\ln \Gamma_k - \ln \Gamma_k^i \right)$$

where $\ln \Gamma_k$ and $\ln \Gamma_k^i$ can be calculated using the following expression:

$$\ln \Gamma_k = Q_k \left[1 - \ln \left(\sum_m \theta_m \psi_{mk} \right) - \sum_m \frac{\theta_m \psi_{km}}{\sum_n \theta_n \psi_{nm}} \right]$$

$$\theta_m = \frac{X_m Q_m}{\sum_n X_n Q_n}; \qquad \psi_{mn} = \exp \left(-\frac{a_{mn}}{T} \right)$$

where $i, j, and\ k$ are the indices of components, $m, n, and\ k$ are indices of groups, ϕ_i is the segment fraction of component i, x_i is the liquid mole fraction, z is a coordination number equal to 10, q_i area parameter of component i, θ_i is the area fraction of component i, r_i is the volume parameter of component i, v_k^i is the number of k groups in component i, Γ_k is the residual activity coefficient of group k, Γ_k^i is the residual activity coefficient of group k in a reference solution of component i, Q_k is the area parameter of group k, R_k is the volume parameter of group k, ψ_{mn} is the group interaction parameter between m and n, a_{mn} is the interaction energy between m and n. The DPC production reactions shown in Figure 4.1 have been studied experimentally from thermodynamic point of view (Haubrock et al., 2008a). The reaction equilibrium coefficients have been presented in term of activities and mole fractions, and the activity based equilibrium constants have been reported. To correct the liquid phase non ideality, UNIFAC activity coefficient model presented above have been considered to calculate the activity coefficient (γ) (Haubrock et al., 2008a).

4.5 Reactions Kinetics

To solve RCMs models, we also need to include the appropriate reaction rate expression for each reaction. Since the reaction is assumed to be in the liquid phase, the rate of reaction expression should be based on the activity coefficient. As an extension to the thermodynamics work presented in the previous section, the same group bed by Haubrock have been able to publish the reactions kinetics parameters and model (Haubrock et al., 2008b). The rates of the three reactions can be represented by the following relations:

$$R_1 = k_1 x_{cat} \left(\gamma_{PhOH} x_{PhOH} \gamma_{DMC} x_{DMC} - \frac{\gamma_{MPC} x_{MPC} \gamma_{MeOH} x_{MeOH}}{K_{A,1}} \right) \qquad (4.19)$$

$$R_2 = k_2 x_{cat} \left(\gamma_{PhOH} x_{PhOH} \gamma_{MePC} x_{MePC} - \frac{\gamma_{DPC} x_{DPC} \gamma_{MeOH} x_{MeOH}}{K_{A,2}} \right) \qquad (4.20)$$

$$R_3 = k_3 x_{cat} \left(\gamma_{MPC}^2 x_{MPC}^2 - \frac{\gamma_{DPC} x_{DPC} \gamma_{DMC} x_{DMC}}{K_{A,3}} \right) \qquad (4.21)$$

The symbol γ_i is referred to the activity coefficient of the relevant component i while x denotes the mole fraction of the relevant component. The x_{cat} is molar fraction amount of catalyst. The equation of equilibrium constants based on activity is tabulated with its parameters in Table 4.1.

Table 4.1: Equilibrium Constants Data

$\ln K_{A,i} = A + \dfrac{B}{T}$ where T in K		
$i = 1$	$i = 2$	$i = 3$
A	82.718	95.444	58.033
B	-6904.5	-10113	-5991.3

The rates constant k_{jf} for each forward reaction j can be calculated by Arrhenius equation which is tabulated with its necessary data in Table 4.2.

Table 4.2: Arrhenius Equation Data of Forward Reactions

$k_{jf} = k_{0,jf} \exp\left(-\dfrac{E_{A,jf}}{R_{gas}T}\right)$		
j	$k_{0,jf}$ [s^{-1}]	$E_{A,jf}$ [kJ/mole]
1	2.42E+8	73.50
2	6.61E+6	59.90
3	14.88	--

Using Table 4.1 and Table 4.2, the rate constant k_{jb} for the backward reactions is tabulated with its necessary data in

Table 4.3: Arrhenius Equation Data of Backward Reactions

$k_{jb} = k_{0,jb} \exp\left(-\dfrac{E_{A,jb}}{R_{gas}T}\right)$		
j	$k_{0,jb}$ [s^{-1}]	$E_{A,jb}$ [kJ/mole]
1	2.42E+8	73.50
2	6.61E+6	59.90
3	14.88	--

4.6 RCMs Results

The azeotropes can be attained using Aspen Plus. Besides the pure components, the system has one binary azeotrope between MeOH and DMC at 337.18 K with mole fractions of 0.8507 and 0.1493 for MeOH and DMC, respectively. The pure components are all saddle points except the DPC component which is stable node. The binary azeotrope of MeOH and DMC is shown to be unstable node. We could reproduce these results by solving (4.3) numerically using DAEs technique solver available in MATALB. The mixture of MeOH-DMC-PhOH-MPC is considered. The RCM of the non-reactive case is represented by Figure 4.4.
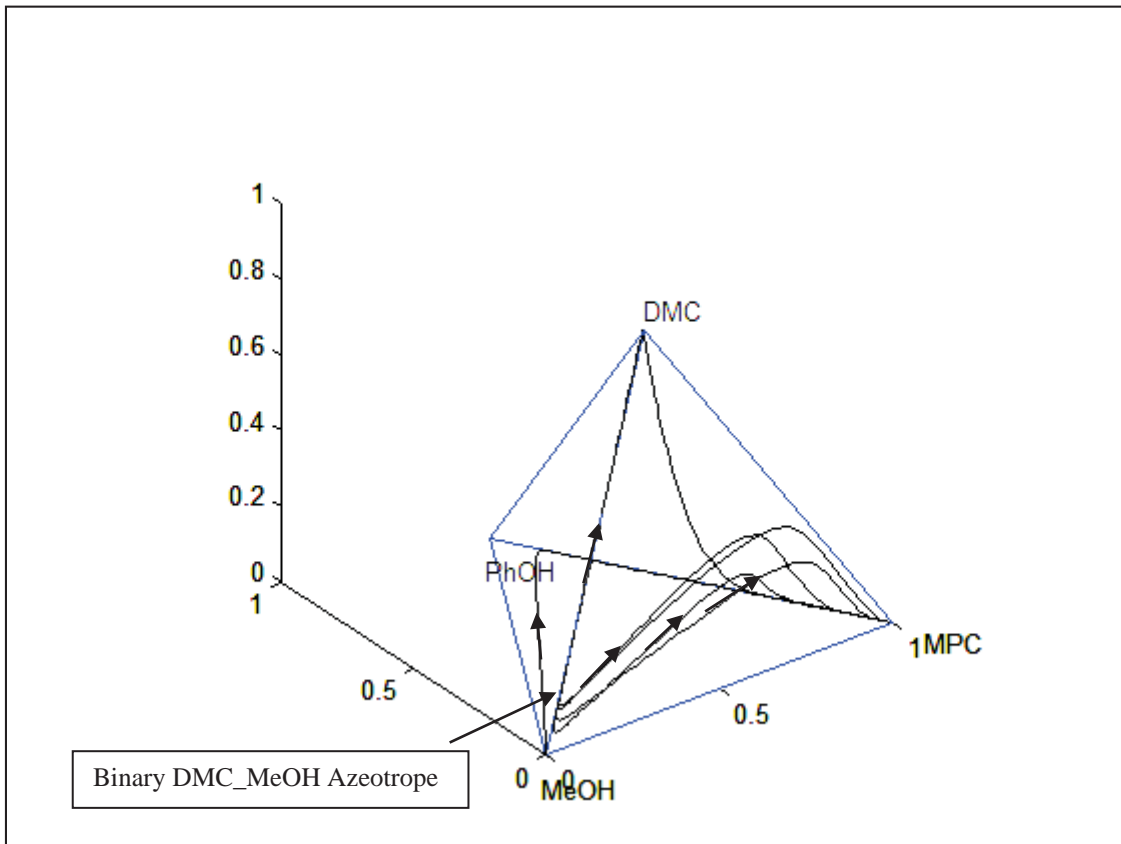
Figure 4.4: Non-Reactive RCM for the System MeOH-DMC-PhOH-MPC

On the other hand, the equilibrium reactive RCM has been generated by solving equation (4.10) which shows that the binary azeotrope is affected by moving its location to another different point called binary reactive azeotrope as shown by Figure 4.5. Based on the starting composition, the RCMs start from the binary reactive azeotrope to end in a pure MPC. Although it is still one distillation region we have, the azeotropic mixture could not be removed totally from the system. This means that the azeotropic mixtures coming from the top of the reactive distillation has to be treated using different column. However, this will not affect the purity on the bottoms of the column because the azeotropic mixture is shifted up during the process time leaving the high boiling MPC that is used directly to produce our main product (DPC).
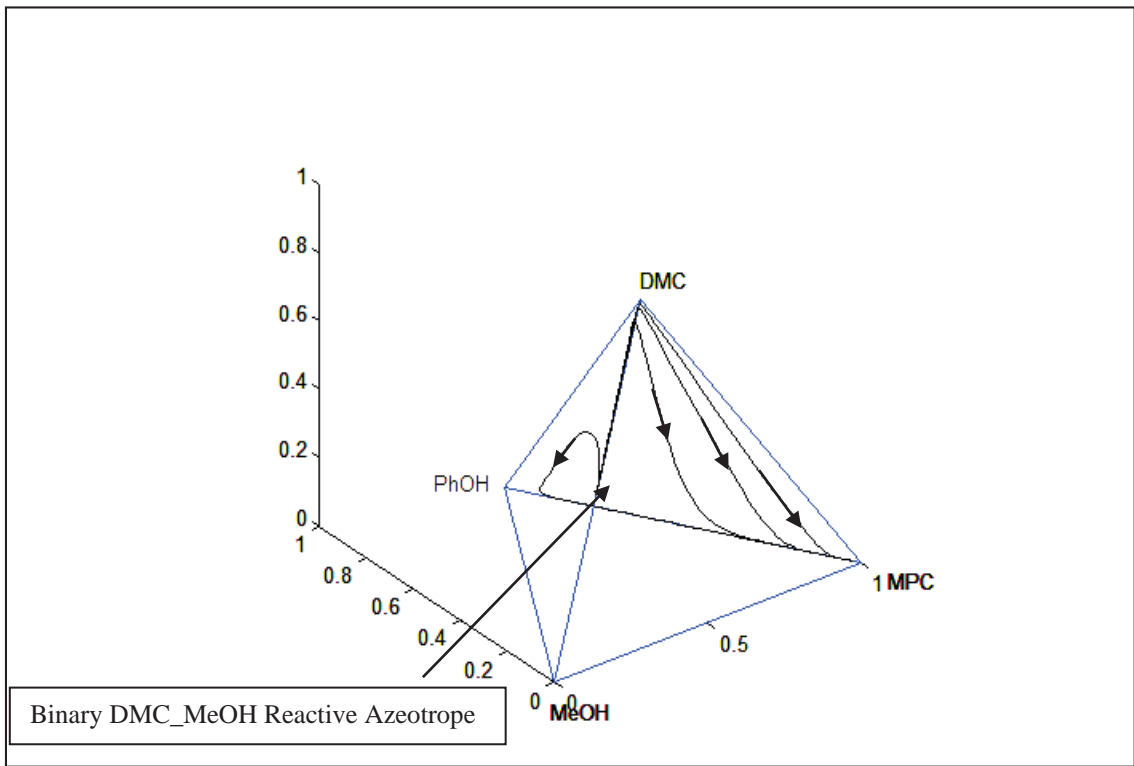
Figure 4.5: Equilibrium Reactive RCM

74

5. Steady State and Control of DPC System

To start the steady state simulation and analysis of DPC system, the design procedure of this system is a pre-step that should be considered. Our design will be based on optimizing the yield and purity while observing the total annual cost (TAC). From the design step, the physical equipments sizes and its optimal operation conditions would be determined based on the required specifications of the final product. An initial guess of the design variables still would be crucial in the design study until meeting the specifications of our product. In the next section, a preliminary design procedure of DPC system is presented.

5.1 Background

As for the system under study (DPC), the overall reaction is considered by Tung and Yu (Luyben and Yu, 2009; Tung and Yu, 2007). By just taking the net reaction, it would be the easiest way to idealize the DPC complex reactions. Therefore, by assuming no side reactions, the overall reaction with heterogeneous catalyst can be net as

$$DMC + 2PhOH \leftrightarrow DPC + 2MeOH$$
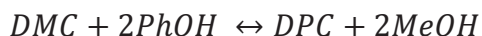
Based on the boiling points of the components in the above reaction, the lightest key is the methanol (MeOH) while diphenyl carbonate (DPC) is the heaviest key. The dimethyl carbonate is lighter than phenol. Ignoring the reality of the chemical system, this ideal system would be appropriate for reactive distillation because the lightest and heaviest components are the desired products. As we can see in the next sections, the non ideal case of this system is extremely different from the ideal one; however, it would be instructive to go first through this ideal case. Based on the available and hypothetic data they had as in Table 5.1, we could reproduce their results using our MATLAB code that have been developed for quaternary system in chapter 3. We believe that the slight difference between our results and their ones is coming from the numerical method. However, the difference still minor, and generally the results agree to each other. The compositions and temperature profiles are shown in Figure 5.1, and Figure 5.2, respectively.

Table 5.1: The Required Parameters for Ideal DPC Simulation

Feed flow of A at Stage 11 (mole/s)	12.6
Feed flow of B at Stage 16 (mole/s)	12.6
Reflux flow (mole/s)	33.55
Rectifying stages including condenser	5
Reactive stages	16
Stripping stages including reboiler	5
Stages Holdup (mole)	1110
Pressure (atm)	7
Conversion (%)	95

Product Purity (Mole Fraction)	Distillate	Bottoms
A	0.045	0.005
B	0.005	0.045
C	0.950	0.000
D	0.000	0.950

Kinetic Parameters	
Forward pre-exponential factor (s^{-1})	0.008
Backward pre-exponential factor (s^{-1})	0.004
Forward activation energy (cal/mole)	12000
Forward activation energy (cal/mole)	17000
Heat of Reaction (cal/mole)	-5000
Heat of Vaporization (cal/mole)	6944

Pure Component Vapor pressure $\quad \ln P_{s,i} = a_j - \dfrac{b_i}{T} \quad$ **where T in K**

Comp i	DMC	PhOH	MeOH	DPC
a	12.34	11.45	13.04	10.96
b	3862	3862	3862	3862
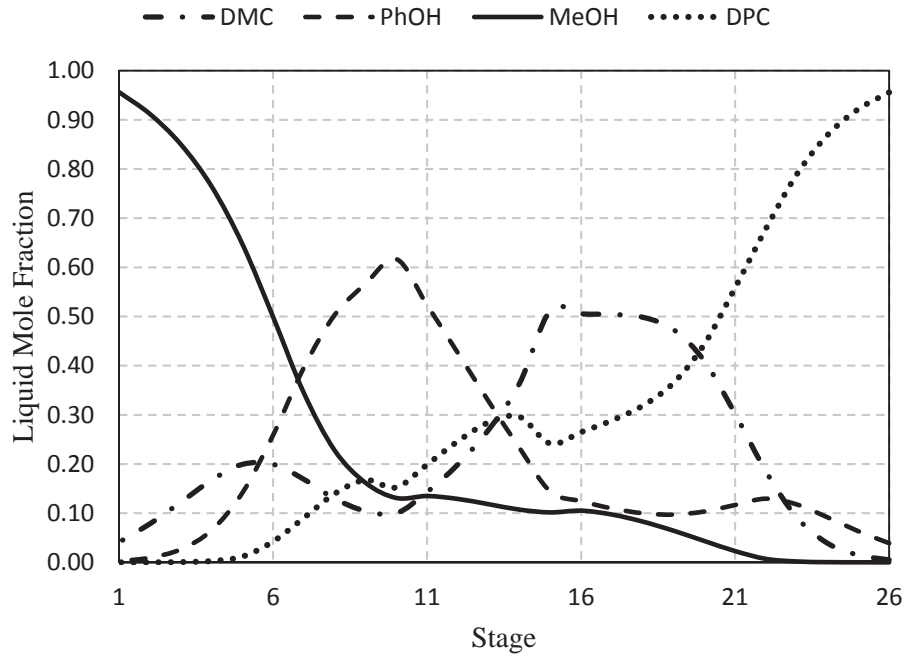
Figure 5.1: Ideal DPC Composition Profiles
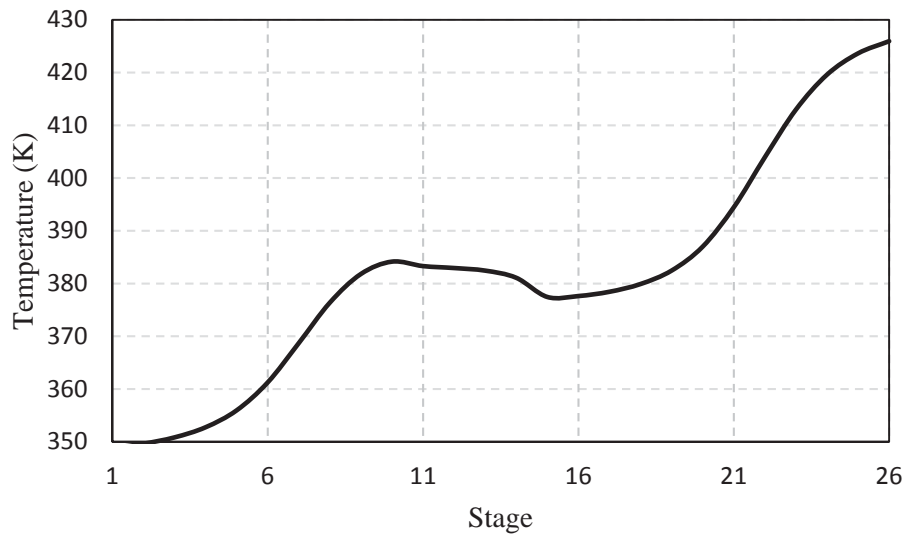
Figure 5.2: Temperature Profile of Ideal DPC System

5.2 Preliminary Design of DPC System

Since we are dealing with a homogeneous system, the reactive distillation of the real system study will be different from the ideal system we presented in the third chapter. The ideal system is based on assuming heterogeneous catalyst so that it would be possible to divide the column into three different sections (rectifying, reactive and stripping). This is not true for the real system that is fed with homogeneous catalyst because the liquid including the catalyst is flowing down from the upper feed stage till the end of the column. Therefore, the reactive distillation configuration of the real DPC system consists of only two sections. The upper part of the column is for the rectifying process while the lower part will be for the reactive process as illustrated by Figure 5.3. The design procedure of this study can be extended based on the optimization complexity used for the design. This complex optimization is beyond this dissertation. The following are some possible variables that can be used to optimize the yield or/and the cost of the DPC system:

1- The number of the reactive stages (N_{rx}).
2- The number of the rectifying stages (N_r).
3- The upper feed location.
4- The lower feed location.
5- The boilup ratio.
6- The reflux ratio.
7- The two feeds flow ratio.
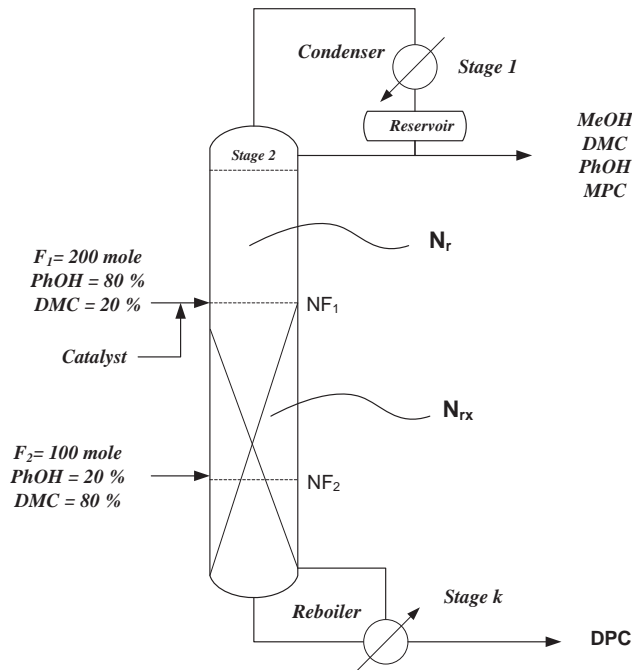
Figure 5.3: Real DPC System

Preliminary Design Procedures:

The following steps can be used to explore the effect of different variables on the yield of DPC while observing the column cost.

1- The pressure is fixed at 1 atm.
2- The catalyst amount is fixed so that its concentration would be constant at 200 ppm which would be sufficient to drive the reaction conversion toward the product side.
3- The total number of stages is guessed to be 74.
4- The number of reactive stages (N_{rx}) is guessed to be 70 so that the good conversion can be achieved. This means the number of the rectifying stages is 4.

5- The upper feed is located at the first reactive stage.

6- The catalyst is fed at the first reactive stage.

7- The lower feed (F_2) is located at stage 65.

8- The steady state simulation is run while controlling the composition of the required chemical (DPC) to reach mole purity of 99.5%

9- The reflux ratio is changed until the maximum yield is found. It is found that the maximum DPC yield is achieved at reflux ratio of 1.2 with mole purity of 99.5% as shown in Figure 5.4.
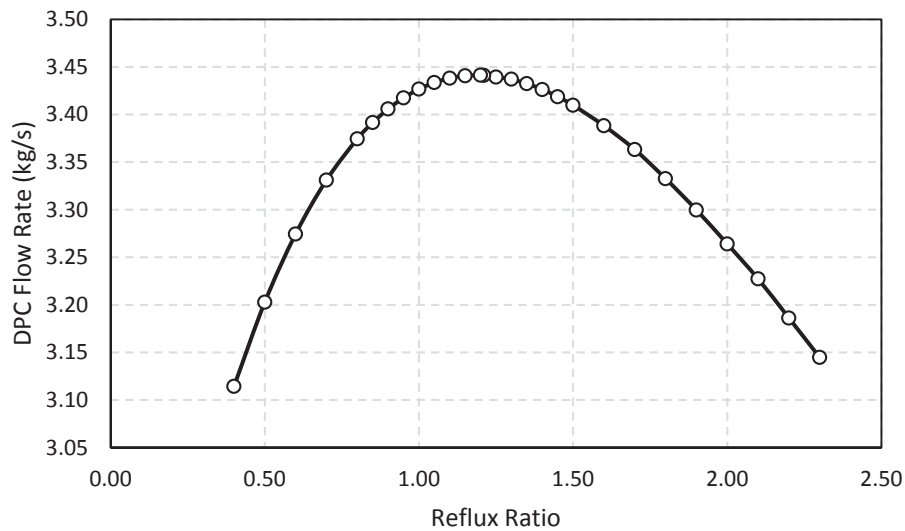
Figure 5.4: Reflux Ratio Effect on the DPC Production

10- Back to step 7, N_{rx} is fixed and NF_2 is changed, and the reflux ratio is changed at each new NF_2 keeping the yield at an optimal value with respect to the new NF_2. The total annual cost (TAC) is observed using the following model as the cost function (Douglas, 1988):

$$TAC = Operations\ Cost + \frac{Capital\ Cost}{Payback\ Period} \tag{5.1}$$

The payback period is usually assumed to be 3 years (Luyben and Yu, 2009). It can be read from both Figure 5.5 and Figure 5.6 that the stage 69 can be found to be the best location choice of the lower feed (F_2) which gives the largest yield comparing to the previous stages while TAC still not that large. After stage 69, the TAC of the column is increased dramatically as shown in Figure 5.6. Also, the simulation convergence becomes very poor.
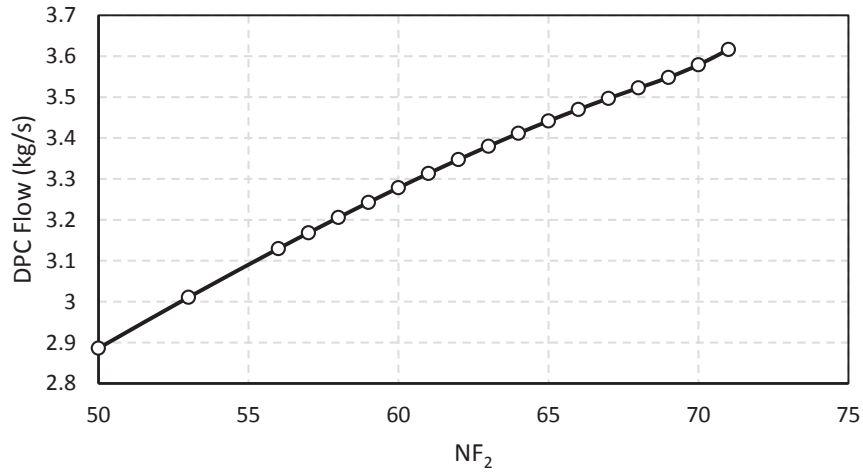
Figure 5.5: Effect of NF2 on DPC Production
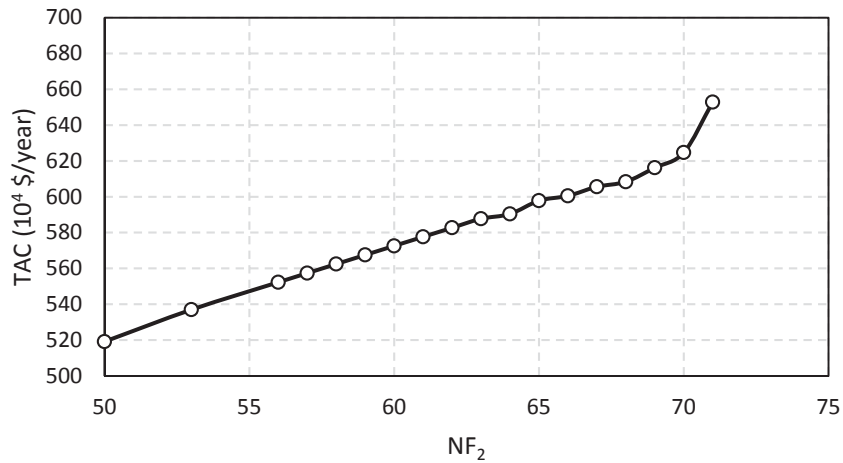
Figure 5.6: TAC Response to Lower Feed Stage (NF2)

5.3 Steady State Simulation

In the previous section, some optimal variables could be explored. Therefore, the steady state simulation can be carried out based on the conditions presented in Table 5.2. Our production target is to yield pure DPC with mole purity 99.5% using one reactive distillation column. The operation temperature for producing DPC should not exceed 350° C (Fukuoka et al., 2009). It is claimed that operating at high temperatures will allow for side reactions to take place giving undesired products such as Anisole. The rigorous RadFrac model in Aspen Plus has been used to simulate this system. All the necessary phase equilibria and kinetics data are presented in the previous chapter (sections 4.2.2 and 4.2.3). The steady state temperature is plotted in Figure 5.7. The composition profiles are presented in two separate graphs for better representation. The components MeOH, PhOH, and DMC are shown in Figure 5.8 while MPC and DPC are plotted in Figure 5.9. It is clear that DPC with mole purity of 99.5% can be achieved directly by one column holding the temperature at the column base at 339° C.

Table 5.2: Steady State Conditions of DPC System

Parameter	Value	Unit
Upper Feed (80% PhOH, 20% DMC)	200	mole/s
Lower Feed (20% PhOH, 80% DMC)	100	mole/s
Reflux ratio	1.27	[ ]
Rectifying stages including condenser	4	[ ]
Reactive stages including reboiler	70	[ ]
Holdup	20	liter
Upper Feed Stage	5	[ ]
Lower Feed Stage	69	[ ]
Pressure	1.0	atm
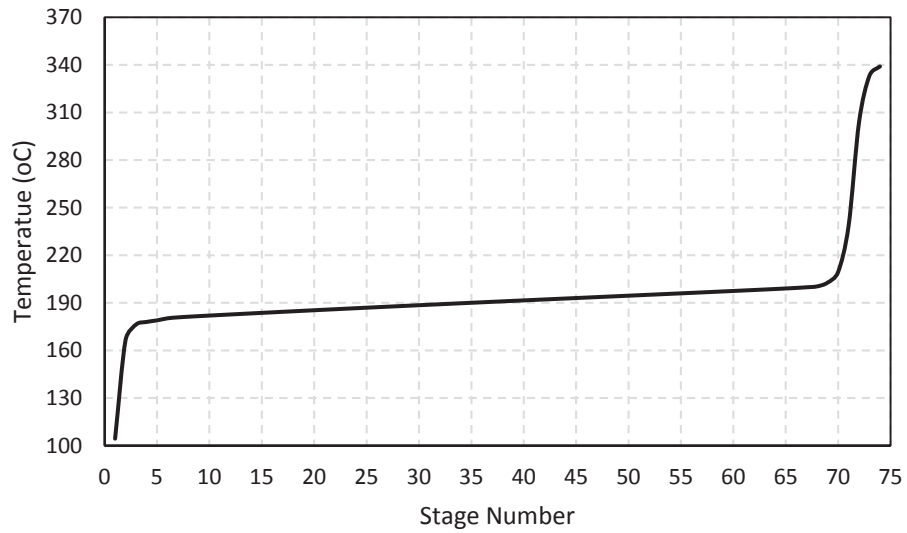
Figure 5.7: Temperature Profile of Real DPC System
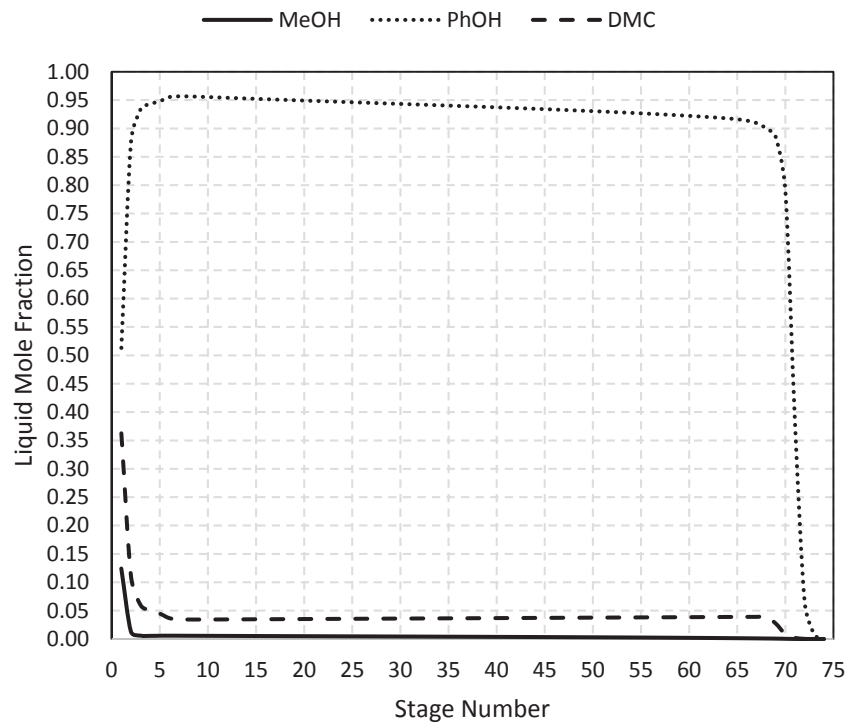
Figure 5.8: Composition Profiles of DMC, PhOH, and MeOH
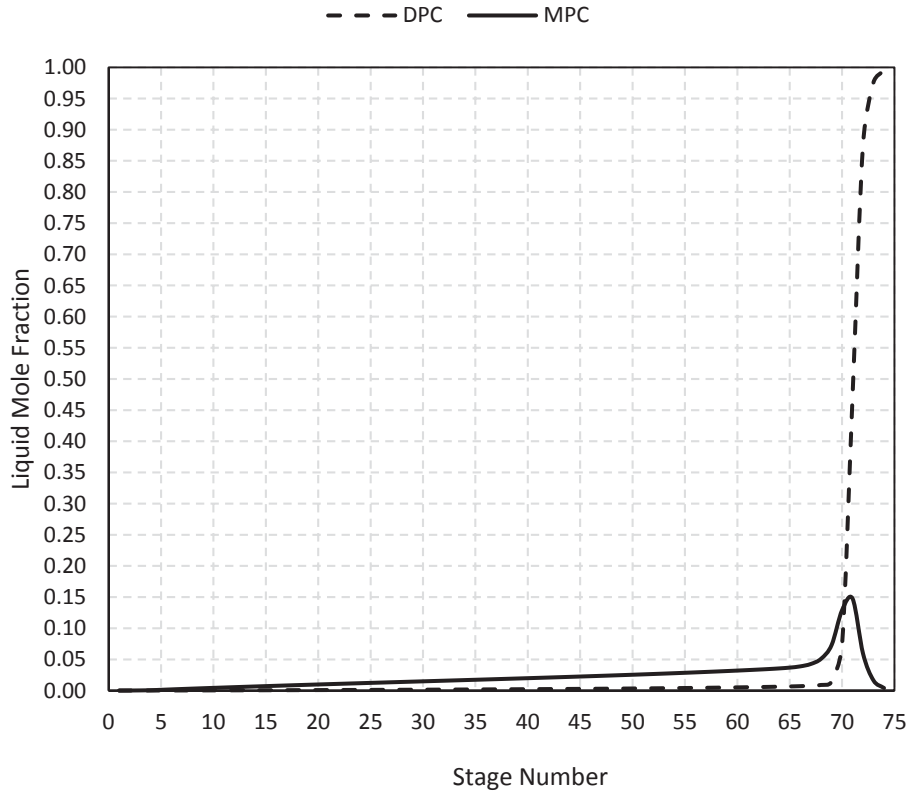
Figure 5.9: Composition Profiles of DPC and MPC

5.4 Catalyst Effect

Although it would be interesting to achieve high conversions by increasing the catalyst amount in each reactive stage (holdup), the holdup will also increase at each reactive stage. In the DPC system, the relationship between the catalyst amount and the DPC yield is represented by Figure 5.10. It has been found that there is steady state for the catalyst amount at about 5.4 Kmole as shown by the graph. Since the mole purity of DPC is held at 99.5%, the temperature remains constant while increasing the catalyst. However, the rate of the reboiler heat would be decreasing as the catalyst increases which obvious fact because the catalyst helps the reaction to be faster consuming less energy.
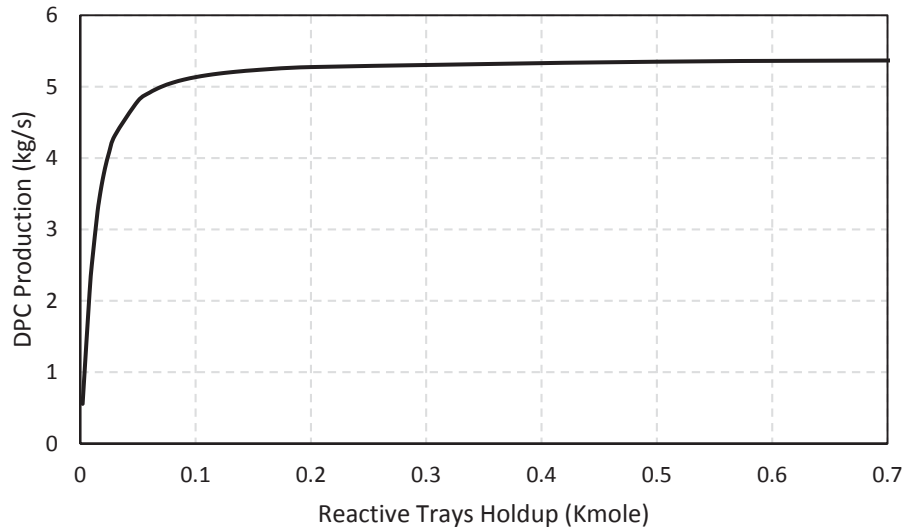
Figure 5.10: Catalyst Effect on DPC Productivity

5.5 Feed Compositions Effect

The feed compositions ratio has significant effect on the DPC productivity. While holding the flow rate of feeds at specified values, different compositions for the two feed streams were tested. Table 5.3 shows the DPC amount that can be produced at these different compositions. When the pure heavy reactant is fed from the upper feed stream and the pure light reactant is fed from lower feed stream, the amount of DPC has been found to be more than those systems with mixture feeds. As will be shown later, pure feeds are considered when feeding the simulation to the Aspen dynamics engine. This will be helpful for control purposes as well.

Table 5.3: Feed Compsitions Effect

Run	$F_1 = 200\ mole/s$		$F_2 = 100\ mole/s$		DPC Yield (kg/s)
	PhOH %	DMC %	PhOH %	DMC %	
1	0.8	0.2	0.2	0.8	3.763837
2	0.2	0.8	0.8	0.2	1.61409
3	0.5	0.5	0.5	0.5	2.875677
4	0.6	0.4	0.4	0.6	3.199524
5	1	0	0	1	4.245146

5.6 Control of DPC System

After the parametric study we made based on the steady state mode, we focused on the dynamic system based on the steady state conditions found in the previous sections. As for the feeds, run 5 in Table 5.3 is considered. In the real system, it can be noticed from the temperature profiles that the lower trays are needed to be controlled. Using another criterion such as the temperature slope shown in Figure 5.11, the stages that should be controlled are stage 1 and stage 71. More analysis and observations can be done during dynamic mode to explore effects of changing different parameters.
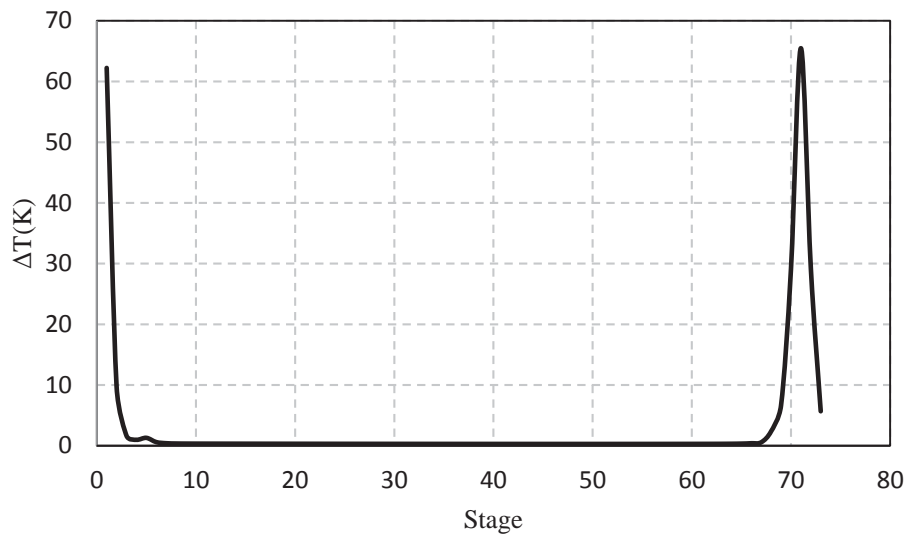
Figure 5.11: Temperature Slope of Real DPC System

5.7 Control Structure

The control configuration structure is built based on the temperature slope as shown in Figure 5.12 having seven controls including the control of the temperature on stages 1 and 71. These controls are listed below:

1- P controller for the column base level (CBC).
2- PI controller for the feed flows (FC1 and FC2).
3- P controller for the accumulator level at the top (ALC).
4- PI controller for the column pressure (CPC).
5- PI controller for the stage 1 temperature (T1C).
6- PI controller for the stage 71 temperature (T71C).
7- Composition controller (CC) in cascade with T71C to hold the purity of DPC.

The proportional controls (CBC and ALC) are used with 2.5 gains while the PI flow control is used with the conventional flow controller tuning (gain of 0.5 and integral time of 0.3) (Luyben and American Institute of Chemical Engineers., 2006). The temperature controller (T1C) was first tuned with 1 min dead time using the relay-feedback method for calculating the ultimate gain and frequency. The gain and integral time is determined by Tyreus-Luyben equations (3.4) and (3.5). The calculated gain and integral time for T1C are 6.995 and 11.88, respectively. The gain of T71C is 1.2 and its integral time is 18.3. To explore the importance of choosing the temperature stage that has to be controlled, the T71C is replaced by another control called T74C which control the temperature at stage 74. Although, the stable steady state could be achieved by this control, the energy needed for this steady state is more than that needed for T71C. The temperature profiles for the system under both controls are shown by Figure 5.13.
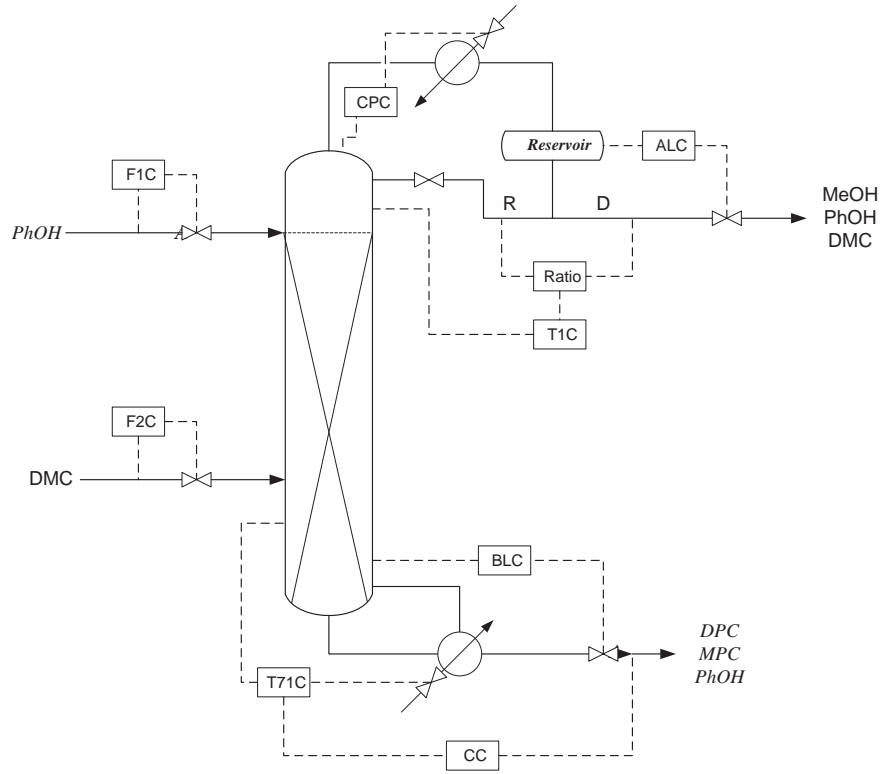
Figure 5.12: Control Configuration of Real DPC System
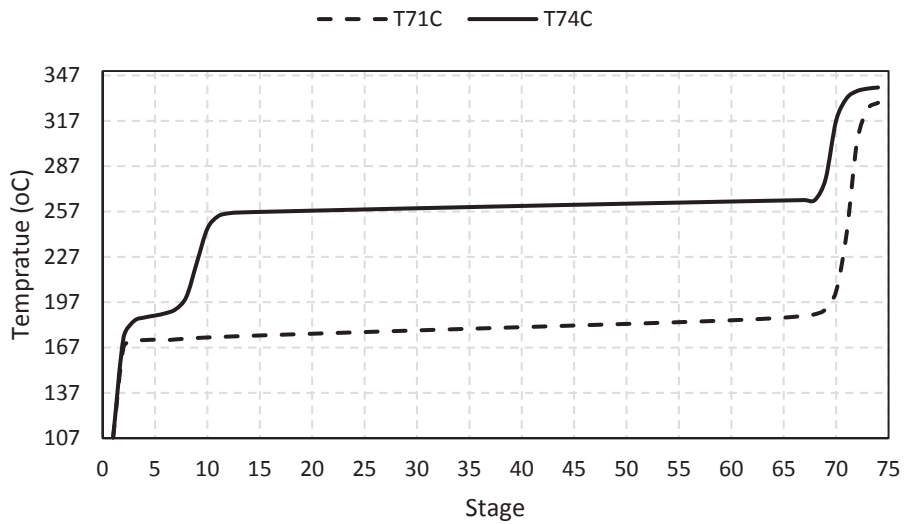
Figure 5.13: Temperature Profiles of DPC System under Two Different Controls

5.8 Response of DPC Control to Disturbances

To examine the disturbance effect on the control structure of DPC system, amount of +10% and -10% of the feed flow on both feed streams are applied. The responses are shown in Figure 5.14 and Figure 5.15. This shows the effectiveness of the chosen controllers to handle feed disturbances.
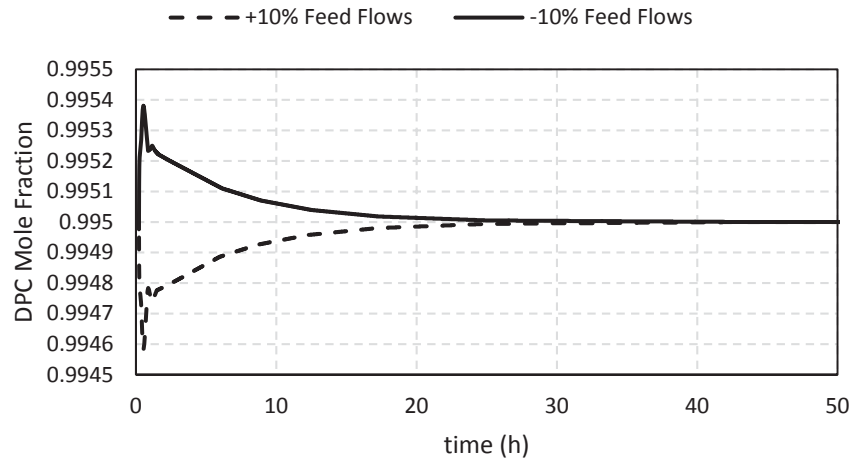
Figure 5.14: DPC Purity Response after Adding Disturbance
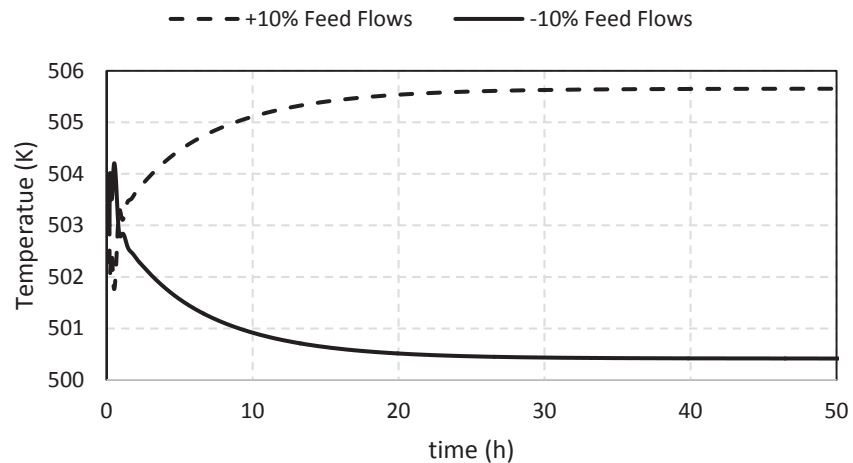
Figure 5.15: Temperature 71 Response to Disturbances

6. Conclusions

The application of reactive distillation technology is investigated in this study. Our study involves both ideal and real systems and shows that reactive distillation can help shift equilibrium reactions toward the desired products. A binary reactive distillation system is the first ideal system example. The reversible reaction from A to B is considered to represent an isomerization chemical system. The study made on this binary system explored why reactive distillation is useful for difficult reversible reactions. A comparative study between the binary reactive and non-reactive distillation shows that the number of stages of reactive distillation will be much fewer than those needed for the conventional distillation. Although the combination of reaction and separation increases system complexity, the exothermic reaction could reduce the energy and the capital cost significantly. Another class of reactive distillation systems is presented which involves a quaternary ideal reactive distillation. Simulation environment using MATLAB have been developed to reproduce a previous work in the literature. The differential algebraic equations (DAEs) could be used efficiently in the simulation to solve the set of the ordinary differential equations and the set of algebraic equations simultaneously based on Rung-Kutta numerical method instead of Euler method. Our results show improved accuracy compared with those presented in the literature.

The study is then extended from ideal systems to non-ideal cases by focusing on the DPC chemical system due to its industrial importance. Information about DPC system is limited in the literature, but fortunately, new data from Haubrock's group (Haubrock et al., 2008a; Haubrock et al., 2008b) has been incorporated in our study. As shown in the DPC study, it is possible to shift the reactions toward the final product (DPC) with high purity (99.5%) while attaining the optimal yield. The study presented in this document shows the possibility of producing DPC via one reactive distillation instead of two, with a production rate of 16.75 tons/h corresponding to start reactants materials of 74.69 tons/h of Phenol and 35.75 tons/h of Dimethyl Carbonate.

The mass and heat transfers in the reactive distillation unit allow for the most volatile components to leave the reaction area, thus minimizing the reverse reactions. The reactions are shifted toward the production of desired product, which is the main objective of using reactive distillation technology.

Aspen Plus software has been used for simulating the real DPC system using the RadFrac module. This model is one of the most rigorous available models for reactive systems simulation. As shown in Figure 5.9, the growing of DPC is dependent to the amount of produced MPC. In addition, Figure 5.8 shows that MeOH and DMC are always together along the column due to the binary azeotrope between them. This azeotrope enhances the reverse reaction between MPC and MeOH backward to the reactants PhOH and DMC slowing the conversion of MPC to DPC.

At the lower part of the column, the conversion to the DPC is sharply increased because there is enough energy for the needed accumulated reactant (i.e. the produced MPC through the column is fallen down since it is the high boiling point component) to be converted to the final DPC product. Therefore, there are two regimes for this system. The first one is the MPC regime which is necessary to be achieved efficiently through reaction 1 shown in Figure 4.1. After getting MPC, the system would be able to move to the second regime called DPC regime mainly achieved via reaction 3. The azeotropes study we have done through chapter 4 tells us that this system is azeotropic system. The main azeotrope is the binary one between DMC and MeOH. However, these two components are not involved in the DPC regime because DMC and MeOH are the most volatiles keys. The azeotropic mixture can be withdrawn from the top of the DPC reactive distillation which needs more treatments to break the azeotrope between DMC and MeOH which is beyond this study. The area of the second regime is completely dependent to the first regime. In other words, as much the MPC is produced as much the DPC would be produced. Although getting pure DPC with the required yield is attractive by just one column, the practical people have claimed in their patents that this system should be carried out using more than one column in order to operate at low temperatures.

91

On the control side, the steady state gain matrix and temperature slope methods are used to identify our control variables. This analysis specify stage 72 to be the most sensitive temperature stage, however, the temperature slope shows that the first stage temperature is also sensitive beside different lower stage which is 71 as shown in Figure 5.11. Thus, the temperature that should be controlled has to be chosen with more care. It might be possible to control the system with some stage that will need huge amount of heat. The control of the temperature of stage 74 instead of 71 has been investigated. The system could be controlled but with high duty on both reboiler and condenser.

7. Recommendations

Based on our study, the following ideas are recommended:

1- The thermodynamic is important for studying the non-ideal chemical system. The DPC system has binary interaction parameters that are still absent in the literature. It is recommended to establish an experimental work that would provide vapor liquid equilibrium data for this new system. The kinetics should be also considered.

2- The DPC plant has a lot of reactants going from the top of the column. The top stream can be fed to a normal distillation column to separate the azeotropic mixture of MeOH and DMC from the top of this new column. A large amount of DMC and PhOH can be withdrawn from the bottoms and then recycled to the DPC reactive distillation feed streams.

3- Economic optimization should be explored further for the overall plant.

4- Plant wide control would be needed for the plant configuration presented in the second recommendation given above.

5- If the DPC system should be operated at low temperature, the purity would be poor as the temperatures are getting lower. However, it can be operated with adding crystallization or extractive equipment to purify the DPC since its chemical structure can assist the crystallization process to be achieved.

Appendix A: Economic Costs Model

Although our study is focused on optimizing the yield and purity of the products, it is some time necessary to incorporate another important cost function for better design decisions as explained through the design of DPC column presented in this document. The total annual cost (TAC) is optimization cost function which should be at its minimum edge. The reboiler heat transfer area is estimated as

$$A_r(ft^2) = \frac{Q_r}{U_r \, \Delta T_r}$$

where

Q_r = the reboiler heat duty (Btu/h),

U_r = the overall heat transfer coefficient (assumed 250 Btu/h ft²),

ΔT_r = the temperature driving force (assumed 86º F),

The condenser heat transfer area is estimated as

$$A_c(ft^2) = \frac{Q_c}{U_c \, \Delta T_c}$$

where

Q_c = the rebiler heat duty (Btu/h),

U_c = the overall heat transfer coefficient (assumed 250 Btu/h ft²),

ΔT_c = the temperature driving force (assumed 41º F),

Cost Model*:*

$$Total \; Anual \; Cost \; (TAC) = Operations \; Cost + \frac{Capital \; Cost}{Payback \; Period}$$

We used a simple effective economic model which is summarized as following (Douglas, 1988):

$$Heat\ Exchanger\ Cost\ [\$] = \frac{M\&S}{280}[A^{0.65}(2.29 + F_c]$$

where $M\&S$ is Marshall and Swift index for 2014

$$F_{c,rebiler} = (F_d + F_p)F_m = (1.35 + 0.00) * 3.75$$

$$F_{c,condenser} = (F_d + F_p)F_m = (1.00 + 0.00) * 3.75$$

$$Column\ Cost\ [\$] = \frac{M\&S}{280}[101.9\ D_c^{1.066}L_c^{0.802}(2.18 + F_c)]$$

where $F_c = F_m F_p = 3.67$

$$Tray\ Cost\ [\$] = \frac{M\&S}{280}(4.7\ D_c^{1.55}\ L_c\ F_c)$$

where $F_c = F_s + F_t + F_m = 1.00 + 1.8 + 1.7$

where

F_c = Correction factor of the installed cost.

F_d = Design correction factor.

F_m = Equipment material correction factor

F_s = Tray spacing correction factor

F_t = Tray material correction factor

F_p = Design pressure correction factor

$$Oil\ Cost\ \left[\frac{\$}{year}\right] = (Oil\ price) * Q_r * (8150\frac{h}{year})$$

$$Steam\ Cost\ \left[\frac{\$}{year}\right] = \left(\frac{Steam\ price}{1000\ lb}\right) * \frac{Q_r}{steam\ latent\ heat} * (8150\frac{h}{year})$$

$$Cooling\ Water\ Cost\ \left[\frac{\$}{year}\right] = \left(\frac{\$0.03}{1000\ gal}\right) * \frac{1\ gal}{8.34\ lb} * \frac{Q_c}{30} * \left(8150\frac{h}{year}\right)$$

Appendix B: Thermodynamic and Physical Properties

Table B.1: Extension Antoine Parameters

$\ln P = A + \dfrac{B}{T} + C \ln T + D\, T^E$, where T in K and P in Pa					
	MeOH	PhOH	DMC	MPC	DPC
A	82.718	95.444	58.033	74.8195	85.8202
B	-6904.5	-10113	-5991.3	-9308.19	-11718.8
C	-8.8622	-10.09	-5.0971	-7.16437	-8.48664
D	7.47e-06	6.76e-18	1.34e-17	2.79e-18	1.56e-18
E	2	6	6	6	6
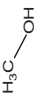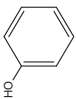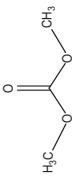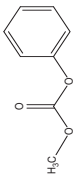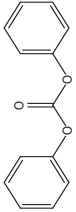
Table B.2: UNIFAC Interaction Parameters (Haubrock et al., 2008a)

Interaction Group$_m$-Group$_n$	$A_{m,n}$	$A_{n,m}$
CH3OH-OCOO	180	300
OH-OCOO	80	250
CH2-OCOO	450	500
ACH-OCOO	-220	250
ACOH-OCOO	189	187

Table B.3: Complete UNIFAC Interaction Parameters Used for DPC System

GROUP	AC	ACH	ACOH	CH3	CH3OH	OCOO
AC	0	0	1329	-11.12	637.4	-220
ACH	0	0	1329	-11.12	637.4	-220
ACOH	25.34	25.34	0	275.8	-265.2	189
CH3	61.13	61.13	1333	0	697.2	450
CH3OH	-50	-50	-101.7	16.51	0	180
OCOO	250	250	187	500	300	0

Table B.4: Pure Components Properties

	Methanol	Phenol	Dimethyl Carbonate	Methyl Phenyl Carbonate	Diphenyl Carbonate
	(MeOH)	(PhOH)	(DMC)	(MPC)	(DPC)
Structure					
Molecular Formula	CH_3OH	C_6H_5OH	$C_3H_6O_3$	$C_8H_8O_3$	$C_{13}H_{10}O_3$
Structure					
Basic Properties					
Molecular Weight (M_w) [g/mol]	32.0400	94.1100	90.0779	152.1473	214.2167
Boiling Temperature (T_b) [K]	338.000	455.000	363.700	491.7600	572.9900
Critical Temperature (T_c) [K]	513.000	671.010	575 ± 2	711.7600	799.3200
Critical Pressure (P_c) [bar]	78.5000	61.3	48 ± 1.5	34.41136	27.96493

* The data in this table can be found *via* Aspen Plus databank **APV80 PURE27**. MPC boiling point and molecular weight are taken from the Dictionary of Organic Compounds, then; Aspen Plus estimation engine can be used to estimate the rest of the basic properties.

Appendix C: Aspen and MATLAB Programs

Binary System

Input Summary created by Aspen Plus Rel. 27.0

PROP

DYNAMICS

DYNAMICS RESULTS=ON

IN-UNITS SI

DATABANKS 'APV80 PURE27' / 'APV80 AQUEOUS' / 'APV80 SOLIDS' / &

    'APV80 INORGANIC' / NOASPENPCD

PROP-SOURCES 'APV80 PURE27' / 'APV80 AQUEOUS' / 'APV80 SOLIDS' &

    / 'APV80 INORGANIC'

COMPONENTS

N-BUT-01 C4H10-1 / ISOBU-01 C4H10-2

PROPERTIES SYSOP0

PROPERTY-REP NOPARAM-PLUS

REACTIONS R-1 REAC-DIST

  REAC-DATA 1 KINETIC CBASIS=MOLEFRAC

  REAC-DATA 2 KINETIC CBASIS=MOLEFRAC

  RATE-CON 1 PRE-EXP=0.06 ACT-ENERGY=15200000. T-REF=360.

  RATE-CON 2 PRE-EXP=0.03 ACT-ENERGY=32300000. T-REF=360.

  STOIC 1 N-BUT-01 -1. / ISOBU-01 1.

  STOIC 2 ISOBU-01 -1. / N-BUT-01 1.

  POWLAW-EXP 1 N-BUT-01 1.

  POWLAW-EXP 2 ISOBU-01 1.

Real DPC System

;Input Summary created by Aspen Plus Rel. 27.0 at 17:35:11 Fri Apr 18, 2014

DYNAMICS

   DYNAMICS RESULTS=ON

IN-UNITS SI

DEF-STREAMS CONVEN ALL

SIM-OPTIONS MASS-BAL-CHE=YES UTL-REQD=NO

DATABANKS 'APV80 PURE27' / 'APV80 AQUEOUS' / 'APV80 SOLIDS' / &

   'APV80 INORGANIC' / 'APV80 ASPENPCD' / 'APV80 BIODIESEL' &

   / 'APV80 COMBUST' / 'APV80 ELECPURE' / 'APV80 EOS-LIT' &

   / 'APV80 ETHYLENE' / 'APV80 HYSYS' / 'APV80 INITIATO' &

   / 'APV80 NRTL-SAC' / 'APV80 PC-SAFT' / 'APV80 POLYMER' &

   / 'APV80 POLYPCSF' / 'APV80 PURE11' / 'APV80 PURE12' &

   / 'APV80 PURE13' / 'APV80 PURE20' / 'APV80 PURE22' / &

   'APV80 PURE24' / 'APV80 PURE25' / 'APV80 PURE26' / &

   'APV80 SEGMENT' / 'FACTV80 FACTPCD' / 'NISTV80 NIST-TRC'

PROP-SOURCES 'APV80 PURE27' / 'APV80 AQUEOUS' / 'APV80 SOLIDS' &

   / 'APV80 INORGANIC' / 'APV80 ASPENPCD' / &

   'APV80 BIODIESEL' / 'APV80 COMBUST' / 'APV80 ELECPURE' &

   / 'APV80 EOS-LIT' / 'APV80 ETHYLENE' / 'APV80 HYSYS' &

   / 'APV80 INITIATO' / 'APV80 NRTL-SAC' / 'APV80 PC-SAFT' &

   / 'APV80 POLYMER' / 'APV80 POLYPCSF' / 'APV80 PURE11' &

   / 'APV80 PURE12' / 'APV80 PURE13' / 'APV80 PURE20' / &

   'APV80 PURE22' / 'APV80 PURE24' / 'APV80 PURE25' / &

   'APV80 PURE26' / 'APV80 SEGMENT' / 'FACTV80 FACTPCD' / &

   'NISTV80 NIST-TRC'

COMPONENTS

   METHANOL CH4O /

   PHENOL C6H6O /

   DIMET-01 C3H6O3-D3 /

   DIPHE-01 C13H10O3 /

   MPC

GROUPS AC 1100 / ACH 1105 / ACOH 1350 / CH3 1015 / &

    CH3OH 1250 / OCOO 4001

SOLVE

  RUN-MODE MODE=SIM

FLOWSHEET

  BLOCK C1 IN=3 4 OUT=D1 B1

  BLOCK V11 IN=F1 OUT=4

  BLOCK V12 IN=F2 OUT=3

  BLOCK V13 IN=6 OUT=7

  BLOCK V14 IN=9 OUT=10

  BLOCK P11 IN=D1 OUT=6

  BLOCK P12 IN=B1 OUT=9

PROPERTIES UNIFAC

STRUCTURES

  UNIFAC DIMET-01 1015 2 / 4001 1

PROP-DATA

  PROP-LIST ATOMNO / NOATOM

  PVAL DIMET-01 6 1 8 / 3. 6. 3.

STRUCTURES

  UNIFAC DIPHE-01 1100 2 / 4001 1 / 1105 10

PROP-DATA

  PROP-LIST ATOMNO / NOATOM

  PVAL DIPHE-01 6 1 8 / 13. 10. 3.

STRUCTURES

  UNIFAC METHANOL 1250 1

PROP-DATA

  PROP-LIST ATOMNO / NOATOM

  PVAL METHANOL 6 1 8 / 1. 4. 1.

STRUCTURES

  UNIFAC MPC 1015 1 / 4001 1 / 1100 1 / 1105 5

  UNIFAC PHENOL 1350 1 / 1105 5

PROP-DATA

PROP-LIST ATOMNO / NOATOM

PVAL PHENOL 6 1 8 / 6. 6. 1.

ESTIMATE ALL

PROP-DATA PCES-1

IN-UNITS SI

PROP-LIST RKTZRA / VLSTD / VB

PVAL DIPHE-01 .2427315250 / .1696134320 / .2192824960

PROP-LIST RKTZRA / VLSTD / TC / DHVLB / VB / VC / ZC / &

OMEGA

PVAL MPC .2524809090 / 0.0 / 719.2376000 / 4.37957801E+7 / &

.1629296210 / .4417024490 / .2541745150 / .4134257100

PROP-DATA REVIEW-1

IN-UNITS SI

PROP-LIST DGFORM

PVAL DIPHE-01 -1.3197000E+8

PROP-LIST DHVLB / VB / VLSTD

PVAL METHANOL 3.51406000E+7 / .0427452000 / .0403346000

PVAL PHENOL 4.64772000E+7 / .1016090000 / .0897171000

PVAL DIMET-01 3.36244000E+7 / .0924129000 / .0847244000

PROP-DATA USRDEF

IN-UNITS SI PRESSURE=bar DIPOLEMOMENT=debye PDROP='N/sqm'

PROP-LIST TB / MW / MUP / PC

PVAL MPC 491.76 / 152.15 / 5.18 / 34.41136

PROP-LIST MUP

PVAL DIPHE-01 2.20

PROP-DATA CPIG-1

IN-UNITS SI

PROP-LIST CPIG

PVAL DIPHE-01 -25830.00000 963.0000000 -.5402000000 &

8.26000000E-5 0.0 0.0 280.0000000 1100.000000 &

36029.20000 35.69515140 1.500000000

PVAL METHANOL 7270.000000 132.8200000 -.0610000000 &

1.05000000E-5 0.0 0.0 280.0000000 1100.000000 &

36029.20000 5.2765282E-15 7.300842390

PVAL PHENOL -59690.00000 709.0000000 -.6572000000 &

   2.43700000E-4 0.0 0.0 280.0000000 1100.000000 &

   36029.20000 .8581158430 1.969415160

PVAL DIMET-01 51070.00000 170.8400000 .0662000000 &

   -8.7400000E-5 0.0 0.0 280.0000000 1100.000000 &

   36029.20000 14.11809910 1.500000000

PVAL MPC 12620 566.92 -0.237 -2.4E-006 0 0 280 1100 &

   36029.2 24.9066252 1.5

PROP-DATA DHVLWT-1

  IN-UNITS SI

  PROP-LIST DHVLWT

  PVAL MPC 4.37957801E+7 491.7600000 .3800000000 0.0 &

   491.7600000

PROP-DATA KLDIP-1

  IN-UNITS SI

  PROP-LIST KLDIP

  PVAL MPC -1.850805510 .0141416801 -3.7820529E-5 &

   4.43840474E-8 -1.959812E-11 491.7600000 712.0452240

PROP-DATA MULAND-1

  IN-UNITS SI

  PROP-LIST MULAND

  PVAL DIPHE-01 136.3121670 -10444.43690 -19.87828890 &

   582.3530000 811.8000000

  PVAL MPC 110.9567200 -7432.734220 -16.78453110 491.7600000 &

   712.0452240

PROP-DATA PLXANT-1

  IN-UNITS SI PRESSURE=atm PDROP='N/sqm'

  PROP-LIST PLXANT

  PVAL METHANOL 70.41098945 -7416.518200 0.0 0.0 &

   -8.328241770 2.2184032E-17 6.000000000 337.8500000 &

   512.5000000

  PVAL PHENOL 61.05415905 -8794.655460 0.0 0.0 -6.822057360 &

3.1427158E-18 6.000000000 454.9900000 694.2500000

PVAL DIMET-01 53.85276135 -6478.361230 0.0 0.0 &

  -6.115467080 1.2125475E-17 6.000000000 363.4000000 &

  548.0000000

PVAL DIPHE-01 69.27153225 -11368.73160 0.0 0.0 &

  -7.821324910 1.2668131E-18 6.000000000 582.3530000 &

  820.0000000

PVAL MPC 58.56070015 -8871.240640 0.0 0.0 -6.543419120 &

  2.4749999E-18 6.000000000 491.7600000 719.2376000

PROP-DATA SIGDIP-1

  IN-UNITS SI

  PROP-LIST SIGDIP

  PVAL DIPHE-01 .0694159535 1.222222220 -3.262278E-11 &

    3.6789711E-11 -1.464829E-11 582.3530000 803.6000000

  PVAL MPC .0706632843 1.222222220 -1.3846453E-9 &

    1.55017767E-9 -6.193815E-10 491.7600000 704.8528480

PROP-DATA U-1

  IN-UNITS MET PRESSURE=bar TEMPERATURE=C DELTA-T=C PDROP=bar &

    INVERSE-PRES='1/bar'

  PROP-LIST GMUFQ / GMUFR

  PVAL AC 0.12 / 0.3652

  PVAL ACH 0.4 / 0.5313

  PVAL ACOH 0.68 / 0.8952

  PVAL CH3 0.848 / 0.9011

  PVAL CH3OH 1.432 / 1.4311

  PVAL OCOO 1.3937 / 1.5821

PROP-DATA GMUFB-1

  IN-UNITS MET PRESSURE=bar TEMPERATURE=C DELTA-T=C PDROP=bar &

    INVERSE-PRES='1/bar'

  PROP-LIST GMUFB

  BPVAL AC AC 0

  BPVAL AC ACH 0

  BPVAL AC ACOH 1329

BPVAL AC CH3 -11.12

BPVAL AC CH3OH 637.4

BPVAL AC OCOO -220

BPVAL ACH AC 0

BPVAL ACH ACH 0

BPVAL ACH ACOH 1329

BPVAL ACH CH3 -11.12

BPVAL ACH CH3OH 637.4

BPVAL ACH OCOO -220

BPVAL ACOH AC 25.34

BPVAL ACOH ACH 25.34

BPVAL ACOH ACOH 0

BPVAL ACOH CH3 275.8

BPVAL ACOH CH3OH -265.2

BPVAL ACOH OCOO 189

BPVAL CH3 AC 61.13

BPVAL CH3 ACH 61.13

BPVAL CH3 ACOH 1333

BPVAL CH3 CH3 0

BPVAL CH3 CH3OH 697.2

BPVAL CH3 OCOO 450

BPVAL CH3OH AC -50

BPVAL CH3OH ACH -50

BPVAL CH3OH ACOH -101.7

BPVAL CH3OH CH3 16.51

BPVAL CH3OH CH3OH 0

BPVAL CH3OH OCOO 180

BPVAL OCOO AC 250

BPVAL OCOO ACH 250

BPVAL OCOO ACOH 187

BPVAL OCOO CH3 500

BPVAL OCOO CH3OH 300

BPVAL OCOO OCOO 0

STREAM F1

  SUBSTREAM MIXED TEMP=180. <C> PRES=5. <atm> &

    MOLE-FLOW=200. <mol/sec>

  MOLE-FRAC METHANOL 0.0 / PHENOL 1. / DIMET-01 0.

STREAM F2

  SUBSTREAM MIXED TEMP=150. <C> PRES=7. <atm> &

    MOLE-FLOW=100. <mol/sec>

  MOLE-FRAC METHANOL 0.0 / PHENOL 0. / DIMET-01 1.

BLOCK C1 RADFRAC

  PARAM NSTAGE=74 ALGORITHM=NONIDEAL INIT-OPTION=STANDARD &

    MAXOL=50

  COL-CONFIG CONDENSER=TOTAL

  FEEDS 3 69 / 4 5

  PRODUCTS D1 1 L / B1 74 L

  P-SPEC 1 1. <atm> / 2 1.1 <atm>

  COL-SPECS QN=32051800. DP-STAGE=0.01 <atm> MOLE-RR=1.27

  REAC-STAGES 5 74 R-2

  HOLD-UP 5 74 MOLE-LHLDP=0.02

  SPEC 1 MOLE-FRAC 0.995 COMPS=DIPHE-01 STREAMS=B1 &

    SPEC-ACTIVE=YES

  VARY 1 QN 32050. 320518000. VARY-ACTIVE=YES

  TRAY-SIZE 1 2 73 SIEVE FLOOD-METH=FAIR

  PROPERTIES UNIFAC FREE-WATER=STEAM-TA SOLU-WATER=3 &

    TRUE-COMPS=YES

BLOCK P11 PUMP

  PARAM DELP=6. <atm>

BLOCK P12 PUMP

  PARAM DELP=6. <atm>

BLOCK V11 VALVE

  PARAM P-OUT=1.13 <atm> NPHASE=1 PHASE=L

  BLOCK-OPTION FREE-WATER=NO

BLOCK V12 VALVE

  PARAM P-OUT=1.77 <atm> NPHASE=1 PHASE=L

BLOCK-OPTION FREE-WATER=NO

BLOCK V13 VALVE

PARAM P-DROP=3. <atm> NPHASE=1 PHASE=L

BLOCK-OPTION FREE-WATER=NO

BLOCK V14 VALVE

PARAM P-DROP=3. <atm> NPHASE=1 PHASE=L

BLOCK-OPTION FREE-WATER=NO

EO-CONV-OPTI

STREAM-REPOR MOLEFLOW MASSFLOW MOLEFRAC MASSFRAC

PROPERTY-REP PCES NOPROP-DATA NODFMS NOPARAM-PLUS

REACTIONS R-2 REAC-DIST

REAC-DATA 1 KINETIC CBASIS=MOLE-GAMMA

REAC-DATA 2 KINETIC CBASIS=MOLE-GAMMA

REAC-DATA 3 KINETIC CBASIS=MOLE-GAMMA

REAC-DATA 4 KINETIC CBASIS=MOLE-GAMMA

REAC-DATA 5 KINETIC CBASIS=MOLE-GAMMA

REAC-DATA 6 KINETIC CBASIS=MOLE-GAMMA

RATE-CON 1 PRE-EXP=242000000. ACT-ENERGY=73500. <kJ/kmol>

RATE-CON 2 PRE-EXP=203150000. ACT-ENERGY=51035.6 <kJ/kmol>

RATE-CON 3 PRE-EXP=14.88 ACT-ENERGY=0. <kJ/kmol>

RATE-CON 4 PRE-EXP=236.1905 ACT-ENERGY=0.0030845 <kJ/kmol>

RATE-CON 5 PRE-EXP=6610000. ACT-ENERGY=59900. <kJ/kmol>

RATE-CON 6 PRE-EXP=88110000. ACT-ENERGY=40520.1 <kJ/kmol>

STOIC 1 PHENOL -1. / DIMET-01 -1. / MPC 1. / METHANOL 1.

STOIC 2 METHANOL -1. / MPC -1. / PHENOL 1. / DIMET-011.

STOIC 3 MPC -2. / DIPHE-01 1. / DIMET-01 1.

STOIC 4 DIPHE-01 -1. / DIMET-01 -1. / MPC 2.

STOIC 5 MPC -1. / PHENOL -1. / DIPHE-01 1. / METHANOL 1.

STOIC 6 METHANOL -1. / DIPHE-01 -1. / MPC 1. / PHENOL 1.

POWLAW-EXP 1 PHENOL 1. / DIMET-01 1.

POWLAW-EXP 2 METHANOL 1. / MPC 1.

POWLAW-EXP 3 MPC 2.

POWLAW-EXP 4 DIPHE-01 1. / DIMET-01 1.

POWLAW-EXP 5 MPC 1. / PHENOL 1.

POWLAW-EXP 6 METHANOL 1. / DIPHE-01 1.

Reactive Distillation MATLAB Code

The run code is used to run the ideal reactive distillation using separate m.file called Run.m which is as following:

```
tic
clear
clc
x_B = [0.0174 0.0326 1.2964e-5 0.95];
x_D = [0.0326 0.0174 0.95 3.4584e-5];
M_D = 2720;
M_B = 2440;
T   = [430.953951954286 426.136915084861  418.075998243212
       408.016976377953 399.302465882202  393.701031978044
       390.401503336020 395.320229029940  397.251165997253
       397.387934312360 396.242652290624  394.321763243214
       392.173611297302 390.178261134218  388.459399911798
       382.619614389805 374.196512242938  365.179911095489
       358.599396874920 355.018709851250  353.000000000000];
NT = 21;
M1 = eye(4*NT+3,4*NT+3);
M2 = zeros(NT,4*NT+3);
M3 = zeros(5*NT+3,NT);

options=odeset('Mass',[[M1;M2],M3],'MaxStep',1,'InitialStep',1);

Xinit = [x_B(1) 0.25*ones(1,19) x_D(1) x_B(2) 0.25*ones(1,19)...
         x_D(2) x_B(3) 0.25*ones(1,19) x_D(3) x_B(4) ...
         0.25*ones(1,19) x_D(4) M_B M_D 0 T];

[t,X]=ode15s(@Reactive_Distillation,[0 8500],Xinit',options,Vs,R_F);


NT =21;

N_R = size(X,1);                         % Final Row Number of Marix X

LiqComp = X(N_R,:);

ind = 4*NT+1:5*NT+3;

LiqComp(ind) = [];

LiqComp = [LiqComp(1:NT);LiqComp(NT+1:NT*2);LiqComp(NT*2+1:NT*3);...
           LiqComp(NT*3+1:NT*4)]';

Trays = 0:NT-1;
figure(1)

plot(Trays,LiqComp)
```

```matlab
grid

figure(2)

T = X(N_R,:);
ind = 1:4*NT+3;
T(ind) = [];
plot(Trays,T)
grid

toc
```

The function Reactive_Distillation that is used in the ode15s solver is written in separate m.file as following:

```matlab
function dx = Reactive_Distillation_2(~,X,Vs,R_F)


%% Kinetic Parameters

K_EQ = 2;            % Chemical Equilibrium Constant           [-]
ko_F = 0.008;        % Forward Pre-Exponential of Reaction      [s^-1]
ko_B = ko_F/K_EQ;    % Backward Pre-Exponential of Reaction     [s^-1]
E_F  = 30000;        % Activation Energy of Forward Reaction
[cal/mole]
E_B  = 40000;        % Activation Enegry of Backward Reaction
[cal/mole]
H_RX = -10000;       % Heat of Reaction
[cal/mole]
H_V  = 6944;         % Heat of Vaporization
[cal/mole]

alphaf = ko_F*exp(E_F/(1.99*366));
alphab = ko_B*exp(E_B/(1.99*366));

%% Steady State Conditions and Design Parameters

NT      = 21;          % Total Number of Trays Including Reboil and
Conds
NS      = 6;           % Number of Stripping Trays Including Reboiler
NRX     = 9;           % Number of Reactive Trays
NR      = NT-NRX-NS;   % Number of Rectifying Trays Including
Condenser
Fo_A    = 12.6;        % Fresh Feed Flowrate of A         [mole/s]
Fo_B    = 12.6;        % Fresh Feed Flowrate of B         [mole/s]
P       = 8;           % Column Pressure                  [bar]
D       = 12.6;        % distllate flow rate
B       = 12.6;        % bottom flow rate
```

110

```matlab
MBs     = 2440;           % Nominal Base holdup - these are rather small
ncomps  = 4;              % --new-- number of components


%% Extract x(i,j), M(i) and T(i) where i=ith tray and j=jth component
    ncNT    = ncomps*NT;
    x       = reshape(X(1:ncNT),NT,ncomps);     % concentrations
%   M       = X(ncNT+(1:NT));                   % holdups
    M(1)    = X(ncNT+1);
    M(NT)   = X(ncNT+2);
    T       = X((ncNT+3)+(1:NT));               % temperature


 % Trays holdups
    M(2:NS)=400;
    M((NS+1):(NS+NRX))=1000;
    M((NS+NRX+1):(NT-1))=400;


%% Calculate tray temperatures and vapor compositions
    f       = zeros(NT,1);
    y       = zeros(NT,ncomps);
    for i = 1:NT    %--modified--
        [T(i),y_T]  = VLLE(x(i,:),P,T(i));
        f(i)        = 1-sum(y_T);
        y(i,:)      = y_T;
    end


%% P contol of base holdup
%   Vss     = Vs;                       % Nominal Vapor Flow
    MB      = M(1);                     % Actual reboiler and condenser holdup
    KcV     = -10;                      % controller gain
    Vs      = Vs +(MBs-MB)*KcV;         % Bottoms flow


%% PI controller for the component C compostion at distillate (mole% C)
    ncc         = 3;                    % comp to be controlled in distillate
    xccset      = 0.95;                 % set point
    xcc         = x(NT,ncc);            % output signal
    ubias       = 0.5;                  % controller bias
    k_p         = 0.5;                  % prop gain
    tau_i       = 1/0.2;               % integral constant
    error       = (xccset-xcc);        % error signal
    reset       = 20*60;
    int_error   = X(ncNT+3);           % integral of error
    op          = ubias + k_p*( error + int_error/tau_i );
    op          = min(1,max(op,0.2));
    R_F         = R_F*op*2;


%% Reactions Rate Calculations
    R           = 1.99;                % ideal Gas Constant    %
[cal/K.mole]
    rts         = NS+(1:NRX);          % reaction trays
    den         = R*T(rts);
    rx_F        = alphaf*exp(-E_F./den).*x(rts,1).*x(rts,2);   % [s^-1]
    rx_B        = alphab*exp(-E_B./den).*x(rts,3).*x(rts,4);   % [s^-1]
    RX(rts)     = M(rts).*(rx_F - rx_B)';
```

111

```matlab
%% Vapor and Liquid Flows
    srx                = NS+NRX ;
    V(2:NS)            = Vs;
    for i = NS+(1:NRX)
        V(i)           = V(i-1)-RX(i)*H_RX/H_V;
    end
    V(srx+(1:NR-1)) = V(srx);
%  V(NT-1)            = V(NT-2);
    L((srx+1):(NT))  = R_F ;
    L(srx)            = R_F+Fo_B+RX(srx)*H_RX/H_V;
    for i = (srx-1):-1:(NS+2)
        L(i)           = L(i+1)+RX(i)*H_RX/H_V;
    end
    L(NS+1)           = L(NS+2)+Fo_A + RX(NS+1)*H_RX/H_V;
    L(2:NS)           = L(NS+1);

%% Calculation of holdup changes --modified--
    dMdt(1)                = L(2)-B-Vs;
    dMdt(2)                = 0;
    dMdt(3:NS)             = 0;
    dMdt(NS+1)             = 0;
    dMdt(NS+2:srx-1)       = 0;
    dMdt(srx)              = 0;
    dMdt(srx+1:NT-2)       = 0;
    dMdt(NT-1)             = 0;
    dMdt(NT)               = V(NT-1) - R_F - D;

%% Reboiler
    dMxdt1            = (L(2)*x(2,:)-Vs*y(1,:) - B*x(1,:));
    dxdt(1,:)         = (dMxdt1 - x(1,:)*dMdt(1))/M(1);
%% Calculation of dxdt in each tray
    dxdt(2,:)         = (L(3)*x(3,:)-L(2)*x(2,:)+Vs*y(1,:)-
V(2)*y(2,:))/M(2); % Vs is cosidered because it is manipulated variable
    for i = 3:NS
        dxdt(i,:)     = (L(i+1)*x(i+1,:)-L(i)*x(i,:)+V(i-1)*y(i-1,:)- ...
                        V(i)*y(i,:))/M(i);
    end
    lastStripAdd     = [Fo_A;0;0;0] + RX(NS+1)*[-1;-1;1;1] ;
    dxdt(NS+1,:)     = (L(NS+2)*x(NS+2,:) - L(NS+1)*x(NS+1,:) + ...
                        V(NS)*y(NS,:) - V(NS+1)*y(NS+1,:) + ...
                        lastStripAdd' )/M(NS+1);
    for i = NS+2:srx-1
        rxnadd       = RX(i)*[-1;-1;1;1];
        dxdt(i,:)     = (L(i+1)*x(i+1,:) - L(i)*x(i,:) + ...
                        V(i-1)*y(i-1,:) - V(i)*y(i,:)+ rxnadd')/M(i);
    end
    lastRxnAdd       = [0;Fo_B;0;0] + RX(srx)*[-1;-1;1;1] ;
    dxdt(srx,:)       = (L(srx+1)*x(srx+1,:)-L(srx)*x(srx,:)+ ...
                        V(srx-1)*y(srx-1,:)-V(srx)*y(srx,:)+...
                        lastRxnAdd')/M(srx);
    for i = srx+1:NT-2
        dxdt(i,:)     = (L(i+1)*x(i+1,:)-L(i)*x(i,:)+V(i-1)*y(i-1,:)-...
                        V(i)*y(i,:))/M(i);
    end
```

112

```
    dxdt(NT-1,:)      = (R_F*x(NT,:)-L(NT-1)*x(NT-1,:)+V(NT-2)*y(NT-2,:)-
...
                         V(NT-1)*y(NT-1,:))/M(NT-1);

%% Condenser
    dMxdtNT           = (V(NT-1)*y(NT-1,:) - R_F*x(NT,:) - D*x(NT,:));
    dxdt(NT,:)        = (dMxdtNT - x(NT,:)*dMdt(NT) )/M(NT);

%% Form dx vector
    xdot(1:ncNT)              = dxdt(:);
    xdot(ncNT+1)             = dMdt(1);
    xdot(ncNT+2)             = dMdt(NT);
    xdot(ncNT+3)             = error/reset;
    xdot(ncNT+3+(1:NT))      = f(:);

    dx                       = xdot';
```

The function Reactive_Distillation has another function in separate m.file called VLLE

which can be written as following:

```
function [temp,y]=VLLE(x,P,tguess)
a_j=[ 12.34 11.65 13.04 10.96];
b_j=[ 3862 3862 3862 3862];
temp=tguess;
for j=1:4;
    ps(j)=exp(a_j(j)-b_j(j)/temp);
    y(j)=ps(j)*x(j)/P;
end
```

Azeotropes Calculations Codes

To calculate the azeotropes in this document, the code of Henk Walpot have been developed (Walpot, 2011). The modifications that have been done on the program can be listed as following:

1- The UNIFAC thermodynamic model is used instead of UNIQUAC.
2- The ideal vapor is assumed.
3- The MATLAB ode15s solver is used instead of ode45 because ode15s is designed for the differential algebraic equations used in this work.

The following are the MATLAB functions used for azeotropes calculations:

Non-Reactive Codes

Run Code:

```
clc
clear all
close all
tic
%% System
comp1 = 'Methanol';
comp2 = 'Dimethyl Carbonate';
comp3 = 'Phenol';
comp4 = 'Methyl Phenyl Carbonate';

[A,Rv,Qr,a,v,Properties,nij,P,R] = physical_data;

%% Initial liquid compositions in mole fractions
Data = [0.5 0.5 0.0
        0.10 0.00 0.80
        0.50 0.50 0.00
        0.00 0.60 0.20
        0.30 0.30 0.02
        0.25 0.20 0.05
        0.30 0.10 0.20
        0.40 0.23 0.08];
% %     0.05 0.23 0.08
%       0.01 0.20 0.05
%       0.20 0.20 0.25
%       0.15 0.70 0.02
%       0.85 0.05 0.05
%       0.10 0.85 0.02
%       0.19 0.40 0.10];
```

```matlab
%% Antoine coefficient matrix for initial guess calculation


B = [23.35 3555.30 -37.16
     21.72 3253.60 -44.25
     21.47 3610.50 -91.90
     7.54048 2778.727 14.953
     19.55 0.7448e4 0];

for i = 1:3;    Ts0(i) = B(i,2)/(B(i,1)-log(P/0.00001))-B(i,3);end

Ts0(4) = B(4,2)/(B(4,1)-log10(P/0.01))-B(4,3);      % MPC

% Ts0(5) = B(5,2)/(B(5,1)-log(P/ 0.001333))-B(5,3);  % DPC

%% Calculating the residue curves for each initial liquid composition

reltol = 1.0e-6; abstol = 1.0e-6;

M = [eye(4,8);zeros(4,8)];

options=odeset('Mass',M,'RelTol',reltol,'AbsTol',abstol);

[m,n] = size(Data);

for i = 1:m

    % Mole fractions
    X1 = Data(i,1);
    X2 = Data(i,2);
    X3 = Data(i,3);

    % Vector of liquid compositions
    Sv_0 = [X1;X2;X3;1-X1-X2-X3;Ts0'];

    %% Solving the differential equation
    % Calculating the forward RC
    tauspan = linspace (0,10);

[tau,Sv] = ode15s(@(tau,Sv)fun_nonreactRCM_for(tau,Sv,A,Rv,Qr,a,v,…
                  Properties,nij,P,R),tauspan,Sv_0,options);

    Xf = Sv(:,1:4);

    [p,q] = size(Xf);

    Xf_end(i,:) = Xf(p,:);
```

115

```matlab
% Calculating the backward RC

    tauspan = linspace (0,10);

tau,Sv] = ode15s(@(tau,Sv)fun_nonreactRCM_back(tau,Sv,A,Rv,Qr,a,v,…
                        Properties,nij,P,R),tauspan,Sv_0,options);

    Xb = Sv(:,1:4);

    [p,q] = size(Xb);

    Xb_end(i,:) = Xb(p,:);


    %% plot in 3-dimension composition space
    % 3D plot
    xaf = Xf(:,1);
    xbf = Xf(:,4);
    xcf = Xf(:,3);
    xdf = Xf(:,2);
    XXf = xbf+0.5*xcf+0.5*xdf;
    YYf = 0.5*sqrt(3)*xcf+1/6*sqrt(3)*xdf;
    ZZf = sqrt(2/3)*xdf;

    xab = Xb(:,1);
    xbb = Xb(:,4);
    xcb = Xb(:,3);
    xdb = Xb(:,2);
    XXb = xbb+0.5*xcb+0.5*xdb;
    YYb = 0.5*sqrt(3)*xcb+1/6*sqrt(3)*xdb;
    ZZb = sqrt(2/3)*xdb;



    figure(2)
    plot3(XXf, YYf, ZZf, '-k')

    hold on
    plot3(XXb, YYb, ZZb,'-k')

    grid off
end

AA = [0 0 0];
BB = [1 0 0];
CC = [0.5 0.5*sqrt(3) 0];
DD = [0.5 (1/6)*sqrt(3) sqrt(2/3)];
allx = [AA(1) BB(1) DD(1) AA(1) CC(1) DD(1) BB(1) CC(1)];
ally = [AA(2) BB(2) DD(2) AA(2) CC(2) DD(2) BB(2) CC(2)];
allz = [AA(3) BB(3) DD(3) AA(3) CC(3) DD(3) BB(3) CC(3)];
```

```
axis square
xlim([0 1])
ylim([0 1])
zlim([0 1])
line(allx, ally, allz);

sp = 0.05;
text(AA(1)-sp,AA(2)-sp,AA(3)-sp, 'MeOH');
text(BB(1)+sp,BB(2)-sp,BB(3)-sp, 'MPC');
text(CC(1)-sp,CC(2)-sp,CC(3)-sp, 'PhOH');
text(DD(1),DD(2),DD(3)+sp, 'DMC');

toc
```

In the above code, there are many functions that are called after running the code. Each function can be written as m-file as following:

1- Physical Properties File

```
function [A,Rv,Qr,a,v,Properties,nij,P,R] = physical_data

% Extended Antoine coefficients (P in [Pa] and T in [K])
A = [82.718 -6904.5 0 0  -8.8622 7.4664e-06  2
     58.033 -5991.3 0 0  -5.0971 1.3402e-17  6
     95.444 -10113  0 0  -10.09  6.7603e-18  6
     74.820 -9308.2 0 0  -7.1644 2.7940e-18  6];
%% UNIFAC parameters
% Volume parameters of Subgroups
%        AC        ACH       ACOH      CH3     CH3OH      OCOO
Rv = [ 0.3652   0.5313    0.8952    0.9011   1.43110    1.5821 ];

% Area parameters of Subgroups
%        AC      ACH      ACOH     CH3      CH3OH     OCOO
Qr = [  0.12   0.4      0.68     0.848    1.432     1.3937 ];

% UNIFAC interaction parameters matrix
%       AC     ACH     ACOH     CH3     CH3OH    OCOO
a = [    0       0      1329   -11.12   637.4    -220
         0       0      1329   -11.12   637.4    -220
      25.34   25.34       0    275.80  -265.2     189
      61.13   61.13    1333       0     697.2     450
       -50     -50     -101.7   16.51      0      180
       250     250      187     500      300       0 ];
```

117

```matlab
% Matrix for Identifying the Number of Each Subgroup in Each Component
%    MeOH DMC PhOH MPC
v = [ 0    0    0    1
      0    0    5    5
      0    0    1    0
      0    2    0    1
      1    0    0    0
      0    1    0    1];
%               Mw        Tb(K)     Tc(K)
Properties = [ 32.0400   338.00   513.00
               90.0779   363.70   576.00
               94.1100   455.00   671.01
              152.1473   491.76   711.76];


% Pressure [bar]
P = 1.013;


% Universal Gas Constant [L bar/mol K]
R = 8.314472;


-------------------------------------------------------
```

2- UNIFAC Function File

```matlab
function GAMMA = unifac1(T,x,a,Rv,Qr,v)
%% -------------- Combinatorial Part of GAMMA ---------------------
-------
power     = 1;
r         = Rv*v;
q         = Qr*v;
SUM_V     = x'*(r'.^power);
SUM_F     = x'*q';
V         = (r.^power)/SUM_V;
F         = q/SUM_F;
L         = 5*(r - q) - (r - ones(1,4));
SUM_L     = x'*L';
L_Gamma_C = log(V) + 5*q.*log(F./V) + L - V*SUM_L;
3- %% ---------------- Residual Part of GAMMA --------------------
    ----------
% Residual activity coefficient of sub-group k in the mixture
(L_Gamma_R_K)
SUM_X         = v*x;
SUM_X_mixture = sum(SUM_X);
X             = SUM_X/SUM_X_mixture;
SUM_TETA      = Qr*X;
TETA          = (Qr.*X')/SUM_TETA;
SAI           = exp(-a/T);
SUM_SAI       = TETA*SAI;
SUM_SAI_SAI   = SAI*(TETA./SUM_SAI)';
L_Gamma_R_K   = Qr.*(ones(1,6) - log(SUM_SAI) - SUM_SAI_SAI');
%-------------------------------------------------------
% Residual activity coefficient of sub-group k in a pure solution of
component i (L_Gamma_R_K_Component)
SUM_X_mixture_Component = ones(1,6)*v;
```

```matlab
X_Component            = bsxfun(@rdivide, v,SUM_X_mixture_Component);
SUM_TETA_Component     = Qr*X_Component;
TETA_Component         = bsxfun(@times,X_Component,Qr');
TETA_Component         = bsxfun(@rdivide,TETA_Component,...
SUM_TETA_Component);
SUM_SAI_Component      = SAI'*TETA_Component;
SUM_SAI_SAI_Component  = bsxfun(@rdivide,TETA_Component,...
                                  SUM_SAI_Component);
SUM_SAI_SAI_Component  = SAI*SUM_SAI_SAI_Component;


L_Gamma_R_K_Component  = bsxfun(@times,(ones(6,4) - ...
                                  log(SUM_SAI_Component)- ...
                                  SUM_SAI_SAI_Component), Qr');
L_Gamma_R              = bsxfun(@minus, L_Gamma_R_K',...
L_Gamma_R_K_Component);
L_Gamma_R              = bsxfun(@times, v, L_Gamma_R);
L_Gamma_R              = sum(L_Gamma_R);
%% -------------------------------------------------
GAMMA                  = exp(L_Gamma_R + L_Gamma_C);
GAMMA                  = GAMMA';


-------------------------------------------------
```

4- Antoine Equation File

```matlab
function Ps = Antoine(T,A)

[n,m] = size(A);

for i=1:n
    Ps(i)= (1e-5)*exp(A(i,1) + A(i,2)/(T+A(i,3)) + A(i,4)*T + ...
    A(i,5)*log(T) + A(i,6)*T^A(i,7));
end

Ps;

end
```

5- Vapor Liquid Equilibrium Function

```matlab
function[Y, Ps_j] = vapor_comp(X,Ts,A,Rv,Qr,a,v,Properties,nij,P)

T = Ts'*X;

Ps = Antoine(T,A);
GAMMA = UNIFAC(T,X,a,Rv,Qr,v);
Alpha_ki = Ps./Ps(1);
fi_ini = [1 1 1 1];
Y_ini = Ps'.*X.*GAMMA./(fi_ini'.*P);

tol = 1e-12;                    % Tolerance
Y = Y_ini;                      % Initial guess Y
```

```matlab
    for i=1:100

        fi = [1 1 1 1];

        Y_new = Ps'.*X.*GAMMA./(fi'.*P);

        Y_new = Y_new./sum(Y_new);

        dY = abs(Y-Y_new);

        if dY<tol

            break

        else Y = Y_new;

        end
    end


    Ps_j = P./sum(X.*Alpha_ki'.*(GAMMA./fi'));

    Y = Y';
```

6- Forward Function that are Called by ode15s

```matlab
function dx=fun_nonreactRCM_for(tau,Sv,A,Rv,Qr,a,v,…
Properties,nij,P,R)

X = Sv(1:4);
Ts = Sv(5:8);

for i=1:4

    if X(i) < 0.000001;

        X(i)=0;

    end
end

X = X./sum(X);
```

```matlab
% Calculation of the vapor composition in equilibrium with the liquid
    [Y Psj] = vapor_comp(X,Ts,A,Rv,Qr,a,v,Properties,nij,P);
```

```
            for i = 1:4; f(i) = fun_Ts(Ts(i),A,Psj,i);end
            xdot(1:4) = X-Y';
            xdot(5:8) = f;
            dx = xdot'
```

7- Backward Function that are Called by ode15s

```
        function dx=fun_nonreactRCM_back(tau,Sv,A,Rv,Qr,a,v,…
                                  Properties,nij,P,R)


        X = Sv(1:4);
        Ts = Sv(5:8);


        for i=1:4

            if X(i) < 0.00001;

                X(i)=0;

            end
        end


        X = X./sum(X);

% Calculation of the vapor composition in equilibrium with the liquid
        [Y Psj] = vapor_comp(X,Ts,A,Rv,Qr,a,v,Properties,nij,P);

        for i = 1:4; f(i) = fun_Ts(Ts(i),A,Psj,i);end


        xdot(1:4) = Y'-X;
        xdot(5:8) = f;
        dx = xdot';
```

Reactive Codes:

Run Code: (the functions used above for the non-reactive case are used for the below reactive case)

```
clc
clear all
close all
tic
%% System
comp1 = 'Methanol';
comp2 = 'Dimethyl Carbonate';
comp3 = 'Phenol';
comp4 = 'Methyl Phenyl Carbonate';

[A,Rv,Qr,a,v,Properties,nij,P,R] = physical_data;
%% Kinetic parameters
nu = [1 -1 -1 1];
ref = 1;
Comp = [2 3 4];

%% Initial transformed liquid compositions
Data = [0.4 0.30
        0.10 0.10
        0.20 0.20
        0.20 0.79
        0.30 0.69];
%          0.40 0.59
%          0.50 0.49
%          0.60 0.39];
%          0.65 0.34
%          0.70 0.29
%          0.75 0.24
%          0.80 0.19
%          0.90 0.09];

%% Antoine coefficient matrix for initial guess calculation

B = [23.35 3555.30 -37.16
     21.72 3253.60 -44.25
     21.47 3610.50 -91.90
     20.02 3753.55 -48.11];

for i = 1:4;    Ts0(i) = B(i,2)/(B(i,1)-log(P/0.00001))-B(i,3);end

%% Calculating the residue curves for each initial liquid composition

reltol = 1.0e-6; abstol = 1.0e-6;

M = [eye(2,6);zeros(4,6)];
```

```matlab
options=odeset('Mass',M,'RelTol',reltol,'AbsTol',abstol);

[m,n] = size(Data);

for i = 1:m

    % Mole fractions
    XT1 = Data(i,1);
    XT2 = Data(i,2);


    % Vector of liquid compositions
    Sv_0 = [XT1 XT2 Ts0];

    %% Solving the differential equation for the reactive RCM
    % Calculating the forward RC
    tauspan = linspace (0,5);
    [tau,Sv] = ode15s(@(tau,Sv)
fun_reactRCM_for(tau,Sv,A,Rv,Qr,a,v,Properties,nij,P,R,nu,ref,Comp),tau
span,Sv_0,options);

    XTf = [Sv(:,1) Sv(:,2) 1-Sv(:,1)-Sv(:,2)];
    Tsf = [Sv(:,3) Sv(:,4) Sv(:,5) Sv(:,6)];

    for j=1:100

        XT = [XTf(j,1); XTf(j,2); 1-XTf(j,1)-XTf(j,2)];

        Ts = [Tsf(j,1); Tsf(j,2); Tsf(j,3); Tsf(j,4)];

        % Initial guess for the reference composition
        Xref_0 = min(XT(1),XT(2));

        % Using fsolve to calculate the Xref
        options = optimset('MaxIter',100000,'TolX', 1e-6,…
                           'MaxFunEvals',100000);

        Xref = fsolve(@(Xref)
solve_Xref(Xref,XT,Ts,A,Rv,Qr,a,v,Properties,nij,P,R,nu,ref,Comp),Xref_
0,options);

        if Xref > 1

            Xref = 1;

        end

        X = Xrecalc(XT,nu,Xref,ref,Comp);
```

```matlab
    for k=1:4

        if X(k) < 0.000000001;

            X(k) = 0;

        end

    end


    X = X./sum(X);

    Xt = X';
    Xf(j,:) = Xt;
    Xr(j,1) = Xref;

end

[p,q] = size(Xf);

Xf_end(i,:) = Xf(p,:)

% Calculating the backward RC

tauspan = linspace (0,30);
[tau,Sv] = ode15s(@(tau,Sv) fun_reactRCM_back(tau,Sv,A,Rv,Qr,a,v,…
        Properties,nij,P,R,nu,ref,Comp),tauspan,Sv_0,options);

XTb = [Sv(:,1) Sv(:,2) 1-Sv(:,1)-Sv(:,2)];
Tsf = [Sv(:,3) Sv(:,4) Sv(:,5) Sv(:,6)];

for j=1:100

    XT = [XTb(j,1); XTb(j,2); 1-XTb(j,1)-XTb(j,2)];
    Ts = [Tsf(j,1); Tsf(j,2); Tsf(j,3); Tsf(j,4)];

    % Initial guess for the reference composition
    Xref_0 = min(XT(1),XT(2));

    options = optimset('MaxIter',100000,'TolX', 1e-6,…
                        'MaxFunEvals',100000);

    Xref = fsolve(@(Xref) solve_Xref(Xref,XT,Ts,A,Rv,Qr,a,v,…
                    Properties,nij,P,R,nu,ref,Comp),Xref_0,options);

    if Xref > 1

        Xref = 1;

    end
```

```matlab
        X = Xrecalc(XT,nu,Xref,ref,Comp);

        for k=1:4

            if X(k) < 0.000000001;

                X(k) = 0;

            end

        end

        X = X./sum(X);

        Xt = X';
        Xb(j,:) = Xt;
        Xr(j,1) = Xref;

    end


    [p,q] = size(Xb);

    Xb_end(i,:) = Xb(p,:)


    %% plot in 3-dimensional composition space
    xaf = Xf(:,1);
    xbf = Xf(:,4);
    xcf = Xf(:,3);
    xdf = Xf(:,2);
    XXf = xbf+0.5*xcf+0.5*xdf;
    YYf = 0.5*sqrt(3)*xcf+1/6*sqrt(3)*xdf;
    ZZf = sqrt(2/3)*xdf;

    xab = Xb(:,1);
    xbb = Xb(:,4);
    xcb = Xb(:,3);
    xdb = Xb(:,2);
    XXb = xbb+0.5*xcb+0.5*xdb;
    YYb = 0.5*sqrt(3)*xcb+1/6*sqrt(3)*xdb;
    ZZb = sqrt(2/3)*xdb;

    XX(:,i) = [XXf; XXb];
    YY(:,i) = [YYf; YYb];
    ZZ(:,i) = [ZZf; ZZb];

    AA = [0 0 0];
    BB = [1 0 0];
    CC = [0.5 0.5*sqrt(3) 0];
    DD = [0.5 (1/6)*sqrt(3) sqrt(2/3)];
```

125

```matlab
    allx = [AA(1) BB(1) DD(1) AA(1) CC(1) DD(1) BB(1) CC(1)];
    ally = [AA(2) BB(2) DD(2) AA(2) CC(2) DD(2) BB(2) CC(2)];
    allz = [AA(3) BB(3) DD(3) AA(3) CC(3) DD(3) BB(3) CC(3)];
    figure(2)
    plot3(XXf, YYf, ZZf,'-k')
    hold on
    plot3(XXb, YYb, ZZb,'-k')
    hold on

    axis square
    xlim([0 1])
    ylim([0 1])
    zlim([0 1])
    hold on
    line(allx, ally, allz);
    sp = 0.05;
    text(AA(1)-sp,AA(2)-sp,AA(3)-sp, 'MeOH');
    text(BB(1)+sp,BB(2)-sp,BB(3)-sp, 'MPC');
    text(CC(1)+sp,CC(2)+sp,CC(3)-sp, 'PhOH');
    text(DD(1),DD(2),DD(3)+sp, 'DMC');
    grid off
end
toc
```

The following functions are called by the above reactive code to run the reactive system. As for physical properties, UNIFAC, Antoine, vapor liquid equilibrium functions are presented above in the non-reactive system.

1- Forward Function Code called by ode15s

```matlab
function dx =fun_reactRCM_for(tau,Sv,A,Rv,Qr,a,v,…
                              Properties,nij,P,R,nu,ref,Comp)
XT = [Sv(1); Sv(2); 1-Sv(1)-Sv(2)];
Ts = Sv(3:6);

% Initial guess for the reference composition
Xref_0 = min(XT(1),XT(2));

% Using fsolve to calculate the Xref
options = optimset('MaxIter',100000,'TolX', 1e-6,
'MaxFunEvals',100000);
Xref = fsolve(@(Xref)
solve_Xref(Xref,XT,Ts,A,Rv,Qr,a,v,Properties,nij,P,R,nu,ref,Comp)
,Xref_0,options);

X = Xrecalc(XT,nu,Xref,ref,Comp);

for i=1:4
```

126

```matlab
        if X(i) < 0.000000001;

            X(i) = 0;

        end
    end

    X = X./sum(X);

    [Y Psj] = vapor_comp(X,Ts,A,Rv,Qr,a,v,Properties,nij,P,R);

    % T = Ts'*X;
    %
    % Keq = fun_Keq(X,T,Q,RP,UA,UB);

    for i = 1:4; f(i) = fun_Ts(Ts(i),A,Psj,i);end

    Y = Y';

    YT = Ytrans(Y,nu,ref);

    XT = [XT(1); XT(2)];
    YT = [YT(1); YT(2)];

    xdot(1:2) = XT-YT;
    xdot(3:6) = f;

    dx = xdot';
    end
```

2- Backward Function Code called by ode15s

```matlab
function dx = fun_reactRCM_back(tau,Sv,A,Rv,Qr,a,v,…
                                Properties,nij,P,R,nu,ref,Comp)
XT = [Sv(1); Sv(2); 1-Sv(1)-Sv(2)];
Ts = Sv(3:6);
% Initial guess for the reference composition
Xref_0 = min(XT(1),XT(2));

% Using fsolve to calculate the Xref
options = optimset('MaxIter',100000,'TolX', 1e-6,
'MaxFunEvals',100000);
Xref = fsolve(@(Xref)
solve_Xref(Xref,XT,Ts,A,Rv,Qr,a,v,Properties,nij,P,R,nu,ref,Comp)
,Xref_0,options);

Xref;

X = Xrecalc(XT,nu,Xref,ref,Comp);
```

127

```matlab
for i=1:4

    if X(i) < 0.000000001;

        X(i) = 0;

    end
end

X = X./sum(X);

[Y Psj] = vapor_comp(X,Ts,A,Rv,Qr,a,v,Properties,nij,P,R);

% Keq = fun_Keq(X,T,Q,RP,UA,UB);

for i = 1:4; f(i) = fun_Ts(Ts(i),A,Psj,i);end

Y = Y';

YT = Ytrans(Y,nu,ref);

XT = [XT(1); XT(2)];
YT = [YT(1); YT(2)];

xdot(1:2) = YT-XT;
xdot(3:6) = f;

dx = xdot';
```

3- X_ref solver function

```matlab
function F =solve_Xref(Xref,XT,Ts,A,Rv,Qr,a,v,
                        Properties,nij,P,R,nu,ref,Comp)
X = Xrecalc(XT,nu,Xref,ref,Comp);

for i=1:4

    if X(i) < 0.000001;

        X(i) = 0.000001;

    end
end

X = X./sum(X);
% Function calculating the VLE
[Y Psj] = vapor_comp(X,Ts,A,Rv,Qr,a,v,Properties,nij,P,R);

T = Ts'*X;
% Function calculating the chemical equilibrium constant
Keq = fun_Keq(T,X,a,Rv,Qr,v);
```

```matlab
% Keq = X(1)*X(4)/(X(2)*X(3));
F = abs(Keq-exp(-23.8e3/R*T)-(0.346/R));
% F = abs(Keq-exp(-2702/T)+0.175);
end
```

4- Chemical Equilibrium Function

```matlab
function Keq = fun_Keq(T,X,a,Rv,Qr,v)

GAMMA = UNIFAC(T,X,a,Rv,Qr,v);
ACT = GAMMA.*X;

Keq = ACT(1)*ACT(4)/(ACT(2)*ACT(3));
end
```

```matlab
function X = Xrecalc(XT,nu,Xref,ref,Comp)

% Determining the number of components(NC) and number
ofreaction(NR)
NR = size(nu,1);
NC = length(XT)+NR;
m = length(XT);
X = zeros(NC,1);
for i=1:NR
    nu_T(i) = sum(nu(i,:));
    for j = 1:NR
        nu_ref(i,j) = nu(i,ref(j));
    end
end

% Elimate the reference component from the stoichiometric matrix

for i=NR:-1:1

    nu(:,ref(i)) = [];

end

x = XT+(nu*inv(nu_ref)*Xref')';

for i=1:m

    X(Comp(i)) = x(i);
end

for i=1:NR
    X(ref(i)) = Xref(i);
end
X;
end
```

129

5- Compositions Transfer Functions

```matlab
function XT = Xtrans(X,nu,ref)

% Determining the number of components(NC) and number of
% reactions(NR)
NC = length(X);
NR = size(nu,1);

% Isolating the reference component and eliminating it from the X
% vector
Xref = X(ref);
X(ref) = [];

% Sum of the stoichiometric coefficients, total molar change and
% building
% the square matrix of stoichiometric coefficients for the
% reference
% components in the each reaction

for i=1:NR

    nu_T(i) = sum(nu(i,:));

    for j = 1:NR

        nu_ref(i,j) = nu(i,ref(j));

    end

end

% Elimate the reference component from the stoichiometric matrix

for i=NR:-1:1

    nu(:,ref(i)) = [];
end

% Calulating the transformed variable for the liquid composition: XT
XT = (X-nu'*inv(nu_ref)*Xref);

XT;
end
```

```matlab
function YT = Ytrans(Y,nu,ref)

% Determining the number of components(NC) and number of reaction(NR)
NC = length(Y);
NR = size(nu,1);

% Isolating the reference component and eliminating it from the X
vector
Yref = Y(ref);
Y(ref) = [];

% Sum of the stoichiometric coefficients, total molar change and
building
% the square matrix of stoichiometric coefficients for the reference
% components in the each reaction

for i=1:NR

    nu_T(i) = sum(nu(i,:));

    for j = 1:NR

        nu_ref(i,j) = nu(i,ref(j));

    end

end

% Elimate the reference component from the stoichiometric matrix

for i=NR:-1:1

    nu(:,ref(i)) = [];

end

% Calulating the transformed variable for the liquid composition: XT
YT = (Y-nu'*inv(nu_ref)*Yref);

YT;
end
```

References

Agreda V., Partin L., Heise W. (1990) High-purity methyl acetate via reactive distillation. Chemical Engineering Progres:40-46.

Barbosa D., Doherty M.F. (1988) The simple distillation of homogeneous reactive mixtures. Chemical Engineering Science 43:541-550. DOI: http://dx.doi.org/10.1016/0009-2509(88)87015-5.

Brunelle D.J., Korn M.R. (2005) Advances in polycarbonates American Chemical Society, Washington, DC.

Buchanan J.S., Jiang Z., Santiesteban J.G., Weber W.A. (2006) Integrated process for preparing dialkyl carbonates with a circulating catalyst, US Patent 7,084,292,, Google Patents.

Co T.B. (2013) Methods of applied mathematics for engineers and scientists Cambridge University Press, New York.

Doherty M.F., Perkins J.D. (1978) On the dynamics of distillation processes—I: The simple distillation of multicomponent non-reacting, homogeneous liquid mixtures. Chemical Engineering Science 33:281-301. DOI: http://dx.doi.org/10.1016/0009-2509(78)80086-4.

Doherty M.F., Malone M.F. (2001) Conceptual design of distillation systems McGraw-Hill.

Douglas J.M. (1988) Conceptual design of chemical processes McGraw-Hill, New York.

Ferrio J.A. (1999) Nonlinear observers for distillation, Chemical Engineering, Michigan Technological University, Houghton. pp. 230.

Fox D.W. (1964) Polycarbonate polymerization process, US Patent 3,144,432.

Fredenslund A., Jones R.L., Prausnitz J.M. (1975) Group-contribution estimation of activity coefficients in nonideal liquid mixtures. AIChE Journal 21:1086-1099. DOI: 10.1002/aic.690210607.

Fukuoka S. (2012) Non-phosgene polycarbonate from CO2: Industrialization of green chemical process Nova Science Publishers, Hauppauge, N.Y.

Fukuoka S., Tojo M., Kawamura M. (1993) Process for continuously producing an aromatic carbonate, US Patent 5,210,268,.

Fukuoka S., Hachiya H., Matsuzaki K. (2009) Process for industrial production of an aromatic carbonate, US Patent 7,531,616, B2.

Fukuoka S., Hachiya H., Matsuzaki K. (2010a) Industrial process for production of an aromatic carbonate, US Patent 7777067 B2.

Fukuoka S., Miyaji H., Hachiya H., Matsuzaki K. (2006) Industrial process for production of dialkyl carbonate and diol, US Patent Appl. Publ. 2009/0105494 A1.

Fukuoka S., Tojo M., Hachiya H., Aminaka M., Hasegawa K. (2007) Green and Sustainable Chemistry in Practice: Development and Industrialization of a Novel Process for Polycarbonate Production from CO2 without Using Phosgene. Polym. J 39:91-114.

Fukuoka S., Fukawa I., Tojo M., Oonishi K., Hachiya H., Aminaka M., Hasegawa K., Komiya K. (2010b) A Novel Non-Phosgene Process for Polycarbonate Production from CO_2: Green and Sustainable Chemistry in Practice. Catalysis Surveys from Asia 14:146-163. DOI: 10.1007/s10563-010-9093-5.

Fukuoka S., Kawamura M., Komiya K., Tojo M., Hachiya H., Hasegawa K., Aminaka M., Okamoto H., Fukawa I., Konno S. (2003) A novel non-phosgene polycarbonate production process using by-product CO2 as starting material. Green Chemistry 5:497-507.

Hallgren J.E. (1983) Diaryl carbonate process, US Patent 4,410,464,, Google Patents.

Haubrock J., Raspe M., Versteeg G.F., Kooijman H.A., Taylor R., Hogendoorn J.A. (2008a) Reaction from Dimethyl Carbonate to Diphenyl Carbonate. 1. Experimental Determination of the Chemical Equilibria. Industrial & Engineering Chemistry Research 47:9854-9861. DOI: 10.1021/ie0711170.

Haubrock J., Wermink W., Versteeg G.F., Kooijman H.A., Taylor R., van Sint Annaland M., Hogendoorn J.A. (2008b) Reaction from Dimethyl Carbonate (DMC) to Diphenyl Carbonate (DPC). 2. Kinetics of the Reactions from DMC via Methyl Phenyl Carbonate to DPC. Industrial & Engineering Chemistry Research 47:9862-9870. DOI: 10.1021/ie071176d.

Illuminati G., Romano U., Tesei R. (1980) Process for the preparation of aromatic carbonates, US Patent 4,182,726,, Google Patents.

Kaymak D.B., Luyben W.L. (2005) Comparison of Two Types of Two-Temperature Control Structures for Reactive Distillation Columns. Industrial & Engineering Chemistry Research 44:4625-4640. DOI: 10.1021/ie058012m.

King C.J. (1980) Separation processes. 2d ed. McGraw-Hill, New York.

Luyben W.L., American Institute of Chemical Engineers. (2006) Distillation design and control using Aspen simulation Wiley-Interscience, Hoboken, N.J.

Luyben W.L., Yu C.C. (2009) Reactive Distillation Design and Control John Wiley & Sons.

Malone M.F., Doherty M.F. (2000) Reactive Distillation. Industrial & Engineering Chemistry Research 39:3953-3957. DOI: 10.1021/ie000633m.

Okamoto H., Someya K. (2007) Method of manufacturing alkylene carbonate, US Patent 7,199,253, B2, Google Patents.

Ono Y. (1997) Catalysis in the production and reactions of dimethyl carbonate, an environmentally benign building block. Applied Catalysis A: General 155:133-166. DOI: 10.1016/s0926-860x(96)00402-4.

Peppel W.J. (1958) Preparation and Properties of the Alkylene Carbonates. Industrial & Engineering Chemistry 50:767-770. DOI: 10.1021/ie50581a030.

Prausnitz J.M., Lichtenthaler R.N., Azevedo E.G.d. (1999) Molecular thermodynamics of fluid-phase equilibria. 3rd ed. Prentice Hall PTR, Upper Saddle River, N.J.

Raines D.A., Ainsworth O.C. (1980) Ethylene carbonate process, US Patent 4,233,221,, Google Patents.

Rev E. (1994) Reactive Distillation and Kinetic Azeotropy. Industrial & Engineering Chemistry Research 33:2174-2179. DOI: 10.1021/ie00033a022.

Roat S., J. D., Vogel E., Doss J. (1986) Integration of rigorous dynamic modeling and control system synthesis for distillation columns, In: Chemical Process Control-CPC III, Elsevier, Amsterdam, Netherlands.

Romano U., Tesel R., Mauri M.M., Rebora P. (1980) Synthesis of Dimethyl Carbonate from Methanol, Carbon Monoxide, and Oxygen Catalyzed by Copper Compounds. Industrial & Engineering Chemistry Product Research and Development 19:396-403. DOI: 10.1021/i360075a021.

Rose A., Sweeny R.F., Schrodt V.N. (1958) Continuous Distillation Calculations by Relaxation Method. Industrial & Engineering Chemistry 50:737-740. DOI: 10.1021/ie50581a026.

Schnell H. (1959) Linear Aromatic Polyesters of Carbonic Acid. Industrial & Engineering Chemistry 51:157-160. DOI: 10.1021/ie50590a038.

Seader J.D., Henley E.J., Roper D.K. (2011) Separation process principles : chemical and biochemical operations. 3rd ed. Wiley, Hoboken, NJ.

Sharma N., Singh K. (2010) Control of reactive distillation column: a review. International Journal of Chemical Reactor Engineering 8.

Siirola J.J. (1996) Industrial Applications of Chemical Process Synthesis, in: L. A. John (Ed.), Advances in Chemical Engineering, Academic Press. pp. 1-62.

Sørensen E., Skogestad S. (1994) Control strategies for reactive batch distillation. Journal of Process Control 4:205-217. DOI: http://dx.doi.org/10.1016/0959-1524(94)80042-1.

Sundmacher K., Kienle A. (2006) Reactive distillation: status and future directions Wiley-VCH.

Taylor R., Krishna R. (2000) Modelling reactive distillation. Chemical Engineering Science 55:5183-5229.

Thiel C., Sundmacher K., Hoffmann U. (1997) Residue curve maps for heterogeneously catalysed reactive distillation of fuel ethers MTBE and TAME. Chemical Engineering Science 52:993-1005. DOI: http://dx.doi.org/10.1016/S0009-2509(96)00454-X.

Tundo P., Trotta F., Moraglio G., Ligorati F. (1988) Continuous-flow processes under gas-liquid phase-transfer catalysis (GL-PTC) conditions: the reaction of dialkyl carbonates with phenols, alcohols, and mercaptans. Industrial & Engineering Chemistry Research 27:1565-1571. DOI: 10.1021/ie00081a002.

Tung S.-T., Yu C.-C. (2007) Effects of relative volatility ranking to the design of reactive distillation. AIChE Journal 53:1278-1297. DOI: 10.1002/aic.11168.

Ung S., Doherty M.F. (1995a) Calculation of residue curve maps for mixtures with multiple equilibrium chemical reactions. Industrial & Engineering Chemistry Research 34:3195-3202. DOI: 10.1021/ie00037a003.

Ung S., Doherty M.F. (1995b) Vapor-liquid phase equilibrium in systems with multiple chemical reactions. Chemical Engineering Science 50:23-48. DOI: http://dx.doi.org/10.1016/0009-2509(94)00180-Y.

Ung S., Doherty M.F. (1995c) Synthesis of Reactive Distillation Systems with Multiple Equilibrium Chemical Reactions. Industrial & Engineering Chemistry Research 34:2555-2565. DOI: 10.1021/ie00047a002.

Venimadhavan G., Buzad G., Doherty M.F., Malone M.F. (1994) Effect of kinetics on residue curve maps for reactive distillation. AIChE Journal 40:1814-1824. DOI: 10.1002/aic.690401106.

Walpot H. (2011) Theoretical Modeling of Residue Curve Maps for Reactive Distllation Cocept for the Production of n_propyl propionate, Delft Universtiy of Technology. pp. 78.